August 2015

Ph.D. Dissertation

Mechanistic study of intracellular processes of amyloid β-induced cell death: caspase activation related to intrinsic apoptotic pathway and nuclear disruption

Graduate School of Chosun University

Department of Bio-Materials

Md. Imamul Islam

Mechanistic study of intracellular processes of amyloid β-induced cell death: caspase activation related to intrinsic apoptotic pathway and nuclear disruption

아밀로이드 베타에 의한 세포사의 세포내 반응의 기전적 연구: 내부 세포자살 경로에 의한 케스페이즈의 활성화와 세포핵의 해체

August 25, 2015

Graduate School of Chosun University

Department of Bio-Materials

Md. Imamul Islam

Mechanistic study of intracellular processes of amyloid β-induced cell death: caspase activation related to intrinsic apoptotic pathway and nuclear disruption

Advisor: Prof. Il- Seon Park

This dissertation is submitted to the Graduate School of Chosun Univeristy in partial fulfillment of the requirements for the degree of Doctor of Philosophy in Science

April 2015

Graduate School of Chosun University

Department of Bio-Materials

Md. Imamul Islam

This is to certify that the PhD thesis of **Md. Imamul Islam** has successfully met the dissertation requirements of Chosun University.

Chairman (Chosun Univ.) : Prof. Song Yub Shin .....

Member (Chosun Univ.) : Prof. Park Il Seon.....

Member (Chosun Univ.) : Prof. Takbum Ohn.....

Member (Chosun Univ.) : Prof. Lee Jung Hee.....

Member (Yonsei Univ.) : Prof. Cho Beong Yon.....

June 2015

Graduate School of Chosun University

CONTENTS

LIST OF FIGURES

초록

아밀로이드 베타에 의한 세포사의 세포내 반응의 기전적 연구: 내부 세포자살 경로에 의한 케스페이즈의 활성화와 세포핵의 해체

엠디 이마물 이슬람
지도교수: 박 일 선
생물신소재학과
조손대학교 대하권

AD에서 아밀로이드 베타는 노인성 반점의 주 성분으로 세포 사멸을 유도한다. Apoptotic pathway는 세포사멸과정에 활성화 되는 것으로 알려져 있고 케스페이즈 활성화는 그 대표적인 특징 중 하나이다. 그러나 stausporine에 의해 유도되는 내인성 경로 세포사멸은 apaf-1 apoptosome 복합체를 형성하고, caspase-9을 활성화시키며, 하류 케스페이즈의 아밀로이드 베타 펩타이드에 의해 억제된다고 알려져 있다. 따라서 케스페이즈 활성화 메커니즘과 아밀로이드 베타에 의해 유도되는 세포사멸 경로에 대한 연구는 필요하다. 아밀로이드 베타를 2시간 동안 2번 처리하고, 22시간 반응시킨 세포에서는 Apaf-1, caspase-9, cytochrome c등을 포함하는 단백질 복합체인 apoptosome이 발견되었지만, 24시간동안 아밀로이드 베타를 한번 처리한 것은 apoptosome 복합체를 형성을 유도하지 않았다. 케스페이즈-8은 외인성경로인 death inducing signaling complex (DISC)형성으로 인해 활성화될 수 있고, 세포사멸신호의 증폭을 위한

내인성 경로에서는 아밀로이드 베타를 2+22시간 처리한 세포에서 활성되었으나 활성화된 케스페이즈-8은 기질인 Bid를 자르기에는 충분하지 못했다. 따라서, DISC는 형성되지 않았으며, 이것은 케스페이즈-8이 내인성 경로에 의해 활성화 된 것을 의미한다. 케스페이즈-8의 *in vitro* 활성화는 세포추출물과 dATP/사이토크롬 c 또는 정제된 케스페이즈-3과-6에 의해 유도되고, 활성화된 케스페이즈-8(43/41 kDa)은 추가로 처리된 아밀로이드베타에 의해 영향을 받지 않았다. 따라서, 케스페이즈-8은 내인성 경로를 통해 활성화되지만 그것의 약한 활성 때문에 세포사멸 신호전달 메커니즘에서의 역할은 여전히 불분명하다.

Lamin A/C와 B는 케스페이즈-6와 NS 프로테아제의 표적이고, 절단된 단백질 산물이 두 경우에 다르고 세포사멸의 경로는 절단산물에 의해 결정될 수 있기 때문에 아밀로이드 베타를 2+22시간 처리한 세포에서 Lamin A/C와 B 절단을 분석하였다. 아밀로이드베타를 처리한 경우 46kDa와 21kDa의 Lamin A와 B의 양이 모두 줄어든 반면, 28kDa와 46kDa 단백질은 케스페이즈-6의 활성이 있을 것으로 기대된다. 따라서 NS 프로테이즈는 내인성경로에서 케스페이즈-6보다 2+22시간 아밀로이드베타를 처리한 세포에서의 절단에 더 두드러진 역할을 한다.

staurosporin 처리된 세포에서 라민 단백질의 절단을 위해 케스페이즈-6의 활성화는 일어나지만 아밀로이드베타를 2+22시간 처리한 세포에서는 케스페이즈-6 활성화는 현저하게 증가되지만 Lamin 단백질의 절단은 일어나지 않는다. 또한 컨포컬 현미경, size-exclusion 크로마토그래피, immunoprecitation을 통해 케스페이즈는-6와 아밀로이드 베타가 상호작용함을 확인하였고 라민단백질로 케스페이즈-6의 활성은 상호작용을 지연시키는 것으로 보인다.

마지막으로, 아밀로이드 베타의 세포독성이 세포 내 또는 세포외의 과정 때문인지 연구하였다. Tat-Ab42 and flag-Ab42 펩타이드는 각각 세포막과 세포질에 위치한 것으로 밝혀졌다. Tat-Ab42는 강력한 세포독성을 나타냈고, flag-Ab42는 세포독성이 나타나지 않았다. 따라서 세포내 과정이 세포독성에 대한 주요 원인이 될 것으로 보인다. 결론적으로, 아밀로이드 베타는 NS 프로테아제를 포함하는 내인성 세포사멸 경로를 유도하지만, 세포내 세포독성을 증가시키는데 기여할 것으로 보인다.

ABSTRACT

Mechanistic study of intracellular processes of amyloid β-induced cell death: caspase activation related to intrinsic apoptotic pathway and nuclear disruption

Md. Imamul Islam

Advisor: Prof. Il-Seon Park

Department of Biomaterials

Graduate School of Chosun Univeristy

Amyloid β (Aβ), a main component of the senile plaque detected in Alzheimer's disease, induces cell death. Apoptotic pathway is known to be activated in the death process. Caspase activation is one of the hallmarks of the pathway. However, it was previously shown that the intrinsic pathway of apoptosis induced by staurosporine (STS) in which formation of apaf-1 apoptosome complex and activation of caspase-9 and the downstream caspase could be suppressed by Aβ peptide. Thus, the mechanism of activation of caspases and the involved apoptotic pathway induced by Aβ needs to be explored. It was found that apoptosome, a protein complex containing Apaf-1, caspase-9, cytochrome c and others, was formed in cells treated with Aβ twice for 2 h and following 22 h (2+22 h), while a single treatment of Aβ to the cells for 24 h did not induce the formation. Caspase-8 which can be activated by the extrinsic

pathway through the formation of death inducing signaling complex (DISC) and intrinsic pathway for the amplification of the death signal was also activated in the cells treated with Aβ for 2+22 h, although the level was not sufficient to cleave Bid, the substrate of caspase-8. DISC was not formed, implying that caspase-8 was activated by intrinsic pathway. The in vitro activation of caspase-8 using cell extract and dATP/cytochrome c or purified caspase-3 and -6 was observed, and the formation of active caspase-8 fragments 43/41 kDa protein was negatively affected by added Aβ. Thus, we suggest that caspase-8 is activated by the intrinsic pathway, but its role in the apoptotic signal transduction is still obscure because of its weak activity.

Next, the role of the activated intrinsic apoptotic pathway in the Aβ-treated cell death was explored. Cleavage of Lamin A/C and B was examined in the 2+22 h Aβ-treated cells, because the proteins are the target of caspase-6 and NS protease and the cleaved products are different in the two cases, implying that the cell death pathway can be determined by the products. Levels of both Lamin A and B (not C) were reduced by the Aβ treatment to produce 46 (N-terminus detection by western blot) and 21 (C-terminus detection by western blot) kDa proteins, respectively, while 28 and 46 kDa proteins for each protein were expected for caspase-6 activity. Thus, it was concluded that NS protease plays a predominant roles in the cleavage in the 2+22 h Aβ-treated cells rather than caspase-6, activation of which is a part of the intrinsic apoptotic pathway.

Caspase-6 was a protease responsible for the cleavage of Lamin proteins in staurosporin-treated cells, while it was not in the 2+22 h Aβ-treated cells, although the caspase was prominently activated in the cells. It was found in confocal microscope, size-exclusion chromatography and immunoprecitation studies that caspase-6 interacts with Aβ. It appears that the interaction might retard the action of capase-6 to Lamin proteins.

Finally, it was explored whether Aβ cytotoxicity is due to extracellular or intracellular processes. Tat-Aβ42 and flag-Aβ42 peptides were constructed and were found to be located at cytoplasm and cell membrane, respectively. Tat-Aβ42 showed robust cytotoxicity, while flag-Aβ42 was not cytotoxic. Thus, an intracellular process seems to be a major cause for the cytotoxicity.

In conclusion, Aβ induced intrinsic apoptotic pathway and NS-protease-involved process, but the latter appears to contribute more to its cytotoxicity which might be intracellular.

I. Introduction

I - 1. The β-Amyloid peptide and Alzheimer's disease

The ~4 kDa Aβ peptide, derived from its precursor protein called amyloid precursor protein (APP), was first isolated as the principal component of amyloid deposits in the brain and cerebrovasculature of Alzheimer's disease. Although the function of APP itself has yet to be resolved, extensive research has been conducted on how the Aβ peptide is produced, and how it is subsequently degraded within the brain, or transported out into the periphery. And these factors determine the final amount of Aβ that accumulates as amyloid deposits within the brain. Alzheimer's disease is characterized clinically by a progressive and gradual decline in cognitive function and neuropathologically by the presence of neuropil threads, specific neuron loss, and synapse loss in addition to the hallmark findings of neurofibriallary tangles and senile plaques. The composition of this senile plaque is, in large part, highly insoluble Aβ in the parenchymal region of the brain.

Metabolism of APP to Aβ by the enzymatic processes is now reasonably well established. APP is sequentially cleaved by two membrane-bound endoprotease activities, β- and γ-secretase. β-secretase first cleaves APP to release a large secreted derivative, sAPPβ[1, 2]. A fragment of 99 amino acids (CTFβ, which begins with the N-terminal aspartyl residue of Aβ) remains membrane bound, and is in turn rapidly

cleaved by γ-secretase to generate Aβ [3]. Cleavage by γ-secretase is somewhat nonspecific, resulting in the formation of different C-terminal heterogeneous peptides. So, numerous different Aβ species exist, but those ending at position 40 (Aβ40) are the most abundant (~80-90%), followed by 42 (Aβ42, ~5-10%). The marginally longer forms of Aβ, specifically Aβ42, are more hydrophobic and fibrillogenic, and are the principal species deposited in the brain [1, 4, 5]. β-secretase activity is thought to be the rate limiting step in the amyloidogenic pathway, which processes ~10% of the total cellular APP. The residual APP, about 90%, is constitutively cleaved by α-secretase (a group of metalloprotease enzymes), generating sAPPα and the 83 amino acid CTFα.

The subsequent cleavage of CTFα by γ-secretase produces the more benign p3 fragment a 3 kDa peptide, instead of Aβ. γ-Secretase cleavage of either membrane bound CTF also generates a cytosolic element, AICD (APP intracellular domain, sometimes referred to as CTFγ), which may have a role in signaling pathway [4, 6-8]. Because of its essential role in the Alzheimer's disease pathogenesis, the longer form of Aβ, (Aβ42) is considered a major target for the study of its underlying mechanism of cell cytotoxicity. This study was also focused to delineate the mechanism of apoptosis induced by a particular structural form of Aβ42.

I-2. Multimeric Conformation and cytotoxicity of Aβ

The biological effect of different species of Aβ is reported to be dependent on the assembly of Aβ into multimeric structures. There are two phases of assembly which have different characteristics and lead to formation of different species of Aβ with different biological properties. Initial research with the pathogenesis of Aβ focused on the extracellular hallmarks of AD, the amorphous and fibrillar deposits of the peptide. Present focus is on the earlier phase of Aβ assembly which involves soluble oligomers of the peptide. These structures are orders of magnitude more toxic to different types of cells than are the fibrils and trigger a different set of toxic events [9]. They are also different in morphologically and conformationally and recognized by specific antibodies. Oligomer specific antibodies do not recognize fibrils or monomer, and soluble oligomers are not recognized by fibril specific antibodies. Though complete rejection of fibril involvement in Alzheimer's disease at this time point is possibly premature because of the potential for plaque involvement with oligomer species [10], the current focus of the Aβ research field has shifted to soluble oligomers. Aβ42 peptide forms the oligomers more readily than the more abundant Aβ40 [11] . The ratio of Aβ 42/40 and age of disease onset play an important role in familial AD [12, 13]. The C-terminus of Aβ42 is reported to be crucial for oligomer formation [14]. While the early intermediates during oligomerization of recombinant purified peptide are

unstable and require trapping of the intermediates, stable small oligomers can be isolated from biological systems. The reason for this difference in stability is yet to be explored. Chemically stable Aβ oligomers even the dimers, isolated from AD brain and CSF have been shown to disrupt synaptic electrophysiology [15, 16]. On the other hand, fibrillar Aβ is thermodynamically favorable and accomplishes by the addition of monomers to the end of existing nucleus, leading to rapid extension of fibrils [17]. Process of Aβ fibrilization is thought to be preceded by multiple conformational changes including trimer, pentamer or higher molecular weight complex formation, known as Aβ – derived diffusible ligands (ADDL) [18], oligomers consisted of 15-20 monomeric units (AβOs) [19], protofibrils and other higher molecular weight oligomers. It is also reported that there is a linear relationship between the fibril formation and the concentration of monomer present in the sample [20]. Also some study revealed that, insoluble Aβ fibrils may act as the reservoir of soluble and highly toxic oligermic form of Aβ [10]. To study of fibril formation of by synthetic or recombinant Aβ, usually high concentrations (μM) range is used to facilitate the probability of a fibril nucleus formation. But the concentration of soluble oligomers in CSF or brain interstitial fluid is in the pM range, hence there is a chance that in in vivo case, fibril formation is nucleated on extracellular matrix or cell surfaces.

Although, most of the investigators of these days are in consensus that soluble oligomers are biologically active and are the cause of cellular

cytotoxicity under some conditions, the mechanism of action of soluble oligomeric species of Aβ still remains to be resolved. This study was conducted to find out the mechanism of intracellular process of cytotoxicity induced by soluble oligomeric species of $A\beta_{42}$.

I-3. Mechanism(s) of Aβ induced cytotoxity

Though it is thought to be the central role player of the Alzheimer's disease pathology, the mechanism of Aβs mediated cytotoxicity is still inconclusive. The cellular events that occur between the production of Aβ and neuronal loss are yet to be revealed. Several hypotheses have been proposed regarding the relation of Aβ production and neuronal degeneration and toxicity. There is no dispute regarding the presence of intracellular Aβ, but the function of this intracellular Aβ in disease progress remains controversial. The burning question is the source of the accumulated Aβ inside the neuronal cells, whether this accumulations result from the direct deposition of intracellularly produced Aβ or uptake of the extracellularly produced Aβ. Because the APP is reported to be present in membranes of mitochondria, the trans-Golgi network, endoplasmic reticulum (ER), endosomes, autophagosomes, and lysosomes in addition to plasma membrane [21]. β- and γ-secretases have been found to be present in these subcellular compartments. Hence, intracellular accumulation may be occurred by intracellular production of Aβ in favorable condition. Nonetheless, there is no question that significant amount of Aβ is

produced in the plasma membrane by cleaving the APP and make the extracellular deposition. Reports have shown that, this extracellular Aβ can be re-uptake by cells through membrane micro domain called lipid rafts and contribute to intracellular deposition [22, 23]. A positive correlation is shown in several studies between the plasma membrane binding of Aβ and the cytotoxicity induced by the peptide [24, 25]. Aβ has been found to bind with a number of receptors or receptor related proteins such as N-methyl-D-aspartic acid (NMDA) receptor [26], low-density receptor associated protein-1 [27], the α7 nicotinic acetyl choline receptor [28], the p75 neurotrophin receptor [29], and the receptor for advanced glycation endproducts [30]. Membrane binding of Aβ has been reported as a necessary step to exert the toxicity by peptide [31], while the interaction of Aβ with receptor associated protein (RAP) have been found to promote the cellular internalization of the peptide [32]. A recent study has been reported a new interaction of Aβ peptide with lipoprotein lipase (LPL) which promoted the membrane association and cellular uptake of the peptide [33].

The first order interaction of Aβ with cell membrane and receptors, however, facilitate the membrane permeability and internalization of the peptide. The binding of Aβ to membrane stimulates the Aβ aggregation due to the interaction between the anionic lipid and the peptide which enhances the structural transition of the peptide from random coils to β-sheet structure [34]. This enhancement of structural conversion along with increased membrane permeability leads to the

formulation of the 'channel hypothesis', postulated on the evidence of the formation of ion channel by Aβ peptides [35], and at least eight different ion channels have been characterized [36]. A report has been shown that the interaction of Aβs with the membrane leads to the formation of small oligomeric complexes which have been found to form multimeric channels with a central pore- like structure [37].

I-4. Reuptake mechanism of Aβ and interaction with intracellular Protein

The mechanism of intracellular accumulation of Aβ has created a growing interest of concern. Several pathways have been proposed to describe the event. Internalization via endocytosis and accumulation in the endosomal/lysosomal systems have been suggested by an earlier study [38]. Endocytosis is a widely studied phenomenon in cell biology and several different pathways have been proposed for different protein machinery [39].

The conventional endocytic pathway contains invagination of the plasma membrane at the site of the receptor-cargo binding; the invaginated vesicle is then coated with adaptor proteins, which recruit guanosine triphosphatases (GTPases) that provide the necessary energy to facilitate cleavage of the vesicle from the cell membrane and delivery to endosomes or other subcellular compartments. By far the most frequently reported process is dependent on clathrin and dynamins. A recent *in vitro* study demonstrated that endocytosis of Aβ is regulated by

a dynamin dependent and RhoA mediated pathway [40]. LRP1, a receptor protein which facilitates Aβ uptake, is reported to do it via a clathrin dependent manner in neuroblastoma cells and neuronal cell lines [41]. Aside of endocytosis mechanism, selective accumulation of Aβ occurs via a nonstable, energy independent and nonendocytotic pathway is reported in PC12 cells and cortical and hippocampal neurons [42]. Endocytosis mechanism is shown to be varied not only with cell types but also in different regions of neurons [43]. The specific pathways involved in up taking and intracellular accumulation of Aβ peptides, however, remains inconclusive.

Aβ interacts with a number of other proteins as exemplified in a recent proteomic analysis for artificial β protein and Aβ interactor [44]. That report indicated that amyloidogenic aggregation can result in the sequestration of numerous proteins such as translation initiation factors, chromatin regulators, RNA processing proteins, mitochondrial membrane proteins and chaperones. It is certain that the sequestration of essential proteins results in cell death.

Besides the sequestration, Aβ can directly induce cell death by binding to receptors such as the p75 neurotrophin receptor, a member of the TNF-receptor superfamily, which in fact induces cell death [45, 46]. Furthermore, interaction with some intracellular Aβ-binding proteins such as alcohol dehydrogenase (ABAD) and cytochrome c (Cyto c) oxidase also induces cell death [47, 48]. This interaction was shown to

result in free-radical generation in neurons, suggesting direct molecular link from Aβ to mitochondrial toxicity [49]. Further, the mitochondrial dysfunction and synaptic damage induced in Aβ-treated cells results in the loss of mitochondrial membrane potential and increase in mitochondrial superoxides [50]. As result, Bax protein increases and Cyto c is released from mithochondria. Aβ also seems to induce a signal transduction pathway as shown in increase of c-Jun N-terminal kinase activity, which is associated with cell death pathway such as apoptosis [51]. A recent study also shown that, Aβ can bind to procaspase-9 which results in inhibition of the apaf-1 apoptosome assembly the hallmark of the intrinsic apoptotic pathway [52].

I-5. Role of Aβ in Apoptosis

The term ‘apoptosis’ also known and accepted as a distinct and important mode of programmed cell death, involves a series of biochemical events to eliminate the cells which are genetically determined. This is a highly harmonized and energy dependent process which usually requires the activation of a cascade of cysteine proteases called ‘caspases’ that links from the initial stimuli to the final demise of the cells. However, other forms of programmed cell deaths are reported recently and many other programmed cell death mechanism may yet be evolved [53, 54]. The apoptotic processes play important roles during development, aging, homeostatic mechanism to maintain the cell populations and also as a defense mechanism when cells get damaged by

disease or other toxic agents.

To date, according to the investigation reports, there are two main apoptotic pathways: the extrinsic or death receptor pathway and the intrinsic or mitochondrial pathway.

Intrinsic mitochondria-dependent apoptosis is characterized by formation of a multiprotein complex called an apoptosome consisting of Apaf-1, Cyto c, dATP and procaspase-9 after release of Cyto c from mitochondria [55]. The formation of this protein complex is essential for intrinsic apoptosis and is tightly regulated in healthy cells in which Cyto c is stored in mitochondria and the intracellular concentration of K+ is high (~150 mM) enough to inhibit the formation [56]. It is also regulated by other proteins such as heat shock protein 70 which binds to Apaf-1 and prevents the formation of the multiprotein complex [57]. The formation of the apoptosome leads to activation of caspase-9 which proteolytically cleaves caspase-3 for activation [58]. The extrinsic apoptotic pathway is receptor mediated pathway. Extracellular ligands such as, TNFα, CD95 and Trail bind to the death receptors to form death inducing signaling complex (DISC) which activate caspase-8 in non-mitochondrial pathway [59].

Both the intrinsic and extrinsic apoptotic pathways end with execution phase, involves the processing of effector caspases such as caspase-3, -6 and -7 which are involved in most of the downstream effects of apoptotic processes [60, 61]. Involvement of Aβ both in in vitro

and in vivo apoptotic process has been reported in several investigations [62, 63]. To describe the mechanism of Aβ induced apoptosis, several hypothesis have been proposed. The mitochondrial release of apoptosis inducing factor (AIF) in cultured neurons, and the release of cytochrome c from isolated mitochondria in presence of Aβ have been suggested, which subsequently initiates a caspase independent apoptosis by causing DNA fragmentation and chromatin condensation [59, 60, 64]. Binding of Aβ to p75 neurotrophin receptor can trigger the extrinsic pathway, while the mitochondrial dysfunction caused by the peptide can trigger the intrinsic pathway. Beside the two apoptotic pathways, caspase-4-mediated apoptosis is also induced by the unfolded protein response signaling pathway when endoplasmic reticulum stress involved in neurodegenerative disease including AD is prolonged [65].

I-6. Out Line of the Thesis

The thesis includes the investigation of intracellular events occurs in the apoptotic processes induced by oligomeric species of Aβ42. The initial part consists of the study of the conditions in which potential activation of caspases occurs, and elucidation of the related cell death mechanism under the condition. The second part presents a new interaction mechanism of Aβ42 peptide with a protein involved in programmed cell death process. And the last part deals with the purification of a cell penetrating version of Aβ42 that is, TAT- Aβ42 and comparative study of TAT- Aβ42, wild type Aβ42 and FLAG- Aβ42 in terms of cell death and cell penetration characteristics. The rational of these studies is

summarized below:

1. The mechanism and role of apoptotic pathway induced by Aβ42 oligomeric species has been elucidated. Activation of intrinsic and extrinsic apoptotic pathway has been checked and found that only intrinsic apoptotic pathway has been activated by oligomeric species of Aβ42. Then the effects of this activated intrinsic apoptotic pathway have been analyzed.
2. Interaction of Aβ42 with caspases was screened by confocal microscopy. A novel interaction between Aβ42 and caspase-6 has been outlined and the consequences of the interaction have been analyzed.
3. Cell penetrating TAT- Aβ42 was expressed and purified and characterized in terms of cell death and cell penetration ability by comparing with wild type Aβ42 and FLAG- Aβ42.

II. Activation of intrinsic apoptotic pathway by amyloid β

Abstract

Amyloid-β (Aβ), a main component of the senile plaque detected in Alzheimer's disease, induces cell death. Apoptotic pathway accompanying caspase activation is known to be involved in the death process. However, the role of apoptosis in the cell death was questionable, as limited activation of caspases in Aβ-treated cells frequently observed and also found that Aβ peptide could suppress the intrinsic apoptosis pathway. Here we sought conditions in which caspases are potently activated in Aβ-induced cell death and to explore related death pathways under the condition. Single treatments of Aβ42 to cells for up to 48 h barely induce caspase activation. However, when cells were treated with Aβ42 twice for 2 h and following 22 h (2+22 h) or more, caspase-9-activating protein complex apoptosome was found to be formed and caspases could be activated, implying activation of intrinsic apoptosis pathway. 30-kDa and 41/43-kDa fragments derived from procaspase-8 were recognized in the early and later stage of Aβ treatment, respectively. Formation of DISC, caspase-8-activating death inducing signaling complex was absent in the 2+22 h sample, indicating no involvement of extrinsic apoptotic pathway in the process. The fragments of caspase-8 are all found to be produced through intrinsic pathway. We suggest that intrinsic pathway is the main apoptosis pathway in Aβ-treated cells.

II-1. INTRODUCTION

Amyloid β (Aβ) is 36-43 amino acid-long peptides to elicit the neurodegenerative Alzheimer's disease (AD) [66]. The peptide is generated by proteolytic cleavage of the amyloid precursor protein by α-, β- and γ- secretases [4, 67]. Monomeric Aβ is prone to change its conformation to β-sheet-rich intermediate structures. The intermediates interact with each other to form multimeric aggregates such as oligomers, protofibrils and fibrils [19, 68, 69]. The aggregated Aβ progressively deposits in brain parenchyma and cerebral blood vessels [70]. The soluble Aβ oligomers and protofibrils have been found to be more toxic than the fibrils, suggesting that the oligomeric aggregates would be the main factor for AD [19, 71].

Essential role of apoptosis in eliciting Aβ cytotoxicity has been proposed, because caspases are activated in cells treated with the peptide [72-75]. Caspase, a hallmark enzyme of apoptosis, is synthesized as a zymogen form which is activated by apoptotic signal. Caspase-8 is processed and catalytically activated through receptor-mediated apoptosis, or extrinsic apoptosis in which the death-inducing signaling complex (DISC) is form [76]. On the other hand, chemical-induced apoptosis or caspase-dependent intrinsic apoptosis leads to activation of caspase-9 which is associated with cytochrome c released from the mitochondria, dATP and an adaptor protein Apaf-1 to form mutiprotein complex called apoptosome [75-77]. Once activated, caspase-8 and -9 then process effector caspases, including caspase-3, -6 and -7 which subsequently transduce the death signal by cleaving other proteins [60, 61].

Binding of Aβ to receptors such as death receptor or p75 neurotrophin receptor can trigger the extrinsic pathway [45, 46], while impaired autophagic degradation of the damaged mitochondria during aging [78] may lead to the accumulation of Aβ in the mitochondrial membrane in neurons and following release of cytochrome c [78, 79]

which can trigger the caspase cascade of the intrinsic pathway [78]. On the other hand, caspase-4-mediated apoptosis is also induced by the unfolded protein response signaling pathway when endoplasmic reticulum stress is prolonged [65]. The differential activation of each pathway depends on proteins or factors that interact with Aβ [25, 80] and the conformational states of Aβ (oligomer vs. fibril) [75, 81, 82].

Although a major role of apoptosis in Aβ-induced cell death is evident, we often found that caspase activation was not potent in Aβ-treated cells [83], and also see "Result". We recently found that caspase activation and cell death induced by staurosporine (STS), employed to induce the intrinsic mitochondria-dependent apoptotic pathway, was significantly reduced by Aβ42 [52]. The inhibitory effect of Aβ42 on the apoptotic pathway is associated with its interaction with procaspase-9 and consequent inhibition of Apaf-1 apoptosome assembly. It is also possible that Aβ42 interacts with other proteins involved in apoptosis and disturbs their function, resulting in the low levels of caspase activation, as the peptide found to interact with many proteins [84, 85]. However, on the basis of reports regarding Aβ-induced apoptosis we speculate that the inhibitory effect can be overcome such that caspase can be potently activated. In the current study, we probed apoptosis pathways under the experimental condition leading to robust caspase activation in Aβ-treated cells.

II-2. MATERIALS AND METHODS

Materials

Fetal Bovine serum (FBS) was purchased from Life Technology Inc. (Grand Island, USA). Dulbecco's modified Eagles medium, high glucose (DMEM/HG) was obtained from Welgene (Daegu, Korea). Caspase-9, Caspase-8, Caspase-6 and Caspase-3 substrates, N-acetyl Leu-Glu-His-Asp-amino methyl coumarin (Ac-LEHD-AMC), Ac-IETD-AMC, Ac-VEID-AMC and Ac-DEVD-AMC, respectively, were from A.G. Scientific Inc. (San Diego, USA). Ni-NTA column were purchased from Amersham Biosciences (Piscataway, USA). Western blotting detection kit (WEST-ZOL PLUS) from iNtron Biotechnology (Gyeonggi-do, Korea). Phosphate buffer saline (PBS) purchased from Amresco (solon, USA). Anti-caspase-9, anti-caspase-3, anti-lamin-A/C, anti-lamin B and anti-β-actin from Santa Cruz Biotechnology (California, USA), anti-caspase-8 from Cell Signaling Technology (Massachusetts, USA), anti-DFF45 from BD Transduction Laboratory (San Diego, USA), anti-FADD from AbFrontier and anti-Bid developed in laboratory. Polyclonal antibody anti-caspase-9(p10) obtained from Santa Cruz Biotechnology, Urea was from USB chemicals, Acetonitrile from Merck (Darmstadt, Germany). All other chemicals obtained from Sigma (St. Louis, USA), unless otherwise stated.

Preparation of Aβ peptide

The purified peptide was solubilized in 100% 1,1,1,3,3,3,-hexafluoro-2-propanol, and dried under nitrogen flow and subsequently, under vacuum for 30 min. The peptide aliquots were stored at –20 °C until use. Immediately before use, the peptide was dissolved in 0.1% NH_4OH at a concentration of 2 mg/ml followed by bath sonication for 10 min in ice cold water. The solution was diluted at the desired concentration with cell culture media without FBS. Aβ42 oligomers were prepared as described earlier [86] with little modification. Briefly, peptides were diluted in cell culture media without FBS at 100 μM concentration, vortexed for 30 seconds and incubated at 4^{o}C for 12 h. The peptide solution then diluted to the desired concentrations with cell culture media without FBS. To make fibrils, Aβ42 (100 μM) was incubated in presence of 0.02% sodium azide in PBS at 37 ^{o}C for 4 days

Measurement of Caspase activity

Caspase activity was measured as described earlier [56]. Briefly, treated cells were washed twice with ice-cold phosphate-buffer saline (PBS). Then, 40 μl of buffer containing 20 mM HEPES-NaOH, pH 7.0, 1mM EDTA, 1mM EGTA, 20mM NaCl, 0.25% Triton X-100, 1mM dithiothreitol (DTT), 1mM phenylmethanesulphonylchloride (PMSF), 10 μg/ml leupeptin, 5 μg/ml pepstatin A, 2 μg/ml aprotinin, 25 μg/ml ALLN was added into each well and incubated on ice for 20 min. The cell extracts were dispersed intermittently with Gilson pipette. Caspase assay

buffer (final 20mM HEPES-NaOH, pH 7.0, 20mM NaCl, 1.5 mM $MgCl_2$, 1mM EDTA, 1mM EGTA and 10mM DTT) was added and the release of AMC was monitored for 2h in 2 minute interval with respective caspase substrates at excitation and emission wavelengths of 360 nm and 480 nm respectively, using microplate sepectrofluorometer (Molecular Devices, CA, USA). The results were expressed as a slope of total readings versus time.

Cell Culture and Cell death Assay

Human epithelial HeLa cells were cultured in DMEM (High glucose) medium supplemented with 10% (v/v) FBS and 1% antibiotics at 37 °C under 5% CO_2.

For MTT cytotoxicity assay, cells were plated at a density of 15,000 cells/well in 96-well plates (Nunc, Denmark) and cultured for 24 h followed by serum deprivation for another 12 h. Cells were exposed to the Aβ preparation for appropriate time and the viability was assessed by 3-(4,5-dimethylthiazol-2-yl)-2,5-di-phenyltetrazolium bromide formazan (MTT) reduction test. Briefly, 20 μl of 5 mg/ml MTT solution in PBS was added to each well, rapped with aluminum foil and incubated for 2 h. Then 100 μl of solubilization buffer [20% SDS solution in 50% (v/v) DMF (pH 4.7)] was added. After 12-16 h of incubation, absorbance was recorded at 570 nm using a micro plate reader KisanBio plate reader (KisanBio, Seoul, South Korea).

For Alamar blue assay also same cell culture and treatment method was followed. After treatment 10 μl of alamar blue (Life technologies) was added directly to the cells and incubated for 4-16 h, absorbance was recorded at 570 nm using a micro plate reader Spectra Max 190 (Molecular Devices, CA, USA).

Western blot analysis

Cells were harvested, washed with ice-cold PBS for at least twice and resuspended in lysis buffer containing, (50 mM Tris-HCL, pH 8.0, 150 mM NaCl, 1% Triton X-100, 5mM EDTA, 5mM EGTA, 1mM PMSF, 10 μg/ml leupeptin, 2 μg/ml pepstatin A and 2 μg/m aprotinin) for 20 min on ice. The extract was obtained by centrifugation at 13,000 rpm at 4^{o}C for 30 min. The amount of protein was measured through Bradford assay. Equal amounts of proteins were separated on 12–15 % SDS-PAGE and transferred on to a PVDF membrane. The membrane was immunoprobed with primary antibodies and horseradish peroxidase-conjugated secondary antibodies. The blots were visualized using West-Zol plus reagent (iNtron Biotechnology Inc., Seoul, Korea) in a Chemiluminescent detection system (Supernova 1800).

Analysis of Cyto c release

Cells were harvested, washed with ice-cold PBS and resuspended in digitonin buffer (75 mM NaCl, 1 mM NaH2PO4, 8 mM Na2HPO4, 250 mM sucrose, 190 μg/ml digitonin). After 5 min on ice, the cells were spun for 5 min at 14,000 rpm at 4°C in a microcentrifuge. Supernatants

were transferred to fresh tubes and the pellets were resuspended in buffer containing 25 mM Tris-HCl, pH 8.0, and 1% Triton X-100. Equal amount of proteins from each sample were subjected to sodium dodecylsulfate-polyacrylamide gel electrophoresis (SDS-PAGE) and western immunoblot assay as described before [56].

Size exclusion column chromatography (SEC) for monitoring apoptosome and DISC formation

For analysis of apoptosome assembly and death inducing signaling complex (DISC) assembly, cell extracts prepared from the treated cells were subjected to SEC following the procedure described earlier [56]. Briefly, 0.9-2 mg cell extract was loaded onto a Superose 6 HR (10/30) column (Amersham pharmacia biotech, Uppsala, Sweden) and 0.5 ml fractions were collected at a flow rate of 0.2 ml/min. Proteins in the fractions were analyzed by western blot analysis. The column was calibrated with calibration kits that included thyroglobulin (669 kDa), ferritin (440 kDa), catalase (232 kDa), and aldolase (158 kDa).

Preparation of cell extract and cell free system

After harvesting, the cells were washed twice with ice-cold PBS, resuspended in buffer consists of (20 mM HEPES-KOH, pH 7.5, 0.5 mM EDTA, 0.5 mM EGTA, 10 mM KCl, 1mM β-merceptoethanol, 0.1 mM PMSF, 10 μg/ml leupeptin, 5 μg/ml pepstatin A, 2 μg/ml aprotinin, 25 μg/ml ALLN) and dounce-homogenized with 40-50 strokes. Then the

supernatant was obtained by centrifuging at 13000 rpm for 1 h and used immediately.

In vitro apoptosis was induced by incubating the prepared HeLa cell extract (100 μg) with 1 mM dATP and 1- 10 μM cytochrome c in buffer containing 20 mM HEPES-NaoH, pH 7.0, 20 mM NaCl, 1 mM EDTA, 1mM EGTA, 1.5 mM $MgCl_2$, 10 mM DTT for the indicated time period at 30˚ C. The reaction mixture was then resolved with 12-15 % SDS-PAGE and subjected to western blot analysis.

Construction and purification of caspases

The human caspase-8 and caspase-8 double mutants were cloned in bacterial expression pET15b vectors (Novagen), and to generate the mutant version of caspase-8 (DM), point mutations were done using DpnI mediated site directed mutagenesis (New England Biolabs) by PCR. The primers used for double mutant are: D374A (sense 5′-ATACCTGTTGAGACTGCTTCAGAGGAGCAA -3′, anti-sense 5′-TTGCTCCTCTGAAGCAGTCTCAACAGGTAT -3′) and D384A (sense 5′- TATTTAGAAATGGCTTTATCATCACCTCAA -3′, anti-sense 5′- TTGAGGTGATGATAAAGCCATTTCTAAATA -3′). The underlined sequences refer to incorporated alanine sequence in each case. The mutated plasmid was confirmed by sequencing both strands. Then the recombinant caspase was expressed in BL21 pLys *Escherichia coli* strain as N-terminal histidine tag. Protein was purified by two successive chromatographic procedures. Initially, bacterial cell lysates from 2 L

culture were prepared by sonication and centrifugation 20000 rpm for 1 h in lysis buffer (20 mM Tris-HCl, pH 8.0, 10 mM NaCl, 0.1 mM PMSF, 0.1 mM EDTA, 1 mM DTT). The supernatant was loaded onto a Ni^{2+}-NTA column (Qiagen). The column was washed with two column volume of washing buffer (20 mM Tris-HCl, pH 8.0, 10 mM NaCl, 1 mM beta-ME, 10 % glycerol) and eluted with elution buffer (20 mM Tris-HCl, pH 8.0, 10 mM NaCl, 1 mM beta-ME, 10 % glycerol and 250 mM imidazole). The active fractions were then loaded onto a HiTrapQ sepharose column (Amersham Pharmacia Biotech) equilibrated with equilibration buffer (20 mM HEPES-NaOH, pH 7.5, 10 mM NaCl, 0.1 mM EDTA, 1 mM DTT, 10 % glycerol). The protein was then eluted with 1-400 mM NaCl gradient. The concentration of the purified protein was then measured and aliquots were saved at -80˚ C before use.

The caspase assay was performed by using fluorogenic substrate Ac-IETD-amc at 30˚ C by monitoring the release of amc at excitation and emission wavelengths of 360 nm and 480 nm respectively, with a micro plate spectrofluorometer (Spectramax Gemini, Molecular Devices). The catalytic parameters were calculated using Michaelis-Menten equation:

$$V_0 = \frac{V_{\max}[S]}{(K_M + [S])} \quad \text{..... (1)}$$

$$V_{\max} = k_{cat} \,.\, [\mathrm{E}]_{\mathrm{T}} \quad \text{..... (2)}$$

Where, V_0 is the initial velocity, [S] is substrate concentration, and $[\mathrm{E}]_{\mathrm{T}}$ is the total amount of enzyme used in the reaction.

II-3. RESULTS

Single treatment of Aβ42 induce limited activation of caspase-3, -8, and -9

Although many reports including ours indicate the involvement of apoptosis and accompanying caspase activation in Aβ-induced cell death [72-75, 83], we have often observed low activities of caspases as shown in Fig. 1. We evaluated the activity of caspase-3, -8 and -9 which participate in intrinsic and extrinsic pathways, two major caspase dependent apoptotic processes. The activity was measured using 3 different synthetic substrates (DEVD-AMC, IETD-AMC, and LEHD-AMC) for each caspase. The cells were incubated with up to 40 μM of Aβ42 for as long as 48 h (Fig. 1). In the investigation, we employed human epithelial HeLa cells which showed relatively higher caspase activity than other cell lines such as human neuroblastoma SH-SY5Y cells in which death occurred too easily with Aβ treatment and the levels of activated caspase were often inconsistent (data not shown). And oligomeric preparation of Aβ42 was mainly used for the experiments instead of monomeric or fibrillar peptide, otherwise indicated, because it was reported in earlier studies and our laboratory to be superior to the monomer or fibrillar form in inducing caspase activity and cell death [19, 71].

Some levels of caspase activities with the synthetic substrates were detected in Aβ42-treated cells, especially in 48 h-incubation samples (Fig. 1A-1C). However, we are not convinced that this was derived from Aβ42-induced damage, because no Aβ42-concentration dependency of the activity was observed and the activity could be due to the background activities which might be increased by cell division during the treatment time. It is also possible that the serum deprivation of the cells before Aβ42 treatment may cause the increase of background activity. Thus, it is questionable whether the activity is due to Aβ42 or to

other unknown factors. Furthermore, the activity levels were lesser by several times than those induced by other damaging agent such as STS [83].

The caspase activation was further explored in the Aβ42-treated cells, using the immunoblot assay. Cleaved fragments (see Fig. 2) were expected to be seen for each caspase if it is activated. No such fragments were detected in the immunoblotting assay (Fig. 1D). DFF45 and Bid, substrates of caspase-3 and -8 respectively, were not reduced, either (Fig. 1D). Altogether, there is no evidence to support the activation of caspase in the cells treated with Aβ42 under the experimental condition used above.

Aβ42 cytotoxicity was examined to confirm the low level of caspase activation is not due to a possible problem of the peptide preparation. The cell death was mainly assessed by the MTT [52]. However, soluble Aβ can lead to a decrease in MTT formazan production in the absence of overt cell death when cells are incubated for longer time. Thus, alamarBlue assay was also performed to complement the cell death experiments [63]. MTT formazan was reduced in 24-h and 48-h incubation samples in an Aβ42-dose dependent manner (Fig. 1E). AlamarBlue reduction was consistently observed in the 48-h sample, although the levels were less than those of MTT assay (Fig. 1E). These results indicate that cell death occurred in the 24 and 48 h samples. Thus, we concluded that Aβ42 used here was cytotoxic. On the other hand, it is questionable if cell death occurred in 12-h samples which showed decrease of the MTT formazan, but no Aβ42-dose dependency. Furthermore, the levels of cell death in the sample were barely decreased in the alamarBlue assay.

Previously, it was reported that Aβ fibrils induced extrinsic apoptosis which results in activation of caspase-8 and subsequently, caspase-3 [75]. In the current study, the caspase-3-like DEVDase activity was not detected in fibrillar Aβ42-treated cells (Fig. 1A). MTT formazan were reduced in cells treated with the fibrillar form of Aβ42, but it was

not Aβ42-dose dependent (Fig. 1E). It seems that non-specific reduction of MTT formazan caused the ambiguous results. In alamarBlue assay for the same samples, Aβ-dose-dependent reduction was clearly seen, suggesting that Aβ42-dose dependent cell death occurred. Altogether, these data indicate that the fibrillary form of Aβ42 led to cell death in which caspase-dependent apoptosis plays little role.

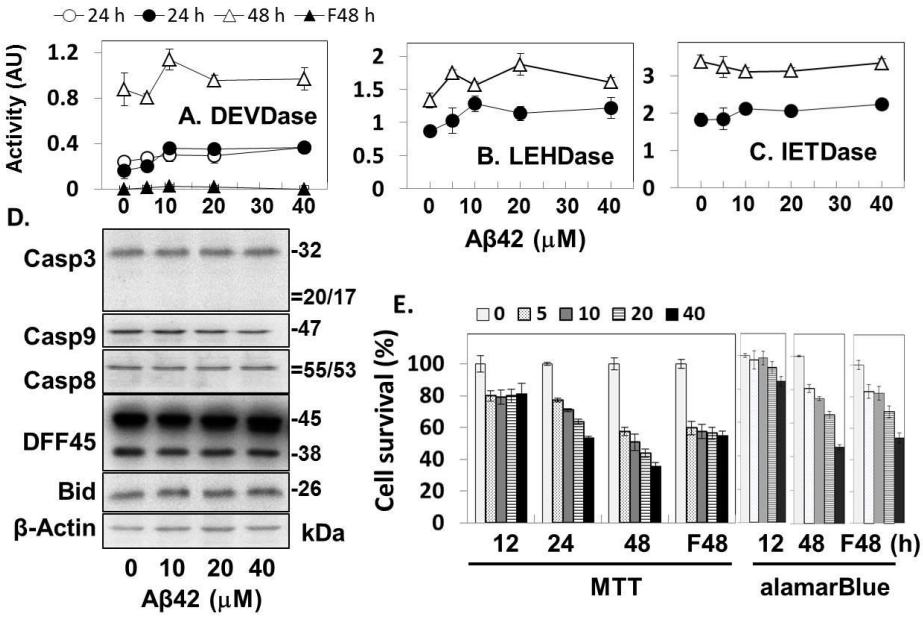

Fig. 1. Effects of single treatment of $A\beta_{42}$ oligomeric species on activation of caspases, processing of caspases and its substrates and cell death in HeLa cells. (**A-C**)Cells ($2x10^4$ /100 μl of culture media) were treated with oligomerized $A\beta_{42}$ at the indicated concentrations and time. The activities of Caspases – 3, -9 and -8 of the cell extracts were measured with their respective synthetic substrates (10 μM DEVD-AMC for caspase-3, 50 μM LEHD-AMC for caspase-9 and 50 μM IETD-AMC for caspase-8). (**D**) Immunoblot analysis of caspase and its substrates. HeLa cells ($2x10^4$ cells/100ul of culture media) treated with oligomeric $A\beta_{42}$ for 48 h at the indicated concentrations. Total cell extracts were prepared and assessed for processing of caspase-3, -9, -8 and its substrates DFF45 and Bid. Actin was employed as loading control. (**E**) to check the effect of $A\beta_{42}$ oligomeric and fibrillar species of cytotoxicity, HeLa cells were plated at a density of $2x10^4$ cells per well and treated with oligomeric and fibrillar $A\beta_{42}$ at the indicated concentration and time point, cell viability was measured by MTT reduction assay and alamrBlue assay.

Double treatment of Aβ induces potent caspase activation.

Next, we sought conditions under which caspases are potently activated and then probed apoptosis pathways accompanying caspase activation under the condition in Aβ42-treated cells. To find those conditions, we tested "double treatment" method in which Aβ42 peptide was sequentially administered to cells twice, referring to a report that nucleation-dependent polymerization is essential for Aβ-mediated cell death [87, 88]. We inferred that the polymerization could give differential or stronger signal to activate caspase. In the previous study, cells were treated with fibrillar form of Aβ42 for 1 h and followed by the treatment of soluble Aβ42. Here we use only soluble oligomeric Aβ42 to facilitate the quantitation of peptide amount and the pretreatment time was determined after testing different time points. Based on the time points tested, cells were initially treated for 2 h with the indicated concentration of oligomeric Aβ42 which then was removed at the end of incubation and subsequently, were further incubated with new preparation of oligomeric Aβ42 peptide at the same concentration for 10 (2+10 h sample), 22 h (2+22 h), 34 h (2+34 h) or 46 h (2+46 h sample).

The 2+22 h and longer incubation samples showed caspase-3-like DEVDase activity in an Aβ42-dose dependent manner (Fig. 2A). ~20 kDa processed fragment of caspase-3 was detected in the 2+22 h and 2+34 h samples treated with the high concentrations of Aβ42, and fully processed ~17 kDa fragment additionally recognized in the 2+46 h samples (Fig. 2D). Although the intensity of processed fragment was strongest in 2+34 h and additional ~17 kDa is present in 2+46 h samples (Fig. 2D), those DEVDase activities were similar with that of 2+22 h sample (Fig. 2A), indicating that correlation of the activity and the processed fragments is not clear. The product fragment of or decrease of DFF45, substrates of caspase-3, were seen (Fig. 2D), confirming the catalytic activation of caspase-3.

Caspase-9-like LEHDase activity was the greatest in the 2+22 h

sample in which also showed Aβ42-dose dependency, and it was decreased in the longer incubation samples (Fig. 2B). Procaspase-9 decrease was clearly shown in 2+22 h or the longer incubation samples treated with the high Aβ42 doses (Fig. 2D). Although ~35/37 kDa cleaved products were barely seen for the enzyme, the fragments were recognized in the analysis of apoptosome (see Fig. 3C). Moreover, the processing of procaspase-3, the substrate of caspase-9, (Fig. 2D) implies catalytic activation of caspase-9. Altogether, these data support activation of caspase-9.

Caspase-8-like IETDase activity was the highest in the same 2+22 h sample, but the correlation of Aβ42-dose and the activity was weak (Fig. 2C). Procaspase-8 was processed in 2+22 h or later samples, but two different types of fragments are observed (Fig. 2D). In 2+22 h samples, ~30 kDa fragment (p30) was mainly detected, while typical 41/43 kDa fragments (p41/43) were recognized in 2+46 h samples. p30 is a fragment of procaspase-8 lacking the prodomain, while p41/43 contains the prodomain and the large domain that becomes large subunit when caspase-8 is fully matured [89]. Thus, the cleavage sites to form the two different fragments are distinct [89]. We further characterized the fragments in the following exploration (see below). The immunoblot signal intensity of Bid, substrate of caspase-8, was rather consistent regardless of the incubation time and dose of Aβ42. Thus, it seems that the catalytic activation of caspase was uncertain in the samples, although a part of it is processed into two different types of fragments.

For a reference for the cytotoxicity of Aβ42 peptide preparation, cell death was assessed in the double treatment samples. All showed Aβ42-dose dependent cell death evaluated by the two methods (Fig. 2E). The levels of cell death evaluated by MTT formazan reduction were generally more than those of alamarBlue assay (2+22 h and 2+46 h samples of MTT vs those of alamarBlue) as in the single treatment samples (Fig. 1E). Reduction of the values was slightly higher in the double treatment sample than in the equivalent single treatment sample

(i.e. 2+22 h vs 24 h). Roughly speaking, we could not detect prominent differences in the single and double treatment samples in induction of cell death.

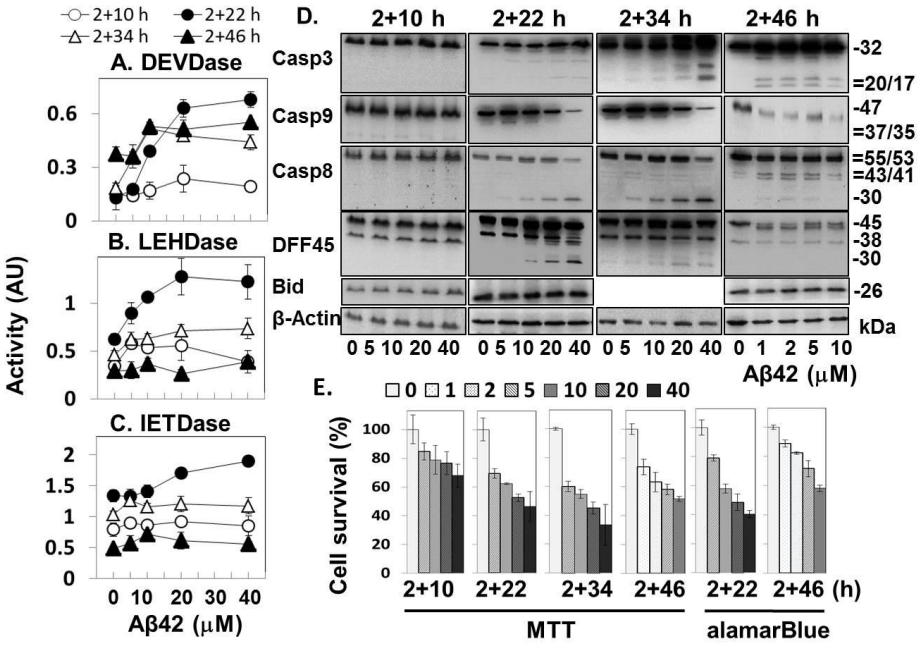

Fig. 2. Effects of double treatment of $A\beta_{42}$ oligomeric species on activation and processing of caspases and its substrates, and cell death in HeLa cells. (**A-C**)Cells ($2x10^4$ /100 μl of culture media) were treated with oligomerized $A\beta_{42}$ at the indicated concentrations and time. The activities of Caspases – 3, -9 and -8 of the cell extracts were measured with their respective synthetic substrates (10 μM DEVD-AMC for caspase-3, 50 μM LEHD-AMC for caspase-9 and 50 μM IETD-AMC for caspase-8). **(D)** Total cell extract were prepared and assessed for processing of caspase-3, -9, -8 and its substrates DFF45 and Bid by western

blotting. HeLa cells were treated for 2+10h but no caspases and its substrates were found to be processed. In case of 2+22h double treatment, caspase-9, -3 and the substrate for caspase-3, DFF45 were processed. Caspase -8 was found to be processed in a unique manner, only p30 processed fraction was observed but neither the p43/41 nor the p18/12 fractions were observed and the substrate Bid was not processed, p30 fraction may be the intermediate stage of caspase-8 processing as longer period double treatment resulted in the formation of the other fractions. With longer period of incubation 2+34h and 2+46h the cleavage of caspase-3, -9, -8 and the substrate of caspase-3 DFF45 was more prominent but Bid was not cleaved even with 2+46h incubation. (**E**) To check the effect of $A\beta_{42}$ oligomeric species of cytotoxicity HeLa cells were plated at a density of $2x10^4$ cells per well and treated with oligomeric $A\beta_{42}$ at the indicated concentration and time point, cell viability was measured by MTT reduction assay and alamarBlue assay.

Cytochrome c release from the mitochondria and formation of the Apaf-1 apoptosome

On the basis of catalytic activity and processing of caspase, it was concluded that intrinsic apoptosis pathway was activated in the Aβ42-doubly treated cells. To confirm activation of the pathway cytochrome c release from the mitochondria were probed in the 2+22 h samples which showed potent activation and processing of caspase-3 and reduction of procaspase-9 (Fig. 2A-D). Cytochrome c was detected in the samples treated with 20 and 40 μM Aβ42, indicating the release (Fig. 3A). Next, formation of apoptosome, a hallmark of the intrinsic pathway, was examined in the 2+22 h samples treated with 20 μM Aβ42. Apaf-1 and caspase-9 were recognized only in the later fractions (>#25) in the analysis of the control sample prepared from Aβ42-non-treated cells by SEC (Fig. 3B), while those proteins were detected in the earlier fractions (~#15-#23) in the 2+22 h sample (Fig. 3C). These data clearly indicate the formation of apoptosome in the sample. It is noted that 35/37 kDa fragments of caspase-9 which were not detected above (Fig. 2D) were seen in the western blotting analysis followed by SEC (Fig. 3C). It was recognized in this experiment probably because the protein was concentrated during the chromatography.

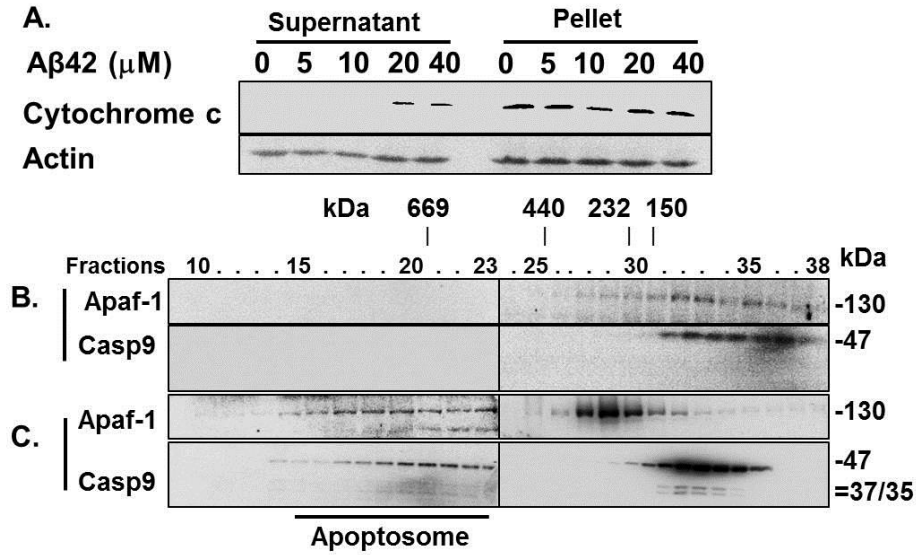

Fig. 3. Double treatment of $A\beta_{42}$ oligomeric species induce cytochrome c realese and the formation of Apaf-1 apoptososme in HeLa cells. (**A**) After HeLa cells were treated with oligomerized $A\beta_{42}$ at the indicated concentrations for 2+22h and the release of cytochrome c was assessed by immunoblot analysis. Supernatant and pellet in cytochrome c release indicate soluble and precipitated parts of the cell extracts respectively. Actin was loaded as loading control. (**B** and **C**) HeLa cells were incubated without or with 20μM oligomerized $A\beta_{42}$ for 2+22h. The extract prepared from the cells (0.8 ~ 1.0 mg) was fractionated by gel filtration chromatography. The fractions were analyzed by immunobloting for Apaf-1 and caspase -9. The standard molecular markers are indicated above the scale with elution fractions.

DISC is not formed in Aβ42-treated cells

The formation of DISC was also probed. Caspase-8 and FADD proteins were detected only in the later fractions (>#22) in the analysis of the control cells by SEC, while ~#14-#21 fractions contained the two proteins in a positive control sample prepared from cells treated with actinomycin-D followed by TNF-α (Fig. 4A and 4B), confirming the formation of DISC. The two proteins were detected in the later fractions (>#22) in the 2+22 h and 2+46 h samples treated with 20 μM Aβ42 (Fig. 4C and 4D). Based on the data, we concluded that DISC was not formed in those samples. However, processed fragment of caspase-8 was recognized. In the 2+22 h sample p30 was seen (Fig. 4C), while p41/43 was also detected in the 2+46 h sample (Fig. 4D). These data indicate that formation of p30 fragment of caspase-8 precedes that of p41/43 fragment, consistent with those of Fig. 2D,

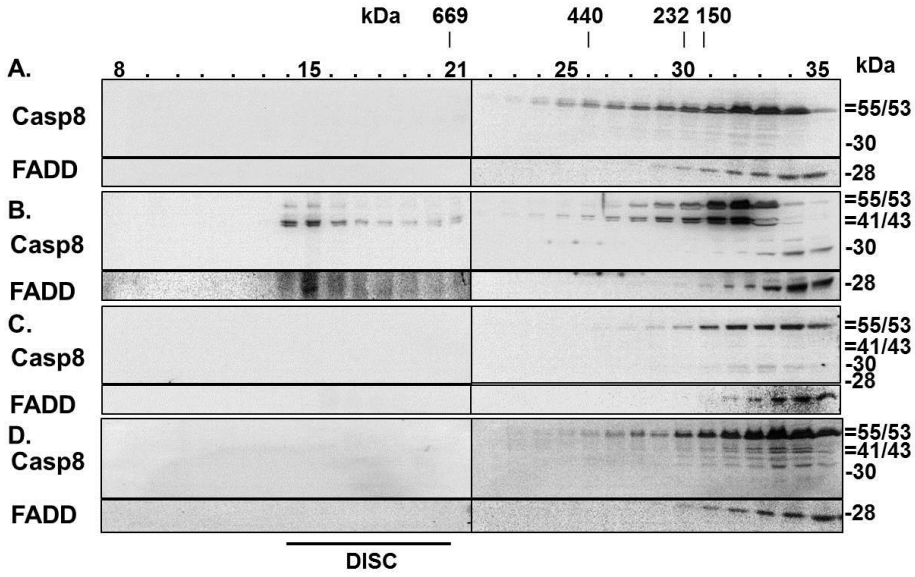

Fig. 4. Effects of $A\beta_{42}$ oligomeric species double treatment DISC assembly in HeLa cells. (A, C and **D**) HeLa cells were incubated without or with 40 μM oligomeric $A\beta_{42}$ for 2+22h and 2+46h respectively, cell extracts prepared from cells (1.0 ~ 1.2 mg) were fractionated by gel filtration chromatography. The fractions were analyzed by immunobloting for caspase-8 and FADD. Only p30 processed fraction was observed but neither the p43/41 nor the p18/12 fractions were observed, p30 fraction may be the intermediate stage of caspase-8 processing as longer period (2+46h) double treatment resulted in the formation of the other fractions. FADD was not detected in any time point with $A\beta_{42}$ treated cell extract. (**B**) HeLa cells were treated with 100ug/ml of Actinomycin D for 2h and then treated with 50nM of TNFα for 24hr. Cell extracts prepared from cells (1.0 ~ 1.2 mg) were fractionated by gel filtration chromatography. The fractions were analyzed by immunobloting for caspase-8 and FADD. Processed caspase-8 and FADD was detected in the earlier fractions which indicate the formation of DISC.

p30 and p41/43 fragments of caspase-8 fragment is formed by caspase-3 and -6.

Because DISC was not formed in the 2+22 samples, we considered intrinsic apoptotic pathway for the induction of formation of the caspase-8 fragments, because caspase-3 and -6 activated in the pathway are also known to induce the fragmentation [90, 91]. The intrinsic apoptosis process was reconstituted in a cell-free experiment in which cell extracts was incubated with dATP and cytochrome c that results in formation of the Apaf-1 apoptosome [52]. As expected, caspase-8 and its substrate Bid was processed, but only p41/43 were detected (the second lane of Fig. 5A). The p30 fragment was seen in the following experiments in which lower dose of cytochrome c was used and caspase-8 processing was not complete (see lanes 3-7 of Fig. 5A), implying that p30 might exist only in the early stage of apoptosis, consistent with the results of Fig. 2D. The apoptosome is a sort of holoenzyme of caspase-9 that leads to activation of caspase-3 and subsequently caspase-6 [92]. Purified caspase-3 could induce the formation of the p30 fragments (Fig. 5B), while caspase-6 induced only the formation of p41/43 fragments (Fig. 5C). Although physiological implication of the differential activity of the two caspases on caspase-8 processing remained to be pursued, they clearly showed that the fragmentation process of caspase-8 could occur through the intrinsic apoptotic pathway.

The levels of Bid were rather consistent under the condition in which caspase-8 was not completely processed (Fig. 5A-C). In fact, the condition seems to better reflect the real situation of samples shown in Fig. 2D, considering the level of Bid and processed caspase-8. Bid processing is essential to strengthen the apoptotic signal in type II cells. It can be hypothesized that the low levels of caspase activation in Aβ42-treated cells may be attributed to the weak activation of the amplification loop.

For a reference, we determined catalytic activity of p30 for Bid. It was assessed by using prodomainless caspase-8 double mutant mimicking p30 (DM, see "Materials and methods", [93]). We also estimated the catalytic activity of enzymes containing p41/43 using enzymes containing the prodomainless equivalent of p41/43 (p18-10) for comparison (Fig. 6A). p18-10 could process procaspase-3 and Bid in the cell extracts as expected, while DM was inefficient in the process (Fig. 6B and 6C). Purified Bid was also cleaved by p18-10 to produce the products (Fig. 6D) which was not detected in the cell-free experiments (Fig. 6C). Consistently, DM could not cleave the purified Bid. k_{cat} of DM was ~800-fold lower than that of p18-10, indicating that the lower activity of DM is due to the slower catalytic velocity (Fig. 6E), consistent with the previous reports [93].

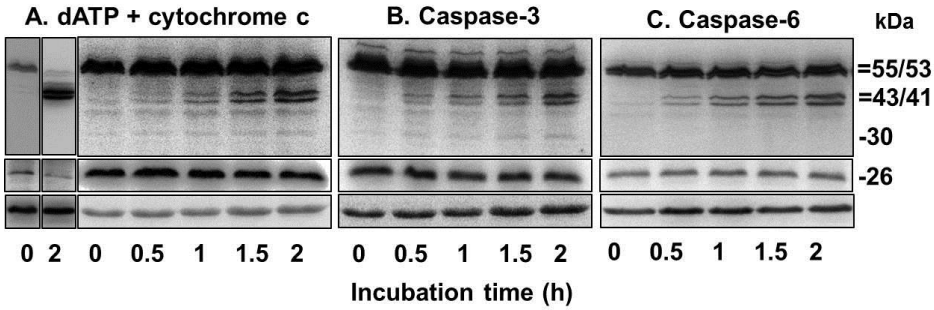

Fig. 5. Caspase-8 is processed by intrinsic apoptotic pathway. To find out the mechanism of caspase-8 processing **(A)** HeLa cell extract was prepared and incubated with cytochrome-c and dATP for the indicated time and immunoblotted for caspase-8 and bid cleavage. It was found that caspase-8 and bid were cleaved in case of high concentration of cytochrome-c (10 μM) (lane-2), but in case of 1 μM of cytochrome-c bid was not processed into truncated bid. Actin was employed as loading control. **(B** and **C)** HeLa cell extract was incubated with purified recombinant active caspase-3 and caspase-6 for indicated time period and probed for caspase-8 and bid processing by western blot. p30 fragment of caspase-8 was found only in the case of in vitro apoptosis and caspase-3 mediated cleavage. Actin was employed as loading control.

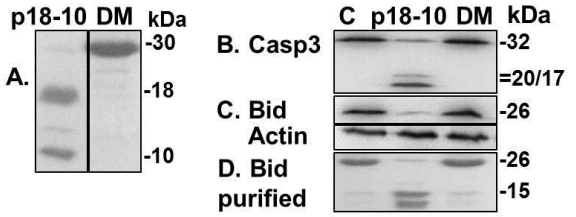

E.

Enzyme	p18-10	DM
K_M (mM)	29.86	28.78
k_{cat} s^{-1}	0.08	0.000098
k_{cat}/K_M ($M^{-1}S^{-1}$)	2680	3.4

Fig. 6. p30 fragment of Caspase-8 is not active but p18 and p12 fragments are active. (A) Recombinant active caspase-8 and caspase-8 double mutant (DM) was purified as described in the materials and method section and run for SDS-PAGE. Lane 1 purified active caspase-8 and lane 2 caspase-8 double mutant. **(B** and **C)** Procaspase-3 and bid processing by wild type caspase-8 and caspase-8 (DM) were checked.70 μg of HeLa cell extracts were incubated with 30 ng of wild type caspase-8 and caspase-8 (DM) for 1 h at 30˚C and the reaction mix was probed for procaspase-3 and bid processing by western blot. Actin was employed as loading control. **(D)** Effect of wild type caspase-8 and caspase-8 (DM) on purified recombinant bid processing. 1 μg of purified bid was incubated with equal amount of (30 ng) wild type and double mutant caspase-8 and incubated for 1 h at 30˚C. The reaction mix was separated by SDS gel electrophoresis. In all **(B, C** and **D)** cases caspase-8 (DM) was found to be inactive. **(E)** Catalytic parameters of purified recombinant wild type and DM caspase-8.

II-4. DISCUSSION

Previously we found that Aβ42 could suppress an apoptosis pathway by interacting with procaspase-9 [52]. However, accumulating data has implicated apoptotic process as a mechanistic feature of the cell death induced by Aβ42 [78, 94]. Although significant progress has been made in understanding the apoptotic pathway related with Aβ42 through extensive studies over decades, cytotoxic properties of Aβ42 and its mechanistic features have been difficult to assess because of variability in culture systems and methods associated with Aβ42 preparation and treatment [24]. In the current study, we sought a condition in which caspases are activated and explored the involvement of apoptosis pathways under the condition. We employed two different treatment ways with the peptide. In the cells treated with Aβ42 “once”, cell death evaluated by MTT and alamarBlue assay occurred in a dose-dependent manner (Fig. 1E). Cells treated with the peptide “twice” showed the similar levels of cell death. This result is inconsistent with the previous report showing that the double treatment of Aβ42 which leads to polymerization of the peptide was necessary to elicit the cell death [88]. Many reports including the present study, however, showed that the single treatment was sufficient to induce cell death.

Caspase activity was detected in the cells treated once with Aβ42 previously [72, 75]. Here, the activity was also detected in the cells singly treated with the peptide (Fig. 1A-C). However, Aβ42-dose-dependency was not seen and furthermore, the processed fragments of caspase were not detected (Fig. 1D). Actually, detection of processed fragment of caspase might not be absolute necessity to prove the activation of the enzyme, because undetectable amount of activated caspase can produce the catalytic activity evaluated with the synthetic substrates (data not shown). Thus, we think that a certain level of caspase activation occurred in the single-treatment sample, although it is questionable whether all

activity is elicited only by Aβ42. A part of the activation could be elicited by other factors. Moreover, we showed previously that apoptosome was not formed in Aβ42-treated cells, which was due to interaction of the peptide with procaspase-9 [52]. We conclude that caspase activation is not potent in the cells singly treated with Aβ42 and the single treatment was not adequate for the purpose of the current study to probe apoptotic pathway leading to caspase activation in Aβ42-treated cells.

The activation of caspase was clearer in cells doubly treated with Aβ42 (Fig. 2A-D). Aβ42-dose dependency was evidently seen and the processed fragments of caspase were detected. The Apaf-1 apoptosome was also formed in Aβ42-doubly treated cells (Fig. 3B), implying that Aβ42 induced the intrinsic pathway in cells. The suppressive effect of Aβ42 on the formation of apoptosome [52] seems to be overcome in the doubly treated cells. Although the mechanism for the necessity of double treatment of Aβ42 to induce robust activation of caspase is not understood yet, polymerization of the peptide [95] is likely to give a strong signal to activate the apoptotic pathway and related caspases.

Previously, Aβ42 fibrils could elicit the extrinsic apoptosis pathway which leads to activation of caspase-8 [75]. In the current study, we failed to detect any activation of caspase in cells treated with Aβ42 fibrils (Fig. 1D), although cell death occurred (Fig. 1E). Again the single treatment of Aβ42 was not efficient in inducing caspase activation regardless of the peptide's form. Fragmentation of caspase-8 to 30 kDa and 41/43 kDa was recognized in the cells doubly treated with Aβ42 oligomeric forms (Fig. 2D). The p41/43 is generally detected in the extrinsic apoptosis process by formation of DISC [96, 97]. But the protein complex was not observed in the cells, implying that p41/43 fragment may be formed by other pathway (Fig. 4C). The fragment can also be produced by the catalytic activity of caspase-3 and -6 [90, 92] that can be processed by the intrinsic pathway. Indeed, the generation of p41/43 was demonstrated in the cell-free experiment in which the intrinsic pathway was reconstituted by addition of dATP and cytochrome

c to the cell extracts (Fig. 5A). The direct addition of purified caspase-3 and -6 to the cell extracts also leads to the fragment production (Fig. 5B and 5C), further supporting the possibility that the intrinsic pathway is responsible for production of caspase-8 fragments.

Here we recognized p30 fragment of caspase-8 formation in Aβ42-treated cells. The caspase-8 fragment p30 was rarely shown in the previous reports. It was generated in cells treated with CD95 by formation of DISC and following autocatalytic process and was further processed to p18 and p10 fragments [89]. Here we firstly showed that p30 was formed in the cells doubly treated with Aβ42 without formation of DISC (Fig. 4C and 4D). It could be produced in the cell-free assay that reconstituted the intrinsic pathway (Fig. 5A and 5B), giving a potential role of the pathway in generation of the fragment. It is also intriguing that p30 fragment was produced only by caspase-3, not by caspase-6 in the cell-free experiments (Fig. 5B and 5C). p30 was produced in earlier stage of the treatment before formation p41/43 fragments (Fig. 2D), consistent with the previous suggestion that p30 can sensitize cells toward death receptor-induced apoptosis [89].

The death signal can be amplified via Bid cleavage in type II cells such as HeLa cells used here [98]. Although p41/43 fragments were formed, its substrate Bid was not processed (Fig. 2D), indicating that the amplification loop was not operated in the Aβ42-treated sample. The levels of caspase activation even in the doubly treated samples was not as high as that that induced by other damaging agents such as STS (data not shown). The weak activation caspase in Aβ42-treated cells can be attributed to the lack of the amplification loop.

In conclusion, we show that intrinsic apoptosis and accompanying caspase activation could be induced by double treatment of Aβ42 to cells. The double treatment seems to be necessary to overcome the inhibitory effect of Aβ42 on the intrinsic pathway. In fact, it is difficult to imagine that neuronal cells are exposed to the Aβ42 just once. Thus, the experimental condition with double or more treatment of

the peptide to cells might be near to the physiological conditions. Hopefully, a full characterization of the nature of the multiple treatment and related cell death pathway will provide novel insight into Aβ-associated pathology and control of AD.

III. Interaction of caspase-6 with amyloid β

Abstract

Amyloid-β (Aβ), a major component of the extracellular senile plaques implicated in the neurodegenerative Alzheimer's disease (AD), elicits apoptosis. However, we previously showed the peptide could suppress formation of the Apaf-1 apoptosome, a key machinery of the intrinsic apoptosis pathway, by interacting with procaspase-9. Here, we screened other caspases for a potential interaction with Aβ42 by analysis of images produced by confocal microscope study. Caspase-6 was found to interact with the peptide. In a subsequent study using size-exclusion chromatography followed by western blot analysis, the two proteins were recovered in the same fractions. Moreover, casepase-6 contained in the fractions could immunoprecipitate concomitantly with Aβ42, giving another evidence for the interaction. Though, caspase-6 was catalytically activated in the Aβ42-treated cells, Lamin A/C and B the substrates of the enzyme were cleaved in a completely different fashion. The sizes of the cleaved fragments of lamin proteins in the Aβ42-treated cells indicated that the lamins seemed to be fragmented by enzyme(s) other than caspase-6, implying that the enzyme was not functionally active in the cells. We suggest that the interaction of caspase-6 and Aβ42 negatively affected the intracellular function of the enzyme.

III-1. INTRODUCTION

Amyloid β (Aβ) peptide is a major component of the extracellular senile plaques implicated in the neurodegenerative Alzheimer's disease (AD) [66]. The peptide is 36-43 amino acid-long and is generated by proteolytic cleavage of the amyloid precursor protein by α-, β- and γ- secretases [4, 67]. Aβ peptide is prone to change its conformation to β-sheet-rich intermediate structures that interact with each other to form soluble aggregates such as oligomers, protofibrils and subsequently insoluble fibrils [19, 68, 69]. The aggregated Aβ progressively accumulates in brain parenchyma and cerebral blood vessels [70]. However, the depositing fibrils was less toxic than the soluble Aβ oligomers and protofibrils, suggesting that the oligomeric aggregates would be the main neurotoxic factor for eliciting AD [19, 71].

The etiology of AD and the mechanistic features of cell death induced by Aβ are not clearly understood, but involvement of apoptosis in the process has been proposed [72-75]. Several apoptotic pathways have been characterized. Binding of death ligands to receptor leads to receptor-mediated apoptosis, or extrinsic apoptosis which is characterized by the formation of the death-inducing signaling complex (DISC) [76]. Caspase-8 is activated as a result of the apoptosis pathway [76, 77]. On the other hand, chemical-induced apoptosis or caspase-dependent intrinsic apoptosis is elicited by mitochondrial damage that results in the release of cytochrome c which associates with procaspase-9, dATP and an adaptor protein Apaf-1 to form a mutiprotein complex called apoptosome [75-77]. Apoptosome complex functions as a holoenzyme of caspase-9 that catalytically activates effector caspases such as caspase-3, -6 and -7 which are responsible for most of the cleavage events observed during apoptosis. The proposal on the involvement of apoptosis in Aβ-induced cell death is based on activation of apoptosis-related proteins such as caspases. Aβ can damage mitochondria leading to cytochrome c

release which can trigger formation of apoptosome and activation of caspases [78, 79]. On the other hand, binding of Aβ to death receptor can elicit the extrinsic apoptosis pathway so that caspase-8 is activated [45, 46].

Although a critical role of apoptosis in Aβ-induced cell death is evident, we recently found that Aβ42 could suppress the activation of the intrinsic apoptosis pathway [52]. The inhibitory effect of Aβ42 on the apoptotic pathway is associated with its interaction with procaspase-9 and consequent inhibition of Apaf-1 apoptosome assembly. Currently, ~15 different caspases have been found and they all share homologous amino acid sequences with each other. Thus, it is possible that Aβ42 might interact with other caspases and affect function of the caspases positively or negatively. In the current study, we made an attempt to recognize caspases that interact with Aβ42 and explore the potential effect of interaction on the apoptosis pathway.

III-2. MATERIALS AND METHODS

Materials

Fetal Bovine serum (FBS) was purchased from Life Technology Inc. (Grand Island, USA). Dulbecco's modified Eagles medium, high glucose (DMEM/HG) was obtained from Welgene (Daegu, Korea). Caspase-9, Caspase-8, Caspase-6 and Caspase-3 substrates, N-acetyl Leu-Glu-His-Asp-amino methyl coumarin (Ac-LEHD-AMC), Ac-IETD-AMC, Ac-VEID-AMC and Ac-DEVD-AMC, respectively, were from A.G. Scientific Inc. (San Diego, USA). Ni-NTA column were purchased from Amersham Biosciences (Piscataway, USA). Western blotting detection kit (WEST-ZOL PLUS) from iNtron Biotechnology (Gyeonggi-do, Korea). Phosphate buffer saline (PBS) purchased from Amresco (solon, USA). Monoclonal anti-Aβ antibody 6E10 was acquired from Signet Laboratories (Dedham, USA), anti-amyloid oligomer polyclonal antibody A11 from Cheimicon International (USA) anti-lamin-A/C, anti-lamin B and anti-β-actin from Santa Cruz Biotechnology (California, USA). Anti-caspase-6 antibody that can detect small domain of caspase-6 was from BD Pharmingen (CA, USA) (named as AbA). Anti-caspase-6 antibody that recognizes the large domain of the enzyme was from Abfrontier (Seoul, Korea) (named as AbB). Anti-caspase-6 antibody used for the immunoprecipitation study recognized the small domain of caspase-6 and was from Santa Cruz Biotechnology (CA, USA) (named as AbC).

Cell Culture

Human epithelial HeLa cells were cultured in DMEM (High glucose) medium supplemented with 10% (v/v) FBS and 100 units of penicillin and 100 μg/ml streptomycin at 37 °C under 5% CO_2. The cells were seeded at 2000 cell/100 μl of culture media and cultured for 24 h. Then, serum deprivation was carried out for another 12 h and treatment was done according to the mentioned time point.

Preparation of Aβ peptide

The purified peptide was solubilized in 100% 1,1,1,3,3,3,-hexafluoro-2-propanol, and dried under nitrogen flow and subsequently, under vacuum for 30 min. The peptide aliquots were stored at –20 °C until use. Immediately before use, the peptide was dissolved in 0.1% NH_4OH at a concentration of 2 mg/ml followed by bath sonication for 10 min. The solution was diluted at the desired concentration with cell culture media without FBS. Aβ42 oligomers were prepared as described earlier [86] with little modification. Briefly, peptides were diluted in cell culture media at 100 μM concentration, vortexed for 30 seconds and incubated at 4^oC for 12 h. The peptide solution then diluted to the desired concentrations.

Confocal microscopy

HeLa cells were seeded in 6 well plate at 70% confluency, cultured for 24h and further incubated for 12h in serum free media and

then treated without or with 20 μM Aβ42 for 12 h. Treated cells were fixed in methanol at -20 ^{o}C and permeabilized by 0.3% Triton X-100. After blocking with 0.1% BSA overnight, primary mouse anti-amyloid beta (6E10), rabbit anti caspase-2, goat anti caspase-4, -6, -7 and -8 antibodies were added to each samples and incubated overnight at 4°C. After washing with PBS, Alexa-Flour-488 conjugated chicken anti mouse IgG, FITC conjugated goat anti-rabbit and Alexa-Fluor-543 conjugated rabbit anti-goat IgG antibodies antibodies (dilution, 1:200) were treated for 2h at room temperature followed by PBS washing. Nuclei were stained with Hoechst and confocal images were obtained with Carl Zeiss LSM510 microscope (Jena, Germany) using vendor provided software (LSM 510).

Size exclusion column chromatography (SEC) for monitoring protein-protein interaction

For analysis of interaction of capsae-6 with $A\beta_{42}$, cell extracts prepared from the treated cells were subjected to SEC following the procedure described earlier [56]. Briefly, 0.9-2 mg cell extract was loaded onto a Superose 6 HR (10/30) column (Amersham pharmacia biotech, Uppsala, Sweden) and 0.5 ml fractions were collected at a flow rate of 0.2 ml/min. Proteins in the fractions were analyzed by western blot analysis. For checking the interaction of $A\beta_{42}$ with caspase-6 in the cell free system, HeLa cell extracts was prepared (1 mg) and incubated with freshly prepared 20 μM of purified $A\beta_{42}$ at 37˚ C for 2 h and the reaction

mixture was separated by SEC and analyzed by western blot.

Interaction of purified caspase-6 (active) with Aβ42 was also analyzed by SEC. 10 μg of each protein incubated with or without 20 μM Aβ42 for 1 h at 30°C was fractionated as above and the collected fractions were analyzed by immunoblot analysis for caspase-6 and Aβ. In both cases, the column was calibrated with calibration kits that included thyroglobulin (669 kDa), ferritin (440 kDa), catalase (232 kDa), and aldolase (158 kDa).

Immunoprecipitation

After size exclusion chromatography, the desired fractions were pooled together and protein concentration was measured. Then the indicated antibodies were added to 100-500 μg of protein (final volume 1 ml) and incubated at 4˚ C overnight with rotor agitation. Next, 40 μl of protein A sepharose beads (Amersham Biosciences, Uppsala, Sweden) were added to each sample and incubated at 4˚ C for 2 h. Beads were precipitated by centrifuging at 13000 rpm at 4˚ C for 5 min and washed 3 times with PBS. 15 μl 2X SDS gel loading buffer was added to the beads, boiled for 5 min and centrifuged at 13000 rpm for 10 min. The obtained supernatants were then analyzed by SDS-PAGE and immunoblotting.

For purified caspase-9 and wild type $A\beta_{42}$, 10 μg of purified active caspase-6 was incubated with 20 μM of $A\beta_{42}$ for 2 h at 30˚ C. Then the antibodies were added to the reaction mixture and kept at 4˚ C for

overnight and analyzed by SDS-PAGE and analyzed by western blot analysis.

Measurement of Caspase activity

Caspase activity was measured as described earlier [56]. Briefly, treated cells were washed twice with ice-cold phosphate-buffer saline (PBS). Then, 40 μl of buffer containing 20 mM HEPES-NaOH, pH 7.0, 1mM EDTA, 1mM EGTA, 20mM NaCl, 0.25% Triton X-100, 1mM dithiothreitol (DTT), 1mM phenylmethanesulphonylchloride (PMSF), 10 μg/ml leupeptin, 5 μg/ml pepstatin A, 2 μg/ml aprotinin, 25 μg/ml ALLN was added into each well and incubated on ice for 20 min. Caspase assay buffer (final 20mM HEPES-NaOH, pH 7.0, 20mM NaCl, 1.5 mM $MgCl_2$, 1mM EDTA, 1mM EGTA and 10mM DTT) was added and the release of AMC was monitored for 2h in 2 minute interval with respective caspase substrates at excitation and emission wavelengths of 360 nm and 480 nm respectively, using microplate sepectrofluorometer (Molecular Devices, CA, USA). The results were expressed as a slope of total readings versus time.

Western blotting

Cells were harvested, washed with ice-cold PBS for at least twice and resuspended in lysis buffer B (50 mM Tris-HCL, pH 8.0, 150 mM NaCl, 1% Triton X-100, 5mM EDTA, 5mM EGTA, 1mM PMSF, 10 μg/ml leupeptin, 2 μg/ml pepstatin A and 2 μg/m aprotinin) for 20 min on

ice. The extract was obtained by centrifugation at 13,000 rpm at 4^{o}C for 30 min. The amount of protein was measured through Bradford assay. Equal amounts of proteins were separated on 12–15 % SDS-PAGE and transferred on to a PVDF membrane. The membrane was immunoprobed with primary antibodies and horseradish peroxidase-conjugated secondary antibodies. The blots were visualized using West-Zol plus reagent (iNtron Biotechnology Inc., Seoul, Korea) in Chemiluminescent detection system (Supernova 1800).

Purification of caspase-6

The human caspase-6 was cloned in bacterial expression pET28b vectors (Novagen). Then the recombinant caspase was expressed in BL21 pLys *Escherichia coli* strain as N-terminal histidine tag. Protein was purified by two successive chromatographic procedures. Initially, bacterial cell lysates from 2 L culture were prepared by sonication and centrifugation 20000 rpm for 1 h in lysis buffer (20 mM Tris-HCl, pH 8.0, 10 mM NaCl, 0.1 mM PMSF, 0.1 mM EDTA, 1 mM DTT). The supernatant was loaded onto a Ni^{2+}-NTA column (Qiagen). The column was washed with two column volume of washing buffer (20 mM Tris-HCl, pH 8.0, 10 mM NaCl, 1 mM beta-ME, 10 % glycerol) and eluted with elution buffer (20 mM Tris-HCl, pH 8.0, 10 mM NaCl, 1 mM beta-ME, 10 % glycerol and 250 mM imidazole). The active fractions were then loaded onto a HiTrapQ sepharose column (Amersham Pharmacia Biotech) equilibrated with equilibration buffer (20 mM HEPES-NaOH, pH 7.5, 10 mM NaCl, 0.1 mM EDTA, 1 mM DTT, 10 % glycerol). The

protein was then eluted with 1-400 mM NaCl gradient. The concentration of the purified protein was then measured and aliquots were saved at -80˚C before use.

III-4. RESULTS AND DISCUSSION

Confocal image analysis of Aβ42-treated cells to probe interaction of Aβ42 and caspase

We explored the interaction of Aβ42 with the selected caspases using confocal microscope image analysis. Previously, procaspase-9 was proven to interact with the peptides. In the current study, we probed caspase-2, -4, -6, -7 and -8. We chose them, because they are known to play a critical role in the intrinsic and extrinsic apoptosis pathway and one aim of this study was characterization of the potential interaction in relation to the apoptosis pathway. Probing of caspase-3 was omitted because the previous study indicated that it did not interact with Aβ42 [52]. In the current investigation, we employed human epithelial HeLa cells which showed relatively high resistance to Aβ42 damage than other cell lines such as human neuroblastoma SH-SY5Y cells in which death occurred too easily with Aβ treatment (data not shown). And oligomeric preparation of Aβ42 was mainly used for the experiments instead of monomeric or fibrillar peptide, otherwise indicated, because it was superior to the monomer or fibrillar form in entering into the cells [19, 71].

We analyzed the images of cells treated with Aβ42 for the peptide and each caspase. The interaction was determined by revealing the yellow-colored spots in the merged images. Among the tested caspases, prominent yellow spots were recognized in caspase-6 samples,

while they were rarely seen in other caspase test group (Fig. 7). In the current study, we focused on exploration of caspase-6 and its potential interaction with Aβ42. We used 3 different antibodies against caspase-6 for this and following experiments (see "Materials and methods").

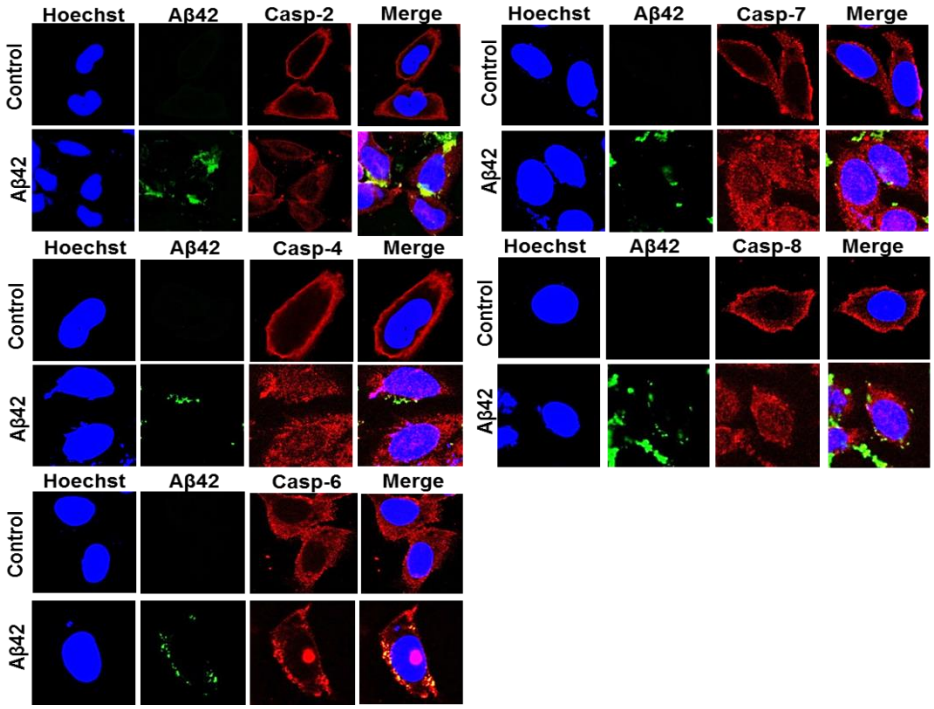

Fig. 7. Aβ42 binds Caspase-6 but not with Caspase -2, -4, -7 and -8. HeLa cells were cultured and treated with 20 μM Aβ42 for 12h. Cells were fixed and permeabilized by methanol and triton x-100. Primary mouse anti amyloid beta (6E10) and rabbit anti caspase-2, goat anti caspase-4, -6, -7 and -8 antibodies in addition to secondary anti-mouse IgG-FITC and anti-rabbit or anti-goat IgG rhodamine antibodies were used to detect intracellular Aβ (green) and caspases (red). Nuclei were seen with the nucleic acid flurochrome Hoechst and images were visualized using a confocal microscope.(LSM 510, Carl Zeiss)

Probing interaction of Aβ42 and caspase-6 by SEC

Immunoblotting analysis can produce frequently false positive results which are partly due to less specific antibodies. In the above confocal studies, caspase-6 was recognized as an Aβ42-interacting protein, but proteins other than caspase-6 were also detected in the western blot analysis as shown in Fig. 8A and Fig. 10C. We made extensive efforts to find more specific anti-caspase-6 antibodies for the confocal and the following studies, but it was not successful (see also Fig. 10C). To reduce this limitation and confirm the interaction, we further investigated the interaction of caspase-6 and Aβ42 using SEC followed by western blotting analysis. It was expected that the two proteins are recognized in the same SEC fractions if they interact with each other. Initially, cell extracts prepared from Aβ42-non-treated cells were analyzed to probe the elution pattern of caspase-6. ~34 kDa band corresponding to procaspase-6 was recognized in fractions #33-#37 (Fig. 8A). In addition to them, other bands were also seen in other fractions among which the fractions around #22 contained the most prominent signals. They were not related with caspase-6, considering the size and the result using purified caspase-6 in which the bands were not seen (Fig. 8E).

Aβ42 peptide was also subjected to SEC and the peptide of the fractions was visualized by western immunoblot analysis using 6E10 and A11 antibodies which bind to different structural species of Aβ [19]. ~9 kDa peptide was detected in #17-25 fractions with 6E10, while ~25 kDa bands was recognized in #14 fraction with A11 (Fig. 8B). Those should

be dimer and oligomers respectively, because the monomeric Aβ42 is 4~5 kDa. However, the sizes of each species estimated by comparison of the molecular weight standard markers of SEC were much bigger, implying that those seen on gels might be an SDS-resistant core of bigger oligomeric species. Monomeric forms of Aβ42 were also detected in the later (>#42) fractions which were not shown here to focus on the caspase-6 containing fractions.

The similar elution pattern of caspase-6 was shown in the fractionation of cell extracts prepared from Aβ42-treated cells by SEC (Fig. 8C). In the analysis of the same cell extracts for Aβ42, only very faint bands estimated as ~9 kDa were detected by western blot analysis with 6E10 antibody in fractions #36-#39, parts of which are caspase-6-containing fractions (Fig. 8C). On the other hand, in the western blot analysis with A11 antibody, protein bands estimated ~25 kDa were recognized in fractions #36-#38 (Fig. 8C). The cell-free experiments using cell extracts and Aβ42 peptide directly added to them also showed the similar ~9 and ~25 kDa bands in the western blot analysis with 6E10 and A11, respectively (Fig. 8D). Similarly, other cell-free experiments using purified caspase-6 and Aβ42 peptide revealed the two protein bands with the same experiments (Fig. 8D), consistent with above results. Altogether, these data suggest a potential interaction of caspase-6 and at least two structural species of Aβ42, though characterization of ~9 kDa and ~25 kDa species remains to be explored.

It is noted that the two bands were also detected in the early

fractions both in the cell-based and cell-free experiments. Those seem to be derived from oligomerized Aβ42 or the peptide that interacts with other cellular proteins, for those were not detected in experiments employing the purified caspase-6 (Fig. 8E). For this western blot analysis, we used AbA which could detect the small domain of caspase-6 (p11) and procaspase-6. However, p11 was very difficult to detect in samples prepared from cells (Fig. 8A, 8C, 8D and Fig. 10C). Only it was recognized in purified caspase-6 (Fig. 8E).

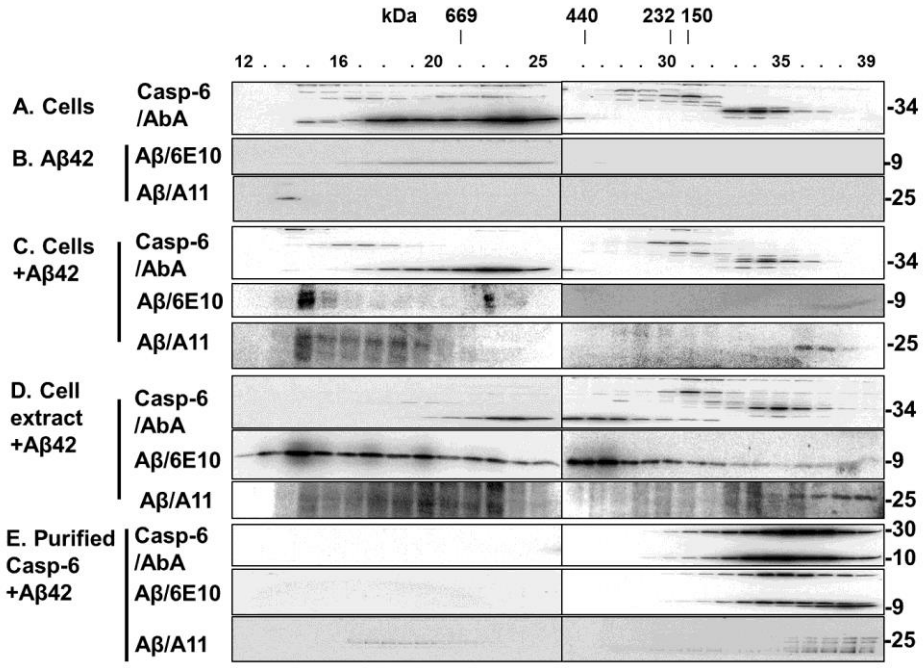

Fig. 8. Aβ42 interacts with Caspase-6. (A, B) HeLa cells were incubated in the absence or presence of 20 μM oligomerized $A\beta_{42}$ for 2+22 h respectively. The extract prepared from the cells (1 ~ 1.5 mg) was fractionated by gel filtration chromatographyas described previously. The fractions were analyzed by immunobloting for caspase-6 and $A\beta_{42}$. The standard molecular markers are indicated above the scale with elution fractions. **(C)** HeLa cell extracts were prepared (1 ~ 1.5 mg) and incubated with 20 μM of $A\beta_{42}$ for 2 h at 30˚C and the reaction mixture was fractionated by gel filtration and analyzed by western blot analysis for caspase-6 and $A\beta_{42}$. **(D)** 10 μg of purified recombinant active caspase-6 was incubated with 20 μM of $A\beta_{42}$ for 2 h at 30˚ C and the reaction mixture was separated and analyzed for caspase-6 and $A\beta_{42}$ as above. **(E)** 20 μM of purified $A\beta_{42}$ was incubated at 30˚C for 2 h and fractionated by gel filtration and probed for $A\beta_{42}$ by western blot analysis.

Probing interaction of Aβ42 and caspase-6 by immunoprecipitation

Immunoprecipitation method was further employed to confirm the interaction (see below). Proteins in the SEC fractions #33-37 of samples shown in Fig. 2B were analyzed for probing the interaction of caspase-6 and Aβ42. We used the fractions instead of cell extract prepared from Aβ42-treated cells, because cells contained many other proteins that could be detected by the antibodies against caspase-6 used here. The immunoprecipitation was performed using AbC, because the other two antibodies (AbA and AbB) were not recommended by the manufacturer for the study. Aβ42 was detected in fractions precipitated with AbC (Fig. 3A), indicating the binding of the peptide to caspase-6. The Aβ42 bands recognized by 6E10 and A11 have sizes different from those in the SEC experiments of Fig. 2 (Fig. 9A). This is probably because the samples were incubated for long time (>12 h) for the immunoprecipitation study and Aβ42 might aggregate during the precipitation procedure. We could not performed the immunoprecipitation with the Aβ antibodies, because of their inability for the experiments. For a reference, purified caspase-6 was incubated with Aβ42 peptide and the reaction mixture was subjected to the same immunoprecipitation study. 6E10 was applicable for this purified caspase-6 experiments. Aβ42 immunoprecipitated with caspase-6 and vice versa (Fig. 9B). Altogether, these all data strongly suggest the binding of Aβ42 to caspase-6.

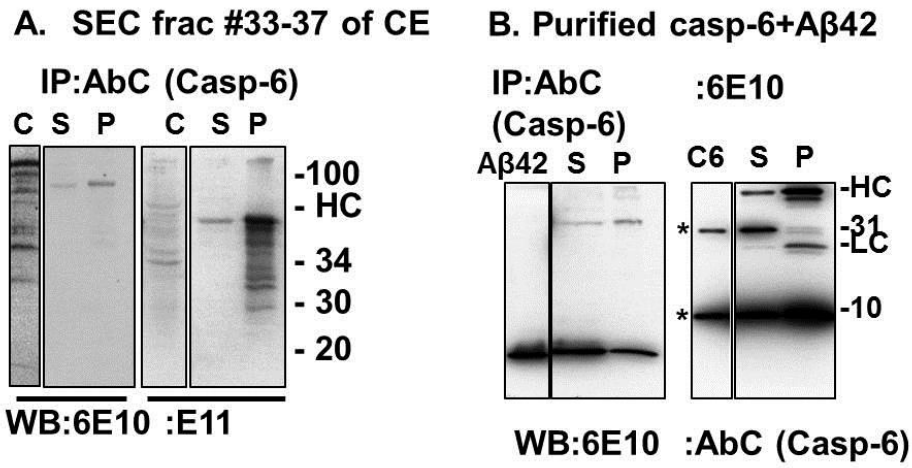

Fig. 9. Immunoprecipitation analysis of the interaction between Aβ42 and Caspase-6. (A) After treating the HeLa cells with 20 μM of $A\beta_{42}$ for 2+22 h, cell extracts were prepared and separated by gel filtration chromatography. Fraction 33-37 as indicated in Fig: 12 were pooled and immunoprecipitated with caspase-6 antibody (Santa Cruz: sc-1232) and probed for $A\beta_{42}$ with 6E10 and A11 antibody. Pooled fractions were loaded as control denoted with C. **(C)** Purified caspase-6 and 20 μM of $A\beta_{42}$ were incubated for 2 h at 30˚ C and immunoprecipated with caspase-6 and 6E10 ($A\beta_{42}$) antibody and western bloted for $A\beta_{42}$ and caspase-6 respectively. Purified $A\beta_{42}$ and caspase-6 (marked with *) was loaded as control.

Activation of caspase-6 and cleavage of lamin A and B

In the above experiments, we used cells in which caspase-6 was potently activated to probe a potential effect of the interaction of caspase-6 and Aβ42 on intracellular function of the caspase. Several different concentrations of Aβ42 and different treatment methods were tested. The "single" treatment of Aβ42 to cells for up to 48 h resulted in a certain levels of activation of caspase-6 that was evaluated by a synthetic substrate VEID-AMC (Fig. 10A). However, it was questionable if the activity was derived from solely Aβ42 treatment, because there was a weak dependency of the activity on concentration of Aβ42. The Aβ42-dose dependency was seen relatively prominently in cells treated twice with Aβ42 (Fig. 10B). Among the "double" treatment conditions, the 2 h pretreatment and subsequent 22 h (2+22 h) treatment induced the most potent activation (Fig. 10B). The 2+22 h samples were employed throughout the current study, because of the prominent activation of caspase-6. We further probed the processing of caspase-6 using western blot analysis. As experiments of Fig. 10, AbA was used initially in the analysis. Although it was difficult to detect the p11, decrease of procspase-6 was clearly seen in the 2+22 h samples with high dose of Aβ42 (20 and 40 μM) (the left panel of Fig. 10C). The same western blot analysis was performed with other anti-caspase-6 antibody, AbB which recognizes the large subunit of the enzyme. ~23 kDa proteins corresponding to the large domain of caspase-6 were clearly seen in the same samples as above (the right panel of Fig. 10C). Altogether, these all data indicated that caspase-6 is activated in the 2+22 h samples treated with Aβ42 at 20 and 40 μM.

We next probed the processing of lamin A/C and B, substrates of catalytically active caspase-6, to know if the enzyme properly functioned inside of cells. While no fragmentation of lamin proteins was observed in cells treated with Aβ42 for 48 h or 2+10 h (Fig. 11A and 11B), the fragmentation was detected in 2+22 h and 2+34 h samples (Fig. 11C and

11D). The detected ~46 kDa lamin A fragment and ~21 kDa lamin B fragment, however, should not be generated by the action of caspase-6, because it produces ~28 kDa lamin A fragment and ~46 kDa lamin B fragment (Fig. 11F). For comparison, caspase-6-dependent fragmentations of lamins were clearly seen in STS-treated cells (Fig. 11E). Thus, it seems that caspase-6 is catalytically active in Aβ42-treated cells, but is not functionally active. Hopefully, understanding the mechanistic details of the caspase-6 in the Aβ42-treated cells will provide novel insight into Aβ-associated pathology and control of AD.

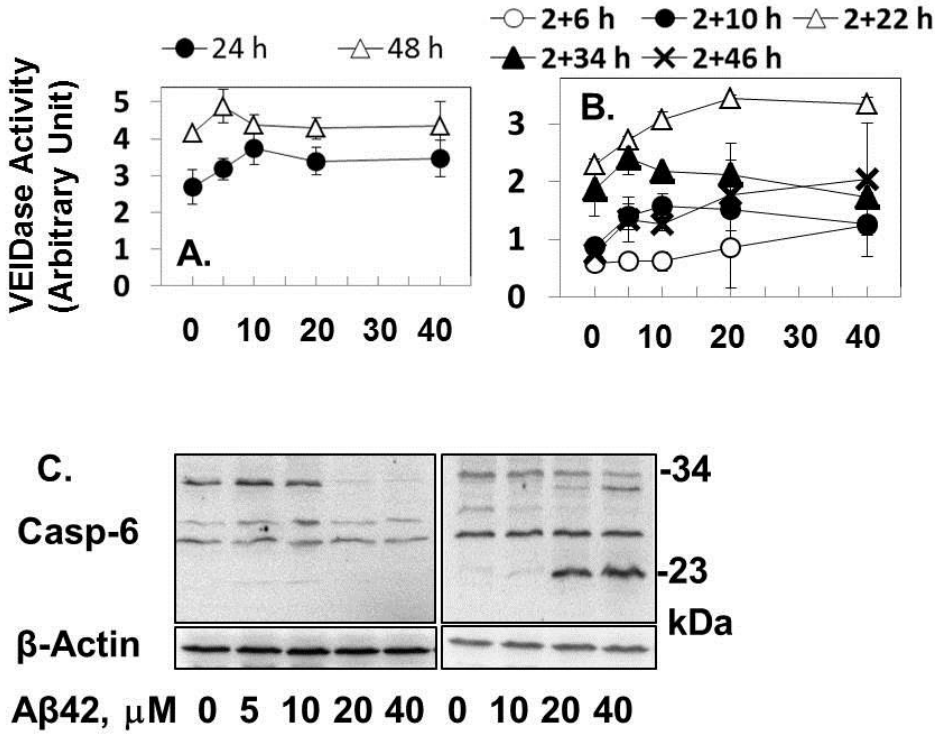

Fig. 10. Double treatment but not single treatment of $A\beta_{42}$ oligmeric species induces caspase-6 activity and cleavage. (A,B) HeLa cells ($2x10^4$ /100 μl of culture media) were treated with oligomerized $A\beta_{42}$ at the indicated concentrations and time. Caspase-6 activity was measured using its synthetic substrate VEID-AMC (50μM). **(C)** HeLa cells ($8x10^5$) were treated with indicated concentration of $A\beta_{42}$ for 2+22 h, total cell lysate were prepared and caspase-6 cleavage was checked by immunoblot analysis with mouse anti-human caspase-6 monoclonal antibody (BD Pharmingen) and rabbit anti-caspase-6 polyclonal antibody (Ab Frontier). Actin was loaded as loading control.

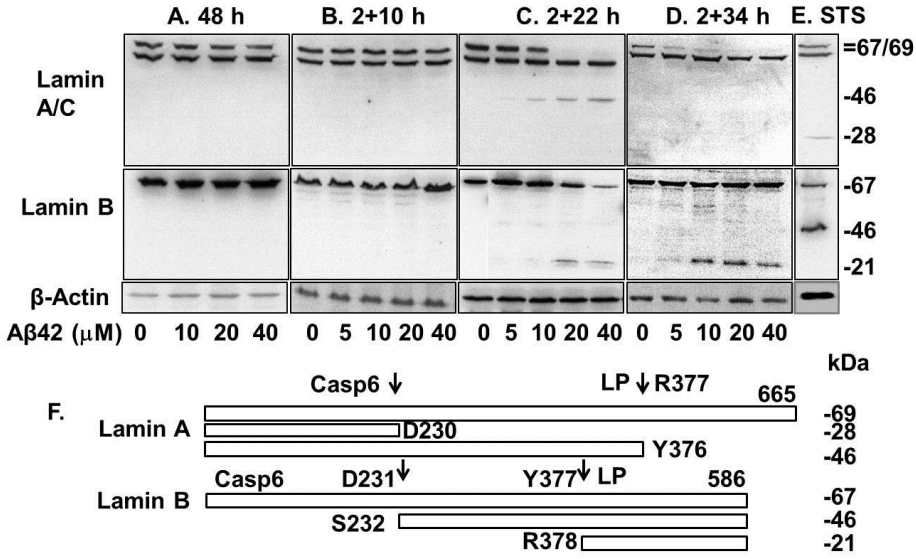

Fig. 11. Time and concentration dependent cleavage of Lamin A and B by $A\beta_{42}$. **(A - D)** HeLa cells ($8x10^5$) were treated with indicated concentration of $A\beta_{42}$ for the indicated time periods, total cell lysate were prepared and analyzed for the cleavage of Lamin A/C and B by immunoblot (antibody for Lamin A/C was raised against N-terminus of human Lamin A/C and for Lamin B was raised against C-terminus of human Lamin B1). Actin was employed as loading control. **(E)** HeLa cells were treated with 5μM of STS for 6 h and after preparation of whole cell lysate probed for the cleavage of Lamin A/C and B by western blot. Actin was loaded as control. **(F)** Schematic drawing of Lamin A and B cleaving sites by caspase-6 and Lamin protease. The predicted sizes of the cleavage fragments are indicated.

IV. Purification and characterization of cell penetrating TAT-Aβ$_{42}$

IV-1. INTRODUCTION

Amyloid beta plaques consisting of fibrillar aggregates of amyloid beta Aβ peptides are the pathological hallmark of Alzheimer's disease. But the detail mechanism of Aβ aggregation, the nature of the toxic species, and the cellular pathway of Aβ induced toxicity is yet to be revealed. It has been proposed that the soluble oligomers as well as the fibrillar aggregates are responsible for the neuronal toxicity. Substantial evidence suggests that, intracellular accumulations Aβ is required to show the toxicity prior to extracellular deposition. Intracellular accumulations is reported to be occurred either by endogenous production of Aβ by some organelles e.g. lysosome, Golgi apparatus, endoplasmic reticulum etc., or by reuptake of extracellular Aβ by endocytosis. Long term expression of APP in rat culture has been shown to induce apoptosis [99]. Presence of intracellular Aβ dimers in primary human neurons and in neuronal cell lines, and accumulation of intracellular Aβ in FAD expressing mice and its correlation to accelerated toxicity clearly implicate the role of intracellular Aβ in neuronal loss [100, 101]. The interaction of amyloid beta with intracellular proteins and the implications of this interaction are also reported [52]. Aβ has been found to bind with a number of receptors or receptor related proteins such

as N-methyl-D-aspartic acid (NMDA) receptor [26], low-density receptor associated protein-1 [27], the α7 nicotinic acetyl choline receptor [28], the p75 neurotrophin receptor [29], and the receptor for advanced glycation endproducts [30]. However, due to lack of specificity of Aβ antibody, sometimes it is difficult to know the exact mechanism of these interactions and their implications on cell cytotoxicity. For the investigation of these mechanisms proposed, large amount of pure Aβ peptides and diverse mutants of Aβ are required. Therefore, cell penetrating version of $A\beta_{42}$, which is the major component of the senile plaques, could be a one interesting option to understand the role of intracellular Aβ in cytotoxicity and to identify Aβ- interacting protein. Cell penetrating version of $A\beta_{42}$ has its advantage over transgenic models, overexpression of APP and expression of cDNA coding Aβ sequence.

The major challenges in expressing this cell penetrating version of $A\beta_{42}$ in *Escherichia coli* is its toxicity towards the bacterial cells, poor expression, inclusion body forming and solubility problem. To overcome these difficulties, the peptide was co-expressed with a fusion protein such as maltose binding protein (MBP), thioredoxin (TRX), transcription pausing factor L (NusA), glutathione-S-transferase [102-104]. The fusion protein technology is beneficial both for high yield and purity, but in most cases, the insoluble inclusion bodies are solubilized by adding strong denaturant such as urea to prevent the aggregation by inhibiting inter and intra molecular interaction. Cleavage of fusion protein in presence of urea is also beneficial in two ways, first, it inhibits the

precipitation of fusion protein before cleavage and second, urea prevents the aggregation of cleaved peptide which is a common phenomenon in aggregation prone peptide. Recently, use of ubiquitin in fusion protein technology has gained considerable interest. Ubiquitin fusion offers efficient cleavage of target by highly specific and robust deubiqutylating enzyme, Usp2-cc. In this study, a recombinant fusion method was used to produce TAT- $A\beta_{42}$. The fusion protein consists of a co-chaperone GroES connected by ubiquitin and then the TAT- $A\beta_{42}$.

IV-2. MATERIALS AND METHODS

Construction and purification of TAT tagged amyloid beta peptides

Genes encoding GroES was PCR amplified (antisense primer, 5'- AAG TCC GCT CTA TTC TTG ATG CGG ATC CCG-3'; sense primer, 5'- GGA ATT CCA TAT GAA TAT TCG TCC ATT GCA -3') using *E. coli* DH5α genomic DNA as template and cloned in *Nde1* and *BamH1* sites of pET28b expression system (Novagen). Ubiquitin gene (kindly provided by Rohan T. Baker) was subcloned in *NdeI/BamHI* sites of a vector containing amyloid beta42 ($A\beta_{42}$). Thereafter, *BamHI* site between ubiquitin and $A\beta_{42}$ were destroyed by site directed mutagenesis to facilitate further cloning. Ubiquitin - $A\beta_{42}$ was PCR amplified (sense 5'- CGC GGA TCC CAG ATC TTT GTG AAG AC -3'; antisense 5'- CCG CTC GAG TCA CGC

TAT GAC AAC ACC GCC -3') and cloned between *BamHI* and *XhoI* sites following C-terminus GroES. TAT tagged Ab42 construct was prepared by inserting TAT sequence between ubiquitin and Ab42 sequence using antisense primer 5'- GGA ATT CTG CAT CGC CAC GAC GCT GAC GAC GTT TTT TAC GGC CTC CAC CGC GGA GGC GCA A -3' and sense primer 5'- CGC GGA TCC CAG ATC TTT GTG AAG AC-3').

Expression of GroES-Ub-TAT-Aβ_{42} fusion protein

The fusion protein was overexpressed as inclusion bodies in *E.coli* BL21 (DE3) pLysS cells. The protocol used as follows: a single colony was inoculated into 50 ml of LB media supplemented with kanamycin to a final concentration of 30 μg/ml and culture for overnight at 37˚ C. The next day, the 50 ml seed culture was transferred into 1L of LB media supplemented with kanamycin with a final concentration of 30 μg/ml and incubated at 37˚ C until the OD_{600} reaches to 0.6 – 0.8. Isopropyl-β- D- thiogalactopyranoside (IPTG) was the added to 0.4 mM concentration for induction. The culture was additionally grown for 4 h and the cells were harvested by centrifuging at 4000 rpm for 10 min at 4˚ C. The cells were then washed with buffer (20ml/1L of culture) containing 50 mM Tris-HCl (pH 8.0), 150 mM NaCl and 5 mM EDTA, collected in 50 ml conical tube and again centrifuged at 4000 rpm for 10 min. The pellets were either used for next step purification or stored at -20˚ C.

Cell lysis and preparation of inclusion bodies

The cell pellet was re-suspended in 20 ml (for 1 L culture) in lysis buffer (50 mM Tris-HCl pH 8.0, 150 mM NaCl, 5 mM EDTA, 0.5% triton X – 100, 1 mM DTT, 0.1 mM PMSF) and kept in ice for 30 min and lysed by sonication at ice cold temperature. The cell extract was then centrifuged at 20000 rpm for 30 min and the supernatant discarded. The pellets were washed 3 times by re-suspending in washing buffer I (50 mM Tris-HCl pH 8.0, 150 mM NaCl. 5 mM EDTA, 0.5% triton X – 100, 1 mM DTT) for 3 times followed by washing with washing buffer II (50 mM Tris-HCl pH 8.0, 150 mM NaCl, 5 mM EDTA, 1 mM DTT) for 2 times. Each time the inclusion bodies were collected by centrifuging at 20000 rpm for 30 min.

Solubilization and digestion of GroES-Ub-TAT-Aβ_{42} fusion protein with Usp2cc enzyme

The extensively washed inclusion bodies were solubilized in 20 ml of solubilization buffer (50 mM Tris-HCl pH 8.0, 150 mM NaCl, 1 mM DTT and 6 M urea) for 1 L of culture and kept at room temperature for 30 min. The soluble proteins were collected by centrifuging at 18000 rpm for 30 min; concentration was measured and adjusted to a final concentration of 9 mg/ml to facilitate the digestion. For digestion, the protein sample was diluted 2 times with buffer (50 mM Tris-HCl pH 8.0,

150 mM NaCl, 1 mM DTT) to maintain the final concentration of urea 3 M to avoid precipitation of fusion protein and to maintain the Usp2cc activity. The digestion reaction was carried with an enzyme : substrate molar ratio 1:100 for 3 h at 37˚ C. After digestion, the sample was sonicated on water bath for 10 min and centrifuged at 18000 rpm for 30 min and the supernatant was collected for next step purification.

HPLC purification of TAT-$A\beta_{42}$ peptide on polymer based column

The reverse phase polymer column was equilibrated with 3 column volume of HPLC buffer A (10 mM Ammonium acetate, pH 10 in 2% acetonitrile) and the sample was injected onto the column. The bound peptide was then eluted with linear gradient of HPLC buffer B (70% acetonitrile) with a flow rate of 10 ml/min. TAT- $A\beta_{42}$ was eluted as a single peak at 30-35% of buffer B. The TAT- $A\beta_{42}$ containing fraction was collected and lyophilized in 50 ml conical tube with Para film cover (~ 48 h).

Preparation of TAT- $A\beta_{42}$ peptides

The purified peptide was solubilized in 100% 1,1,1,3,3,3,-hexafluoro-2-propanol, and dried under nitrogen flow and subsequently, under vacuum for 30 min. The peptide aliquots were stored at –20 °C until use. Immediately before use, the peptide was dissolved in 0.1%

NH4OH at a concentration of 2 mg/ml followed by bath sonication for 10 min. The solution was diluted at the desired concentration with cell culture media without FBS.

Cell culture and cytotoxicity Assay

Human epithelial HeLa cells were cultured in DMEM (High glucose) medium supplemented with 10% (v/v) FBS and 1% antibiotics at 37 °C under 5% CO2.

For MTT cytotoxicity assay, cells were plated at a density of 15,000 cells/well in 96-well plates (Nunc, Denmark) and cultured for 24 h followed by serum deprivation for another 12 h. Cells were exposed to the Aβ preparation for 24 h and the viability was assessed by 3-(4,5-dimethylthiazol-2-yl)-2,5-di-phenyltetrazolium bromide (MTT) reduction test. Briefly, 20 μl of 5 mg/ml MTT solution in PBS was added to each well and incubated for 2 h. Then 100 μl of solubilization buffer [20% SDS solution in 50% (v/v) DMF (pH 4.7)] was added. After 12-16 h of incubation, absorbance was recorded at 570 nm using a micro plate reader KisanBio plate reader (KisanBio, Seoul, South Korea).

Immunocytochemistry to check the entry of $A\beta_{42}$ species inside the cells

HeLa cells were seeded in 6 well plate at 70% confluency, cultured for 24h and further incubated for 12h in serum free media and then treated without or with 5 μM of indicated $A\beta_{42}$ for 24 h. Treated cells were fixed in methanol at -20˚ C and permeabilized by 0.3% Triton X-100. After blocking with 0.1% BSA overnight, primary mouse anti-amyloid beta (6E10), mouse anti-HIV1 tat (N3), mouse anti-FLAG (M2) and rabbit anti caspase-9 antibodies were added to each samples and incubated overnight at 4°C. After washing with PBS, Alexa-Flour-488 conjugated chicken anti mouse IgG, FITC conjugated goat anti-rabbit antibodies (dilution, 1:200) were treated for 2h at room temperature followed by PBS washing. Nuclei were stained with Hoechst and confocal images were obtained with Carl Zeiss LSM510 microscope (Jena, Germany) using vendor provided software (LSM 510).

IV-3. RESULTS AND DISCUSSION

Overexpression of fusion protein and purification

After harvesting the cells by high speed centrifugation, the cells were lysed in lysis buffer and the supernatant solution and the precipitated pellets were checked for the expression and whether the fusion protein appeared in the supernatant or in the inclusion bodies in

SDS-PAGE gel (Lane 1-3 of Fig: 12B). As expected, a large protein band of approximate mass of 25 kDa, that of the fusion protein, was found in the pellets of the cell extracts (Lane: 3). Therefore, the supernatant was discarded and the inclusion bodies were used for further purification.

The pellets of the cell extract were washed extensively 3 times with washing buffer I (described in materials and methods) to remove the traces of other soluble proteins. Then the inclusion bodies were further washed with washing buffer II twice to eliminate the triton X-100 so that it does not interfere with Usp2cc digestion and HPLC purification. The inclusion bodies found after this washing step is mostly free of other contaminants (Lane 4 of Fig: 12B) as found in the SDS-PAGE gel electrophoresis. At this stage, the inclusion bodies were solubilized in 6 M urea and centrifuged in a high speed centrifugation at 18000 rpm to remove the small amount of insoluble proteins. The supernatant was collected, quantified for the protein concentration by Bradford assay and diluted twice to facilitate digestion by Usp2cc in 3 M of urea (Lane 5, Fig: 12B). Bellow this concentration of urea, the inclusion bodies tend to precipitate and over 3 M of urea concentration Usp2cc was found less effective in case of wild type $A\beta_{42}$. Following the cleavage reaction, the cleaved peptide was separated by using reverse phase HPLC polymer based column using the buffers systems mentioned in materials and method section. It is evident from the gel electrophoresis result (Lane 6, Fig: 12B) that the TAT-$A\beta_{42}$ we got finally is quite pure. Approximately 4.0 mg of TAT-$A\beta_{42}$ was obtained from 1 L of bacterial culture.

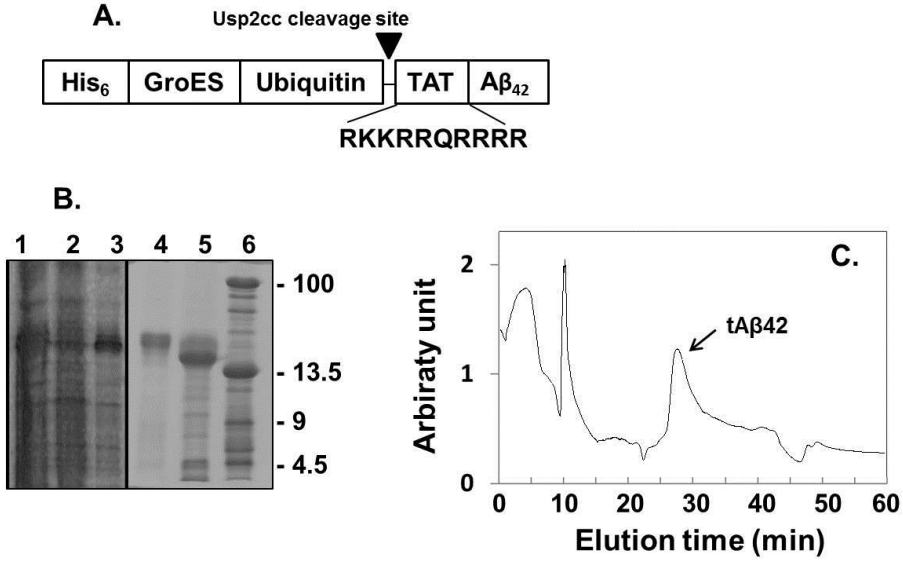

Fig. 12. Construction, Expression and purification of TAT- Aβ$_{42}$. (A) Schematic representation of the TAT- Aβ$_{42}$ construct. **(B)** SDS-PAGE analysis of overexpressed GroES-Ub-TAT- Aβ$_{42}$ fusion protein. Lanes: 1, Cell extracnts, 2, supernatant, 3, precipitant, 4, washed inclusion body of GroES-Ub-TAT- Aβ$_{42}$ fusion protein; 5, Fusion protein digested by Usp2-cc; 6, HPLC purified TAT- Aβ$_{42}$. **(C)** HPLC chromatogram shows elution profile of TAT- Aβ$_{42}$.

Toxicity of TAT, FLAG and wild type $A\beta_{42}$

The exact mechanism of toxicity by Aβ is not well defined till now. Although, the senile plaque consisting of Aβ is primarily extracellular, the role of this extracellular Aβ on cytotoxicity is also unknown to date, though many hypotheses have been proposed. Expression of Aβ inside the cells helps to reveal the role of intracellular accumulation of Aβ, but the consequences of large deposition of extracellular Aβ remains questionable. Moreover, transfection of Aβ plasmids may alter the membrane properties of the cells, which may interfere with the cytotoxicity rendered by Aβ. Considering these things, we treated the cells by three different kinds of Aβ, that is, a cell penetrating version of TAT- $A\beta_{42}$, FLAG- $A\beta_{42}$ which cannot enter into the cells revealed by confocal microscopy, and the wild type $A\beta_{42}$ as mentioned in the materials and methods section. The percentage of cell death induced by these three $A\beta_{42}$ varies significantly. As the data shows (Fig: 13), cell survival rate is the maximum with the cells treated by FLAG- $A\beta_{42}$. In the case of TAT- $A\beta_{42}$, the cell survival rate was the lowest even at very low concentration of TAT- $A\beta_{42}$, while the wild type $A\beta_{42}$ shows moderate cytotoxicity among the three different $A\beta_{42}$ species. The difference in the level of cytotoxicity induced by three groups of $A\beta_{42}$ can be described by the fact that, entry into the cell might be very crucial for $A\beta_{42}$ mediated cell death pathway.

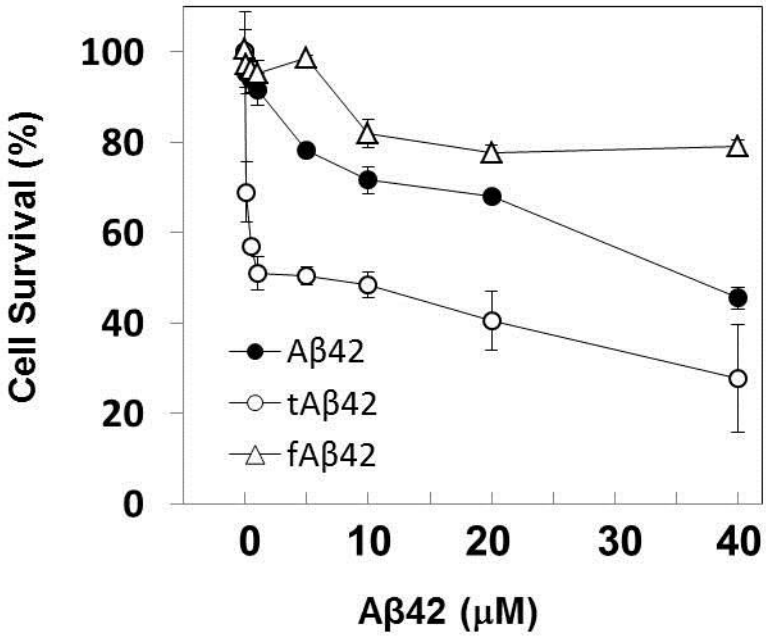

Fig. 13. Cytotoxicity of different species of $A\beta_{42}$ in HeLa cells. Cells were cultured (10000 cells/well) for 24 h and serum deprived for 24 h and then treated with mentioned species of $A\beta_{42}$ at indicated concentration for 24 h. Cytotoxicity was measured by MTT reduction assay. Triplicate experiments were performed and standard deviations were indicated as bars.

TAT- $A\beta_{42}$ preferentially enters into cells than wild type and FLAG- $A\beta_{42}$

It was found from confocal microscopy results that, FLAG- $A\beta_{42}$ was unable to enter into the cells, it accumulates outside the membrane. While, intra cellular accumulation of TAT- $A\beta_{42}$ was much higher than wild type $A\beta_{42}$. In the earlier study from our lab, it was shown that, $A\beta_{42}$ can bind to procaspase-9 and inhibit the caspase cascade initiated by intrinsic apoptotic pathway [52]. To confirm the binding ability of TAT-$A\beta_{42}$ with caspase-9, the interaction of all three groups of $A\beta_{42}$ was checked by concomitant antibody treatment for both Aβ antibodies (TAT, 6E10 and FLAG) and caspase-9 antibody. And the interaction was found very clearly (Fig: 14). The cause of higher cell death by TAT- $A\beta_{42}$ was further substantiated by this entrance into the cells.

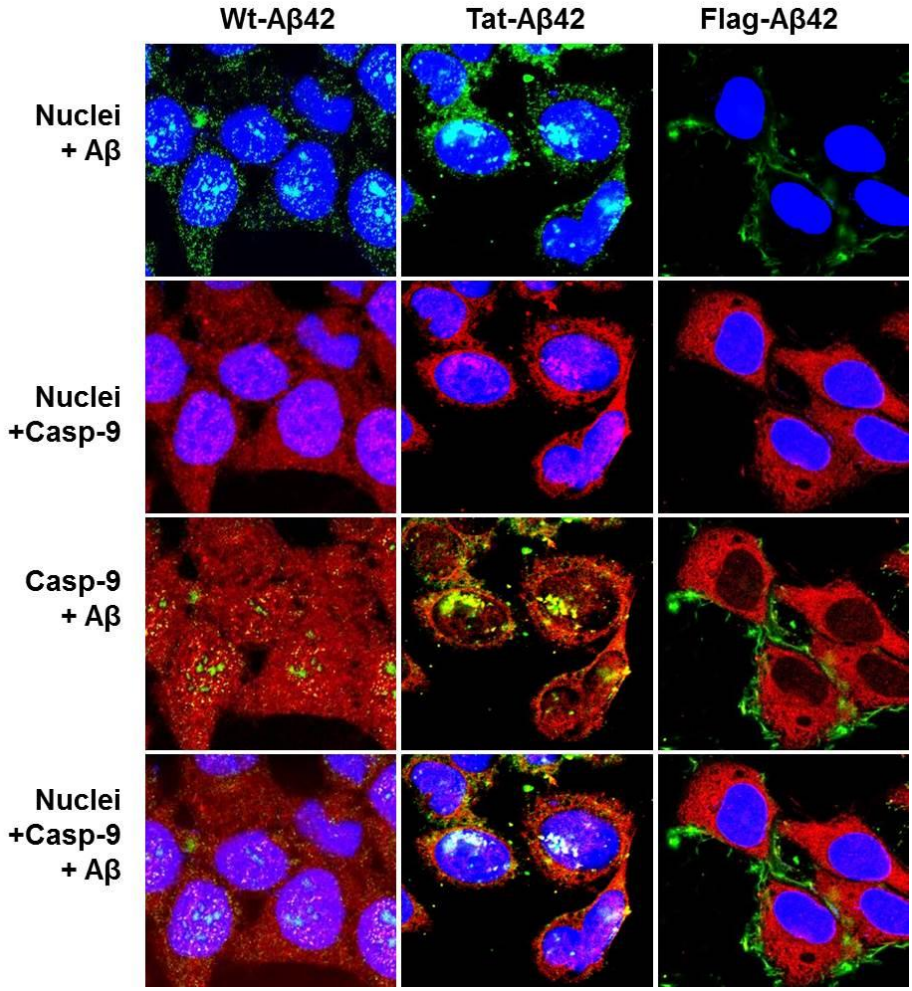

Fig. 14. Confocal microscopy analysis of different species of $A\beta_{42}$. HeLa cells were treated with 20 μM of wild type $A\beta_{42}$ and FLAG- $A\beta_{42}$ and 5 μM of TAT-$A\beta_{42}$ for 24 h. Cells were fixed and permeabilized by methanol and triton x-100. Primary mouse anti-amyloid beta (6E10), mouse anti- FLAG, mouse anti-TAT and rabbit anti-caspase-9 antibodies in addition to secondary anti-mouse IgG-FITC and

anti-rabbit IgG Rhodamine antibodies were used to detect intracellular Aβ (green) and caspase-9 (red) respectively. Nuclei were seen with the nucleic acid fluorochrome Hoechst and images were visualized using a confocal microscope. (LSM 510, Carl Zeiss).

FUTURE RESEARCH

Purification of TAT- $A\beta_{42}$ by Methanol Precipitation method

Purification of recombinant peptide always poses difficulties due to various factors such as: solubility problem, inclusion body formation, precipitation during purification which results in loss of biological activities. To overcome this problem, denaturant buffers e.g. urea or guanidine hydrochloride is used in the purification buffer systems. To remove this denaturant from the purified peptide sample is often problematic, either we have to go for dialysis which is a time consuming process or we have to go for another column chromatographic purification which may be both time consuming and costly. But, we can easily remove the denaturants from the peptide sample by precipitating with different organic solvents like ether, methanol, ethanol or iso-propyl alcohol and then solubilize the peptide in a suitable solvent. In this method, we also tried to precipitate TAT- $A\beta_{42}$ digested inclusion bodies with different solvents among which methanol was the most efficient to precipitate the peptide. The purification scheme is as bellow:

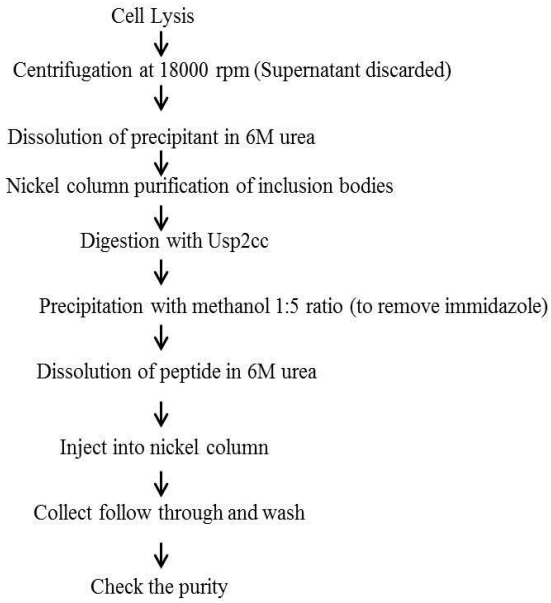

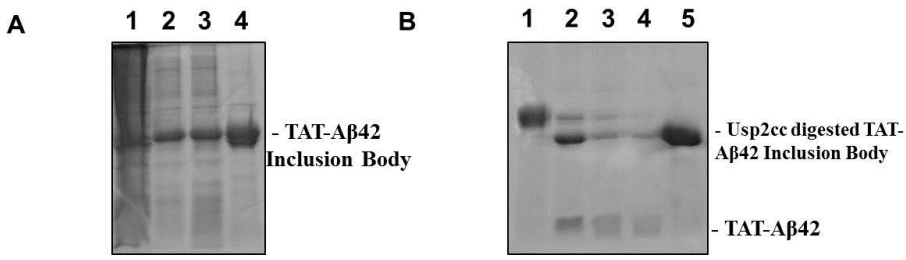

Figure. 15. Purification of TAT- $A\beta_{42}$ by precipitation method. (A) Purification of inclusion bodies by nickel column: lanes are as: 1- precipitant got after centrifugation of cell lysate, 2- follow through collected, 3- wash with washing buffer, 4- elution with imidazole. **(B)** Digestion and purification of TAT- $A\beta_{42}$. Lanes: 1- purified inclusion bodies, 2- inclusion bodies digested with Usp2cc enzyme, 3- follow through after nickel column injection, 4- wash after nickel column injection and 5- elution with imidazole.

V. REFERENCES

1. Selkoe, D.J., *Alzheimer's disease: genes, proteins, and therapy.* Physiol Rev, 2001. **81**(2): p. 741-66.

2. Suh, Y.H. and F. Checler, *Amyloid precursor protein, presenilins, and alpha-synuclein: molecular pathogenesis and pharmacological applications in Alzheimer's disease.* Pharmacol Rev, 2002. **54**(3): p. 469-525.

3. Goate, A., et al., *Segregation of a missense mutation in the amyloid precursor protein gene with familial Alzheimer's disease.* Nature, 1991. **349**(6311): p. 704-6.

4. Hardy, J. and D.J. Selkoe, *The amyloid hypothesis of Alzheimer's disease: progress and problems on the road to therapeutics.* Science, 2002. **297**(5580): p. 353-6.

5. Hardy, J.A. and G.A. Higgins, *Alzheimer's disease: the amyloid cascade hypothesis.* Science, 1992. **256**(5054): p. 184-5.

6. Cao, X. and T.C. Sudhof, *A transcriptionally [correction of transcriptively] active complex of APP with Fe65 and histone acetyltransferase Tip60.* Science, 2001. **293**(5527): p. 115-20.

7. Gao, Y. and S.W. Pimplikar, *The gamma -secretase-cleaved C-terminal fragment of amyloid precursor protein mediates signaling to the nucleus.* Proc Natl Acad Sci U S A, 2001. **98**(26): p. 14979-84.

8. Kimberly, W.T., et al., *The intracellular domain of the beta-amyloid precursor protein is stabilized by Fe65 and translocates to the nucleus in a notch-like manner.* J Biol Chem, 2001. **276**(43): p. 40288-92.

9. Deshpande, A., et al., *Different conformations of amyloid beta induce neurotoxicity by distinct mechanisms in human cortical neurons.* J Neurosci, 2006. **26**(22): p. 6011-8.

10. Koffie, R.M., et al., *Oligomeric amyloid beta associates with postsynaptic densities and correlates with excitatory synapse loss near senile plaques.* Proc Natl Acad Sci U S A, 2009. **106**(10): p. 4012-7.

11. Bitan, G., et al., *Amyloid beta -protein (Abeta) assembly: Abeta 40 and Abeta 42 oligomerize through distinct pathways.* Proc Natl Acad Sci U S A, 2003. **100**(1): p. 330-5.

12. Duering, M., et al., *Mean age of onset in familial Alzheimer's disease is determined by amyloid beta 42.* Neurobiol Aging, 2005. **26**(6): p. 785-8.

13. Shahnawaz, M., et al., *Wild-type, Flemish, and Dutch amyloid-beta exhibit different cytotoxicities depending on Abeta40 to Abeta42 interaction time and concentration ratio.* J Pept Sci, 2013. **19**(9): p. 545-53.

14. Bitan, G., S.S. Vollers, and D.B. Teplow, *Elucidation of primary structure elements controlling early amyloid beta-protein oligomerization.* J Biol Chem, 2003. **278**(37): p. 34882-9.

15. Klyubin, I., et al., *Amyloid beta protein dimer-containing human CSF disrupts synaptic plasticity: prevention by systemic passive immunization.* J Neurosci, 2008. **28**(16): p. 4231-7.

16. Shankar, G.M., et al., *Amyloid-beta protein dimers isolated directly from Alzheimer's brains impair synaptic plasticity and memory.* Nat Med, 2008. **14**(8): p. 837-42.

17. Naiki, H. and K. Nakakuki, *First-order kinetic model of Alzheimer's beta-amyloid fibril extension in vitro.* Lab Invest, 1996. **74**(2): p. 374-83.

18. Lambert, M.P., et al., *Diffusible, nonfibrillar ligands derived from Abeta1-42 are potent central nervous system neurotoxins.* Proc Natl Acad Sci U S A, 1998. **95**(11): p. 6448-53.

19. Kayed, R., et al., *Common structure of soluble amyloid oligomers implies common mechanism of pathogenesis.* Science, 2003. **300**(5618): p. 486-9.

20. O'Nuallain, B., et al., *Seeding specificity in amyloid growth induced by heterologous fibrils.* J Biol Chem, 2004. **279**(17): p. 17490-9.

21. Koo, E.H. and S.L. Squazzo, *Evidence that production and release of amyloid beta-protein involves the endocytic pathway.* J Biol Chem, 1994. **269**(26): p. 17386-9.

22. LaFerla, F.M., K.N. Green, and S. Oddo, *Intracellular amyloid-beta in Alzheimer's disease.* Nat Rev Neurosci, 2007. **8**(7): p. 499-509.

23. Bayer, T.A. and O. Wirths, *Intracellular accumulation of amyloid-Beta - a predictor for synaptic dysfunction and neuron loss in Alzheimer's disease.* Front Aging Neurosci, 2010. **2**: p. 8.

24. Small, D.H., S.S. Mok, and J.C. Bornstein, *Alzheimer's disease and Abeta toxicity: from top to bottom.* Nat Rev Neurosci, 2001. **2**(8): p. 595-8.

25. Verdier, Y. and B. Penke, *Binding sites of amyloid beta-peptide in cell plasma membrane and implications for Alzheimer's disease.* Curr Protein Pept Sci, 2004. **5**(1): p. 19-31.

26. Bi, X., et al., *Uptake and pathogenic effects of amyloid beta peptide 1-42 are enhanced by integrin antagonists and blocked by NMDA receptor antagonists.* Neuroscience, 2002. **112**(4): p. 827-40.

27. Deane, R., et al., *LRP/amyloid beta-peptide interaction mediates differential brain efflux of Abeta isoforms.* Neuron, 2004. **43**(3): p. 333-44.

28. Wang, H.Y., et al., *beta-Amyloid(1-42) binds to alpha7 nicotinic acetylcholine receptor with high affinity. Implications for Alzheimer's disease pathology.* J Biol Chem, 2000. **275**(8): p. 5626-32.

29. Yaar, M., et al., *Binding of beta-amyloid to the p75 neurotrophin receptor induces apoptosis. A possible mechanism for Alzheimer's disease.* J Clin Invest, 1997. **100**(9): p. 2333-40.

30. Du Yan, S., et al., *Amyloid-beta peptide-receptor for advanced glycation endproduct interaction elicits neuronal expression of macrophage-colony stimulating factor: a proinflammatory pathway in Alzheimer disease.* Proc Natl Acad Sci U S A, 1997. **94**(10): p. 5296-301.

31. Simakova, O. and N.J. Arispe, *The cell-selective neurotoxicity of the Alzheimer's Abeta peptide is determined by surface phosphatidylserine and cytosolic ATP levels. Membrane binding is required for Abeta toxicity.* J Neurosci, 2007. **27**(50): p. 13719-29.

32. Kanekiyo, T. and G. Bu, *Receptor-associated protein interacts with amyloid-beta peptide and promotes its cellular uptake.* J Biol Chem, 2009. **284**(48): p. 33352-9.

33. Kulandaivelu, U., et al., *Synthesis, antimicrobial and anticancer activity of new thiosemicarbazone derivatives.* Arch Pharm (Weinheim), 2011. **344**(2): p. 84-90.

34. Davis, C.H. and M.L. Berkowitz, *Structure of the amyloid-beta (1-42) monomer absorbed to model phospholipid bilayers: a molecular dynamics study.* J Phys Chem B, 2009. **113**(43): p. 14480-6.

35. Arispe, N., E. Rojas, and H.B. Pollard, *Alzheimer disease amyloid beta protein forms calcium channels in bilayer membranes: blockade by tromethamine and aluminum.* Proc Natl Acad Sci U S A, 1993. **90**(2): p. 567-71.

36. Kagan, B.L., R. Azimov, and R. Azimova, *Amyloid peptide channels.* J Membr Biol, 2004. **202**(1): p. 1-10.

37. Lal, R., H. Lin, and A.P. Quist, *Amyloid beta ion channel: 3D structure and relevance to amyloid channel paradigm.* Biochim Biophys Acta, 2007. **1768**(8): p. 1966-75.

38. Cataldo, A.M., D.J. Hamilton, and R.A. Nixon, *Lysosomal abnormalities in degenerating neurons link neuronal compromise to senile plaque development in Alzheimer disease.* Brain Res, 1994. **640**(1-2): p. 68-80.

39. Kumari, S., S. Mg, and S. Mayor, *Endocytosis unplugged: multiple ways to enter the cell.* Cell Res, 2010. **20**(3): p. 256-75.

40. Yu, C., et al., *Endocytic pathways mediating oligomeric Abeta42 neurotoxicity.* Mol Neurodegener, 2010. **5**: p. 19.

41. Fuentealba, R.A., et al., *Low-density lipoprotein receptor-related protein 1 (LRP1) mediates neuronal Abeta42 uptake and lysosomal trafficking.* PLoS One, 2010. **5**(7): p. e11884.

42. Kandimalla, K.K., et al., *Mechanism of neuronal versus endothelial cell uptake of Alzheimer's disease amyloid beta protein.* PLoS One, 2009. **4**(2): p. e4627.

43. Lai, A.Y. and J. McLaurin, *Mechanisms of amyloid-Beta Peptide uptake by neurons: the role of lipid rafts and lipid raft-associated proteins.* Int J Alzheimers Dis, 2010. **2011**: p. 548380.

44. Olzscha, H., et al., *Amyloid-like aggregates sequester numerous metastable proteins with essential cellular functions.* Cell, 2008. **144**(1): p. 67-78.

45. Troy, C.M., J.E. Friedman, and W.J. Friedman, *Mechanisms of p75-mediated death of hippocampal neurons. Role of caspases.* J Biol Chem, 2002. **277**(37): p. 34295-302. .

46. Truzzi, F., et al., *p75 neurotrophin receptor mediates apoptosis in transit-amplifying cells and its overexpression restores cell death in psoriatic keratinocytes.* Cell Death Differ., 2011. **18**(6): p. 948-58.

47. Hernandez-Zimbron, L.F., et al., *Amyloid-beta peptide binds to cytochrome C oxidase subunit 1.* PLoS One, 2012. **7**(8): p. e42344.

48. Lustbader, J.W., et al., *ABAD directly links Abeta to mitochondrial toxicity in Alzheimer's disease.* Science, 2004. **304**(5669): p. 448-52.

49. Swerdlow, R.H., *Brain aging, Alzheimer's disease, and mitochondria.* Biochim Biophys Acta, 2011. **1812**(12): p. 1630-9.

50. Liu, T., et al., *Cooperative role of RanBP9 and P73 in mitochondria-mediated apoptosis.* Cell Death Dis, 2013. **4**: p. e476.

51. Hong, Y.K., et al., *Inhibition of JNK/dFOXO pathway and caspases rescues neurological impairments in Drosophila Alzheimer's disease model.* Biochem Biophys Res Commun, 2012. **419**(1): p. 49-53.

52. Sharoar, M.G., et al., *Amyloid beta binds procaspase-9 to inhibit assembly of Apaf-1 apoptosome and intrinsic apoptosis pathway.* Biochim Biophys Acta, 2014. **1843**(4): p. 685-93.

53. Formigli, L., et al., *Aponecrosis: morphological and biochemical exploration of a syncretic process of cell death sharing apoptosis and necrosis.* J Cell Physiol, 2000. **182**(1): p. 41-9.

54. Castro-Obregon, S., et al., *A ligand-receptor pair that triggers a non-apoptotic form of programmed cell death.* Cell Death Differ, 2002. **9**(8): p. 807-17.

55. Reubold, T.F. and S. Eschenburg, *A molecular view on signal transduction by the apoptosome.* Cell Signal, 2012 **24**(7): p. 1420-5. .

56. Karki, P., et al., *Intracellular K(+) inhibits apoptosis by suppressing the Apaf-1 apoptosome formation and subsequent downstream pathways but not cytochrome c release.* Cell Death Differ, 2007. **14**(12): p. 2068-75.

57. Beere, H.M., et al., *Heat-shock protein 70 inhibits apoptosis by preventing recruitment of procaspase-9 to the Apaf-1 apoptosome.* Nat Cell Biol, 2000. **2**(8): p. 469-75.

58. Zou, H., et al., *An APAF-1.cytochrome c multimeric complex is a functional apoptosome that activates procaspase-9.* J Biol Chem, 1999. **274**(17): p. 11549-56.

59. Imai, Y., et al., *The CED-4-homologous protein FLASH is involved in Fas-mediated activation of caspase-8 during apoptosis.* Nature, 1999. **398**(6730): p. 777-85.

60. Boatright, K.M. and G.S. Salvesen, *Mechanisms of caspase activation.* Curr Opin Cell Biol, 2003. **15**(6): p. 725-31.

61. Mace, P.D., S.J. Riedl, and G.S. Salvesen, *Caspase enzymology and activation mechanisms.* Methods Enzymol, 2014. **544**: p. 161-78.

62. Li, Y.P., et al., *Beta-amyloid induces apoptosis in human-derived neurotypic SH-SY5Y cells.* Brain Res, 1996. **738**(2): p. 196-204.

63. Estus, S., et al., *Aggregated amyloid-beta protein induces cortical neuronal apoptosis and concomitant "apoptotic" pattern of gene induction.* J Neurosci, 1997. **17**(20): p. 7736-45.

64. Loo, D.T., et al., *Apoptosis is induced by beta-amyloid in cultured central nervous system neurons.* Proc Natl Acad Sci U S A, 1993. **90**(17): p. 7951-5.

65. Lee do, Y., et al., *Activation of PERK signaling attenuates Abeta-mediated ER stress.* PLoS One, 2010. **5**(5): p. e10489.

66. Esler, W.P. and M.S. Wolfe, *A portrait of Alzheimer secretases--new features and familiar faces.* Science, 2001. **293**(5534): p. 1449-54.

67. Mattson, M.P., *Pathways towards and away from Alzheimer's disease.* Nature, 2004. **430**(7000): p. 631-9.

68. Neudecker, P., et al., *Structure of an intermediate state in protein folding and aggregation.* Science, 2012. **336**(6079): p. 362-6.

69. Selkoe, D.J., P. American College of, and S. American Physiological, *Alzheimer disease: mechanistic understanding predicts novel therapies.* Ann Intern Med, 2004. **140**(8): p. 627-38.

70. Duyckaerts, C., B. Delatour, and M.C. Potier, *Classification and basic pathology of Alzheimer disease.* Acta Neuropathol, 2009. **118**(1): p. 5-36.

71. Walsh, D.M., et al., *The APP family of proteins: similarities and differences.* Biochem Soc Trans, 2007. **35**(Pt 2): p. 416-20.

72. Chong, Y.H., et al., *ERK1/2 activation mediates Abeta oligomer-induced neurotoxicity via caspase-3 activation and tau cleavage in rat organotypic hippocampal slice cultures.* J Biol Chem, 2006. **281**(29): p. 20315-25.

73. Ellerby, L.M. and H.T. Orr, *Neurodegenerative disease: cut to the chase.* Nature, 2006. **442**(7103): p. 641-2.

74. Nikolaev, A., et al., *APP binds DR6 to trigger axon pruning and neuron death via distinct caspases.* Nature, 2009. **457**(7232): p. 981-9.

75. Picone, P., et al., *Abeta oligomers and fibrillar aggregates induce different apoptotic pathways in LAN5 neuroblastoma cell cultures.* Biophys J, 2009. **96**(10): p. 4200-11.

76. Fossati, S., J. Ghiso, and A. Rostagno, *TRAIL death receptors DR4 and DR5 mediate cerebral microvascular endothelial cell apoptosis induced by oligomeric Alzheimer's Abeta.* Cell Death Dis, 2012. **3**: p. e321.

77. Fossati, S., J. Ghiso, and A. Rostagno, *Insights into caspase-mediated apoptotic pathways induced by amyloid-beta in cerebral microvascular endothelial cells.* Neurodegener Dis, 2012. **10**(1-4): p. 324-8.

78. Cha, M.Y., et al., *Mitochondria-specific accumulation of amyloid beta induces mitochondrial dysfunction leading to apoptotic cell death.* PLoS One, 2012. **7**(4): p. e34929.

79. Murakami, Y., et al., *Cytoprotective role of mitochondrial amyloid beta peptide-binding alcohol dehydrogenase against a cytotoxic aldehyde.* Neurobiol Aging, 2009. **30**(2): p. 325-9.

80. Verdier, Y., M. Zarandi, and B. Penke, *Amyloid beta-peptide interactions with neuronal and glial cell plasma membrane: binding sites and implications for Alzheimer's disease.* J Pept Sci, 2004. **10**(5): p. 229-48.

81. Dahlgren, K.N., et al., *Oligomeric and fibrillar species of amyloid-beta peptides differentially affect neuronal viability.* J Biol Chem, 2002. **277**(35): p. 32046-53.

82. Resende, R., et al., *Neurotoxic effect of oligomeric and fibrillar species of amyloid-beta peptide 1-42: involvement of endoplasmic reticulum calcium release in oligomer-induced cell death.* Neuroscience, 2008. **155**(3): p. 725-37.

83. Thapa, A., et al., *Biflavonoids are superior to monoflavonoids in inhibiting amyloid-beta toxicity and fibrillogenesis via accumulation of nontoxic oligomer-like structures.* Biochemistry, 2011. **50**(13): p. 2445-55.

84. Evans, C.G., S. Wisen, and J.E. Gestwicki, *Heat shock proteins 70 and 90 inhibit early stages of amyloid beta-(1-42) aggregation in vitro.* J Biol Chem, 2006. **281**(44): p. 33182-91.

85. Sabirzhanov, B., et al., *Over-expression of HSP70 attenuates caspase-dependent and caspase-independent pathways and inhibits neuronal apoptosis.* J Neurochem, 2012. **123**(4): p. 542-54.

86. Chromy, B.A., et al., *Self-assembly of Abeta(1-42) into globular neurotoxins.* Biochemistry, 2003. **42**(44): p. 12749-60.

87. Xue, W.F., S.W. Homans, and S.E. Radford, *Systematic analysis of nucleation-dependent polymerization reveals new insights into the mechanism of amyloid*

self-assembly. Proc Natl Acad Sci U S A, 2008. **105**(26): p. 8926-31.

88. Wogulis, M., et al., *Nucleation-dependent polymerization is an essential component of amyloid-mediated neuronal cell death.* J Neurosci, 2005. **25**(5): p. 1071-80.

89. Hoffmann, J.C., et al., *A new C-terminal cleavage product of procaspase-8, p30, defines an alternative pathway of procaspase-8 activation.* Mol Cell Biol, 2009. **29**(16): p. 4431-40.

90. Cowling, V. and J. Downward, *Caspase-6 is the direct activator of caspase-8 in the cytochrome c-induced apoptosis pathway: absolute requirement for removal of caspase-6 prodomain.* Cell Death Differ, 2002. **9**(10): p. 1046-56.

91. Monnier, P.P., et al., *Involvement of caspase-6 and caspase-8 in neuronal apoptosis and the regenerative failure of injured retinal ganglion cells.* J Neurosci, 2011. **31**(29): p. 10494-505.

92. Slee, E.A., et al., *Ordering the cytochrome c-initiated caspase cascade: hierarchical activation of caspases-2, -3, -6, -7, -8, and -10 in a caspase-9-dependent manner.* J Cell Biol, 1999. **144**(2): p. 281-92.

93. Salvesen, G.S. and V.M. Dixit, *Caspase activation: the induced-proximity model.* Proc Natl Acad Sci U S A, 1999. **96**(20): p. 10964-7.

94. Morishima, Y., et al., *Beta-amyloid induces neuronal apoptosis via a mechanism that involves the c-Jun N-terminal kinase pathway and the induction of Fas ligand.* J Neurosci, 2001. **21**(19): p. 7551-60.

95. Jan, A., et al., *Abeta42 neurotoxicity is mediated by ongoing nucleated polymerization process rather than by discrete Abeta42 species.* J Biol Chem, 2011. **286**(10): p. 8585-96.

96. Majkut, J., et al., *Differential affinity of FLIP and procaspase 8 for FADD's DED binding surfaces regulates DISC assembly.* Nat Commun, 2014. **5**: p. 3350.

97. Dickens, L.S., et al., *A death effector domain chain DISC model reveals a crucial role for caspase-8 chain assembly in mediating apoptotic cell death.* Mol Cell, 2012. **47**(2): p. 291-305.

98. Hippe, D., et al., *Fas/CD95-mediated apoptosis of type II cells is blocked by Toxoplasma gondii primarily via interference with the mitochondrial amplification loop.* Infect Immun, 2008. **76**(7): p. 2905-12.

99. Kienlen-Campard, P., et al., *Intracellular amyloid-beta 1-42, but not extracellular soluble amyloid-beta peptides, induces neuronal apoptosis.* J Biol Chem, 2002. **277**(18): p. 15666-70.

100. Wirths, O., et al., *Intraneuronal Abeta accumulation precedes plaque formation in beta-amyloid precursor protein and presenilin-1 double-transgenic mice.* Neurosci Lett, 2001. **306**(1-2): p. 116-20.

101. Chui, D.H., et al., *Transgenic mice with Alzheimer presenilin 1 mutations show accelerated neurodegeneration without amyloid plaque formation.* Nat Med, 1999. **5**(5): p. 560-4.

102. Catanzariti, A.M., et al., *An efficient system for high-level expression and easy purification of authentic recombinant proteins.* Protein Sci, 2004. **13**(5): p. 1331-9.

103. De Marco, V., et al., *The solubility and stability of recombinant proteins are increased by their fusion to NusA.* Biochem Biophys Res Commun, 2004. **322**(3): p. 766-71.

104. Kapust, R.B. and D.S. Waugh, *Escherichia coli maltose-binding protein is uncommonly effective at promoting the solubility of polypeptides to which it is fused.* Protein Sci, 1999. **8**(8): p. 1668-74.

ABREVIATIONS USED

The abbreviations used are:

Aβ, amyloid β;

AD, Alzheimer's disease;

DISC, death-inducing signaling complex;

DM, prodomainless caspase-8 double mutant mimicking p30 fragment of caspase-8;

MTT, 3-(4,5-dimethylthiazol-2-yl)-2,5-diphenyl tetrazolium bromide;

p18-10, prodomainless equivalent of p41/43 fragment of caspase-8;

p30, ~30 kDa fragment of caspase-8;

p41/43, ~41/43 kDa fragment of caspase-8;

PBS, phosphate-buffered saline;

SDS-PAGE, sodium dodecylsulfate-polyacrylamide gel electrophoresis;

SEC, Size exclusion column chromatography;

STS, staurosporine;

DMEM, Dulbecco's modified Eagles medium;

DTT, Dithiothreitol;

fAβ, Fibrillar form of Aβ;

FBS, Fetal bovine serum;

ACKNOWLEDGEMENTS

Firstly, I would like to express my wholehearted gratitude to my supervisor Prof. Il-Seon Park for his continuous and judicious supervision, advice, guidance and training throughout this study. His extraordinary knowledge covering the large areas of protein biochemistry has been invaluable and a great support for my dissertation work. I would like to extend my gratitude to Prof. Song Yub Shin, Prof. Takbum Ohn and Prof. Lee Jung Hee for their valuable suggestions and support in various ways.

I reserve the deep note of appreciation to my previous supervisor Prof. Sohel Rana and my mentor in academic and personal life Prof. Gazi Mosharof Hossain for their contribution in my life. I would like to thank National Institute for International Education (NIIED) Korea, for the financial supports I got throughout my study period. I gratefully thank to my seniors Dr. Sharoar and Dr. Vijay for their training at early stage of my research and immense support during my work and to my colleague Aminul for their countless help. All the members of Molecular and cell Biology, Peptide Biochemistry, Peptide Engineering lab and Korea DNA Repair laboratory get warmest thanks for giving the chance of sharing their facilities.

Finally, I would like to thank my parents, my sisters and brothers and my wife for her inspiration, continuous supports and best care and love which made my journey a pleasant one.

August 2015

Ph.D. Dissertation

Mechanistic study of intracellular processes of amyloid β-induced cell death: caspase activation related to intrinsic apoptotic pathway and nuclear disruption

Graduate School of Chosun University

Department of Bio-Materials

Md. Imamul Islam

Mechanistic study of intracellular processes of amyloid β-induced cell death: caspase activation related to intrinsic apoptotic pathway and nuclear disruption

아밀로이드 베타에 의한 세포사의 세포내 반응의 기전적 연구: 내부 세포자살 경로에 의한 케스페이즈의 활성화와 세포핵의 해체

August 25, 2015

Graduate School of Chosun University

Department of Bio-Materials

Md. Imamul Islam

Mechanistic study of intracellular processes of amyloid β-induced cell death: caspase activation related to intrinsic apoptotic pathway and nuclear disruption

Advisor: Prof. Il- Seon Park

This dissertation is submitted to the Graduate School of Chosun Univeristy in partial fulfillment of the requirements for the degree of Doctor of Philosophy in Science

April 2015

Graduate School of Chosun University

Department of Bio-Materials

Md. Imamul Islam

This is to certify that the PhD thesis of **Md. Imamul Islam** has successfully met the dissertation requirements of Chosun University.

Chairman (Chosun Univ.) : Prof. Song Yub Shin .....

Member (Chosun Univ.) : Prof. Park Il Seon.....

Member (Chosun Univ.) : Prof. Takbum Ohn.....

Member (Chosun Univ.) : Prof. Lee Jung Hee.....

Member (Yonsei Univ.) : Prof. Cho Beong Yon.....

June 2015

Graduate School of Chosun University

CONTENTS

LIST OF FIGURES

초록

아밀로이드 베타에 의한 세포사의 세포내 반응의 기전적 연구: 내부 세포자살 경로에 의한 케스페이즈의 활성화와 세포핵의 해체

엠디 이마물 이슬람
지도교수: 박 일 선
생물신소재학과
조손대학교 대하권

AD에서 아밀로이드 베타는 노인성 반점의 주 성분으로 세포 사멸을 유도한다. Apoptotic pathway는 세포사멸과정에 활성화 되는 것으로 알려져 있고 케스페이즈 활성화는 그 대표적인 특징 중 하나이다. 그러나 stausporine에 의해 유도되는 내인성 경로 세포사멸은 apaf-1 apoptosome 복합체를 형성하고, caspase-9을 활성화시키며, 하류 케스페이즈의 아밀로이드 베타 펩타이드에 의해 억제된다고 알려져 있다. 따라서 케스페이즈 활성화 메커니즘과 아밀로이드 베타에 의해 유도되는 세포사멸 경로에 대한 연구는 필요하다. 아밀로이드 베타를 2시간 동안 2번 처리하고, 22시간 반응시킨 세포에서는 Apaf-1, caspase-9, cytochrome c등을 포함하는 단백질 복합체인 apoptosome이 발견되었지만, 24시간동안 아밀로이드 베타를 한번 처리한 것은 apoptosome 복합체를 형성을 유도하지 않았다. 케스페이즈-8은 외인성경로인 death inducing signaling complex (DISC)형성으로 인해 활성화될 수 있고, 세포사멸신호의 증폭을 위한

내인성 경로에서는 아밀로이드 베타를 2+22시간 처리한 세포에서 활성되었으나 활성화된 케스페이즈-8은 기질인 Bid를 자르기에는 충분하지 못했다. 따라서, DISC는 형성되지 않았으며, 이것은 케스페이즈-8이 내인성 경로에 의해 활성화 된 것을 의미한다. 케스페이즈-8의 *in vitro* 활성화는 세포추출물과 dATP/사이토크롬 c 또는 정제된 케스페이즈-3과-6에 의해 유도되고, 활성화된 케스페이즈-8(43/41 kDa)은 추가로 처리된 아밀로이드베타에 의해 영향을 받지 않았다. 따라서, 케스페이즈-8은 내인성 경로를 통해 활성화되지만 그것의 약한 활성 때문에 세포사멸 신호전달 메커니즘에서의 역할은 여전히 불분명하다.

Lamin A/C와 B는 케스페이즈-6와 NS 프로테아제의 표적이고, 절단된 단백질 산물이 두 경우에 다르고 세포사멸의 경로는 절단산물에 의해 결정될 수 있기 때문에 아밀로이드 베타를 2+22시간 처리한 세포에서 Lamin A/C와 B 절단을 분석하였다. 아밀로이드베타를 처리한 경우 46kDa와 21kDa의 Lamin A와 B의 양이 모두 줄어든 반면, 28kDa와 46kDa 단백질은 케스페이즈-6의 활성이 있을 것으로 기대된다. 따라서 NS 프로테이즈는 내인성경로에서 케스페이즈-6보다 2+22시간 아밀로이드베타를 처리한 세포에서의 절단에 더 두드러진 역할을 한다.

staurosporin 처리된 세포에서 라민 단백질의 절단을 위해 케스페이즈-6의 활성화는 일어나지만 아밀로이드베타를 2+22시간 처리한 세포에서는 케스페이즈-6 활성화는 현저하게 증가되지만 Lamin 단백질의 절단은 일어나지 않는다. 또한 컨포컬 현미경, size-exclusion 크로마토그래피, immunoprecitation을 통해 케스페이즈는-6와 아밀로이드 베타가 상호작용함을 확인하였고 라민단백질로 케스페이즈-6의 활성은 상호작용을 지연시키는 것으로 보인다.

마지막으로, 아밀로이드 베타의 세포독성이 세포 내 또는 세포외의 과정 때문인지 연구하였다. Tat-Ab42 and flag-Ab42 펩타이드는 각각 세포막과 세포질에 위치한 것으로 밝혀졌다. Tat-Ab42는 강력한 세포독성을 나타냈고, flag-Ab42는 세포독성이 나타나지 않았다. 따라서 세포내 과정이 세포독성에 대한 주요 원인이 될 것으로 보인다. 결론적으로, 아밀로이드 베타는 NS 프로테아제를 포함하는 내인성 세포사멸 경로를 유도하지만, 세포내 세포독성을 증가시키는데 기여할 것으로 보인다.

ABSTRACT

Mechanistic study of intracellular processes of amyloid β-induced cell death: caspase activation related to intrinsic apoptotic pathway and nuclear disruption

Md. Imamul Islam

Advisor: Prof. Il-Seon Park

Department of Biomaterials

Graduate School of Chosun Univeristy

Amyloid β (Aβ), a main component of the senile plaque detected in Alzheimer's disease, induces cell death. Apoptotic pathway is known to be activated in the death process. Caspase activation is one of the hallmarks of the pathway. However, it was previously shown that the intrinsic pathway of apoptosis induced by staurosporine (STS) in which formation of apaf-1 apoptosome complex and activation of caspase-9 and the downstream caspase could be suppressed by Aβ peptide. Thus, the mechanism of activation of caspases and the involved apoptotic pathway induced by Aβ needs to be explored. It was found that apoptosome, a protein complex containing Apaf-1, caspase-9, cytochrome c and others, was formed in cells treated with Aβ twice for 2 h and following 22 h (2+22 h), while a single treatment of Aβ to the cells for 24 h did not induce the formation. Caspase-8 which can be activated by the extrinsic

pathway through the formation of death inducing signaling complex (DISC) and intrinsic pathway for the amplification of the death signal was also activated in the cells treated with Aβ for 2+22 h, although the level was not sufficient to cleave Bid, the substrate of caspase-8. DISC was not formed, implying that caspase-8 was activated by intrinsic pathway. The in vitro activation of caspase-8 using cell extract and dATP/cytochrome c or purified caspase-3 and -6 was observed, and the formation of active caspase-8 fragments 43/41 kDa protein was negatively affected by added Aβ. Thus, we suggest that caspase-8 is activated by the intrinsic pathway, but its role in the apoptotic signal transduction is still obscure because of its weak activity.

Next, the role of the activated intrinsic apoptotic pathway in the Aβ-treated cell death was explored. Cleavage of Lamin A/C and B was examined in the 2+22 h Aβ-treated cells, because the proteins are the target of caspase-6 and NS protease and the cleaved products are different in the two cases, implying that the cell death pathway can be determined by the products. Levels of both Lamin A and B (not C) were reduced by the Aβ treatment to produce 46 (N-terminus detection by western blot) and 21 (C-terminus detection by western blot) kDa proteins, respectively, while 28 and 46 kDa proteins for each protein were expected for caspase-6 activity. Thus, it was concluded that NS protease plays a predominant roles in the cleavage in the 2+22 h Aβ-treated cells rather than caspase-6, activation of which is a part of the intrinsic apoptotic pathway.

Caspase-6 was a protease responsible for the cleavage of Lamin proteins in staurosporin-treated cells, while it was not in the 2+22 h Aβ-treated cells, although the caspase was prominently activated in the cells. It was found in confocal microscope, size-exclusion chromatography and immunoprecitation studies that caspase-6 interacts with Aβ. It appears that the interaction might retard the action of capase-6 to Lamin proteins.

Finally, it was explored whether Aβ cytotoxicity is due to extracellular or intracellular processes. Tat-Aβ42 and flag-Aβ42 peptides were constructed and were found to be located at cytoplasm and cell membrane, respectively. Tat-Aβ42 showed robust cytotoxicity, while flag-Aβ42 was not cytotoxic. Thus, an intracellular process seems to be a major cause for the cytotoxicity.

In conclusion, Aβ induced intrinsic apoptotic pathway and NS-protease-involved process, but the latter appears to contribute more to its cytotoxicity which might be intracellular.

I. Introduction

I - 1. The β-Amyloid peptide and Alzheimer's disease

The ~4 kDa Aβ peptide, derived from its precursor protein called amyloid precursor protein (APP), was first isolated as the principal component of amyloid deposits in the brain and cerebrovasculature of Alzheimer's disease. Although the function of APP itself has yet to be resolved, extensive research has been conducted on how the Aβ peptide is produced, and how it is subsequently degraded within the brain, or transported out into the periphery. And these factors determine the final amount of Aβ that accumulates as amyloid deposits within the brain. Alzheimer's disease is characterized clinically by a progressive and gradual decline in cognitive function and neuropathologically by the presence of neuropil threads, specific neuron loss, and synapse loss in addition to the hallmark findings of neurofibriallary tangles and senile plaques. The composition of this senile plaque is, in large part, highly insoluble Aβ in the parenchymal region of the brain.

Metabolism of APP to Aβ by the enzymatic processes is now reasonably well established. APP is sequentially cleaved by two membrane-bound endoprotease activities, β- and γ-secretase. β-secretase first cleaves APP to release a large secreted derivative, sAPPβ[1, 2]. A fragment of 99 amino acids (CTFβ, which begins with the N-terminal aspartyl residue of Aβ) remains membrane bound, and is in turn rapidly

cleaved by γ-secretase to generate Aβ [3]. Cleavage by γ-secretase is somewhat nonspecific, resulting in the formation of different C-terminal heterogeneous peptides. So, numerous different Aβ species exist, but those ending at position 40 (Aβ40) are the most abundant (~80-90%), followed by 42 (Aβ42, ~5-10%). The marginally longer forms of Aβ, specifically Aβ42, are more hydrophobic and fibrillogenic, and are the principal species deposited in the brain [1, 4, 5]. β-secretase activity is thought to be the rate limiting step in the amyloidogenic pathway, which processes ~10% of the total cellular APP. The residual APP, about 90%, is constitutively cleaved by α-secretase (a group of metalloprotease enzymes), generating sAPPα and the 83 amino acid CTFα.

The subsequent cleavage of CTFα by γ-secretase produces the more benign p3 fragment a 3 kDa peptide, instead of Aβ. γ-Secretase cleavage of either membrane bound CTF also generates a cytosolic element, AICD (APP intracellular domain, sometimes referred to as CTFγ), which may have a role in signaling pathway [4, 6-8]. Because of its essential role in the Alzheimer's disease pathogenesis, the longer form of Aβ, (Aβ42) is considered a major target for the study of its underlying mechanism of cell cytotoxicity. This study was also focused to delineate the mechanism of apoptosis induced by a particular structural form of Aβ42.

I-2. Multimeric Conformation and cytotoxicity of Aβ

The biological effect of different species of Aβ is reported to be dependent on the assembly of Aβ into multimeric structures. There are two phases of assembly which have different characteristics and lead to formation of different species of Aβ with different biological properties. Initial research with the pathogenesis of Aβ focused on the extracellular hallmarks of AD, the amorphous and fibrillar deposits of the peptide. Present focus is on the earlier phase of Aβ assembly which involves soluble oligomers of the peptide. These structures are orders of magnitude more toxic to different types of cells than are the fibrils and trigger a different set of toxic events [9]. They are also different in morphologically and conformationally and recognized by specific antibodies. Oligomer specific antibodies do not recognize fibrils or monomer, and soluble oligomers are not recognized by fibril specific antibodies. Though complete rejection of fibril involvement in Alzheimer's disease at this time point is possibly premature because of the potential for plaque involvement with oligomer species [10], the current focus of the Aβ research field has shifted to soluble oligomers. Aβ42 peptide forms the oligomers more readily than the more abundant Aβ40 [11] . The ratio of Aβ 42/40 and age of disease onset play an important role in familial AD [12, 13]. The C-terminus of Aβ42 is reported to be crucial for oligomer formation [14]. While the early intermediates during oligomerization of recombinant purified peptide are

unstable and require trapping of the intermediates, stable small oligomers can be isolated from biological systems. The reason for this difference in stability is yet to be explored. Chemically stable Aβ oligomers even the dimers, isolated from AD brain and CSF have been shown to disrupt synaptic electrophysiology [15, 16]. On the other hand, fibrillar Aβ is thermodynamically favorable and accomplishes by the addition of monomers to the end of existing nucleus, leading to rapid extension of fibrils [17]. Process of Aβ fibrilization is thought to be preceded by multiple conformational changes including trimer, pentamer or higher molecular weight complex formation, known as Aβ – derived diffusible ligands (ADDL) [18], oligomers consisted of 15-20 monomeric units (AβOs) [19], protofibrils and other higher molecular weight oligomers. It is also reported that there is a linear relationship between the fibril formation and the concentration of monomer present in the sample [20]. Also some study revealed that, insoluble Aβ fibrils may act as the reservoir of soluble and highly toxic oligermic form of Aβ [10]. To study of fibril formation of by synthetic or recombinant Aβ, usually high concentrations (μM) range is used to facilitate the probability of a fibril nucleus formation. But the concentration of soluble oligomers in CSF or brain interstitial fluid is in the pM range, hence there is a chance that in in vivo case, fibril formation is nucleated on extracellular matrix or cell surfaces.

Although, most of the investigators of these days are in consensus that soluble oligomers are biologically active and are the cause of cellular

cytotoxicity under some conditions, the mechanism of action of soluble oligomeric species of Aβ still remains to be resolved. This study was conducted to find out the mechanism of intracellular process of cytotoxicity induced by soluble oligomeric species of $A\beta_{42}$.

I-3. Mechanism(s) of Aβ induced cytotoxity

Though it is thought to be the central role player of the Alzheimer's disease pathology, the mechanism of Aβs mediated cytotoxicity is still inconclusive. The cellular events that occur between the production of Aβ and neuronal loss are yet to be revealed. Several hypotheses have been proposed regarding the relation of Aβ production and neuronal degeneration and toxicity. There is no dispute regarding the presence of intracellular Aβ, but the function of this intracellular Aβ in disease progress remains controversial. The burning question is the source of the accumulated Aβ inside the neuronal cells, whether this accumulations result from the direct deposition of intracellularly produced Aβ or uptake of the extracellularly produced Aβ. Because the APP is reported to be present in membranes of mitochondria, the trans-Golgi network, endoplasmic reticulum (ER), endosomes, autophagosomes, and lysosomes in addition to plasma membrane [21]. β- and γ-secretases have been found to be present in these subcellular compartments. Hence, intracellular accumulation may be occurred by intracellular production of Aβ in favorable condition. Nonetheless, there is no question that significant amount of Aβ is

produced in the plasma membrane by cleaving the APP and make the extracellular deposition. Reports have shown that, this extracellular Aβ can be re-uptake by cells through membrane micro domain called lipid rafts and contribute to intracellular deposition [22, 23]. A positive correlation is shown in several studies between the plasma membrane binding of Aβ and the cytotoxicity induced by the peptide [24, 25]. Aβ has been found to bind with a number of receptors or receptor related proteins such as N-methyl-D-aspartic acid (NMDA) receptor [26], low-density receptor associated protein-1 [27], the α7 nicotinic acetyl choline receptor [28], the p75 neurotrophin receptor [29], and the receptor for advanced glycation endproducts [30]. Membrane binding of Aβ has been reported as a necessary step to exert the toxicity by peptide [31], while the interaction of Aβ with receptor associated protein (RAP) have been found to promote the cellular internalization of the peptide [32]. A recent study has been reported a new interaction of Aβ peptide with lipoprotein lipase (LPL) which promoted the membrane association and cellular uptake of the peptide [33].

The first order interaction of Aβ with cell membrane and receptors, however, facilitate the membrane permeability and internalization of the peptide. The binding of Aβ to membrane stimulates the Aβ aggregation due to the interaction between the anionic lipid and the peptide which enhances the structural transition of the peptide from random coils to β-sheet structure [34]. This enhancement of structural conversion along with increased membrane permeability leads to the

formulation of the 'channel hypothesis', postulated on the evidence of the formation of ion channel by Aβ peptides [35], and at least eight different ion channels have been characterized [36]. A report has been shown that the interaction of Aβs with the membrane leads to the formation of small oligomeric complexes which have been found to form multimeric channels with a central pore- like structure [37].

I-4. Reuptake mechanism of Aβ and interaction with intracellular Protein

The mechanism of intracellular accumulation of Aβ has created a growing interest of concern. Several pathways have been proposed to describe the event. Internalization via endocytosis and accumulation in the endosomal/lysosomal systems have been suggested by an earlier study [38]. Endocytosis is a widely studied phenomenon in cell biology and several different pathways have been proposed for different protein machinery [39].

The conventional endocytic pathway contains invagination of the plasma membrane at the site of the receptor-cargo binding; the invaginated vesicle is then coated with adaptor proteins, which recruit guanosine triphosphatases (GTPases) that provide the necessary energy to facilitate cleavage of the vesicle from the cell membrane and delivery to endosomes or other subcellular compartments. By far the most frequently reported process is dependent on clathrin and dynamins. A recent *in vitro* study demonstrated that endocytosis of Aβ is regulated by

a dynamin dependent and RhoA mediated pathway [40]. LRP1, a receptor protein which facilitates Aβ uptake, is reported to do it via a clathrin dependent manner in neuroblastoma cells and neuronal cell lines [41]. Aside of endocytosis mechanism, selective accumulation of Aβ occurs via a nonstable, energy independent and nonendocytotic pathway is reported in PC12 cells and cortical and hippocampal neurons [42]. Endocytosis mechanism is shown to be varied not only with cell types but also in different regions of neurons [43]. The specific pathways involved in up taking and intracellular accumulation of Aβ peptides, however, remains inconclusive.

Aβ interacts with a number of other proteins as exemplified in a recent proteomic analysis for artificial β protein and Aβ interactor [44]. That report indicated that amyloidogenic aggregation can result in the sequestration of numerous proteins such as translation initiation factors, chromatin regulators, RNA processing proteins, mitochondrial membrane proteins and chaperones. It is certain that the sequestration of essential proteins results in cell death.

Besides the sequestration, Aβ can directly induce cell death by binding to receptors such as the p75 neurotrophin receptor, a member of the TNF-receptor superfamily, which in fact induces cell death [45, 46]. Furthermore, interaction with some intracellular Aβ-binding proteins such as alcohol dehydrogenase (ABAD) and cytochrome c (Cyto c) oxidase also induces cell death [47, 48]. This interaction was shown to

result in free-radical generation in neurons, suggesting direct molecular link from Aβ to mitochondrial toxicity [49]. Further, the mitochondrial dysfunction and synaptic damage induced in Aβ-treated cells results in the loss of mitochondrial membrane potential and increase in mitochondrial superoxides [50]. As result, Bax protein increases and Cyto c is released from mithochondria. Aβ also seems to induce a signal transduction pathway as shown in increase of c-Jun N-terminal kinase activity, which is associated with cell death pathway such as apoptosis [51]. A recent study also shown that, Aβ can bind to procaspase-9 which results in inhibition of the apaf-1 apoptosome assembly the hallmark of the intrinsic apoptotic pathway [52].

I-5. Role of Aβ in Apoptosis

The term ‘apoptosis’ also known and accepted as a distinct and important mode of programmed cell death, involves a series of biochemical events to eliminate the cells which are genetically determined. This is a highly harmonized and energy dependent process which usually requires the activation of a cascade of cysteine proteases called ‘caspases’ that links from the initial stimuli to the final demise of the cells. However, other forms of programmed cell deaths are reported recently and many other programmed cell death mechanism may yet be evolved [53, 54]. The apoptotic processes play important roles during development, aging, homeostatic mechanism to maintain the cell populations and also as a defense mechanism when cells get damaged by

disease or other toxic agents.

To date, according to the investigation reports, there are two main apoptotic pathways: the extrinsic or death receptor pathway and the intrinsic or mitochondrial pathway.

Intrinsic mitochondria-dependent apoptosis is characterized by formation of a multiprotein complex called an apoptosome consisting of Apaf-1, Cyto c, dATP and procaspase-9 after release of Cyto c from mitochondria [55]. The formation of this protein complex is essential for intrinsic apoptosis and is tightly regulated in healthy cells in which Cyto c is stored in mitochondria and the intracellular concentration of K+ is high (~150 mM) enough to inhibit the formation [56]. It is also regulated by other proteins such as heat shock protein 70 which binds to Apaf-1 and prevents the formation of the multiprotein complex [57]. The formation of the apoptosome leads to activation of caspase-9 which proteolytically cleaves caspase-3 for activation [58]. The extrinsic apoptotic pathway is receptor mediated pathway. Extracellular ligands such as, TNFα, CD95 and Trail bind to the death receptors to form death inducing signaling complex (DISC) which activate caspase-8 in non-mitochondrial pathway [59].

Both the intrinsic and extrinsic apoptotic pathways end with execution phase, involves the processing of effector caspases such as caspase-3, -6 and -7 which are involved in most of the downstream effects of apoptotic processes [60, 61]. Involvement of Aβ both in in vitro

and in vivo apoptotic process has been reported in several investigations [62, 63]. To describe the mechanism of Aβ induced apoptosis, several hypothesis have been proposed. The mitochondrial release of apoptosis inducing factor (AIF) in cultured neurons, and the release of cytochrome c from isolated mitochondria in presence of Aβ have been suggested, which subsequently initiates a caspase independent apoptosis by causing DNA fragmentation and chromatin condensation [59, 60, 64]. Binding of Aβ to p75 neurotrophin receptor can trigger the extrinsic pathway, while the mitochondrial dysfunction caused by the peptide can trigger the intrinsic pathway. Beside the two apoptotic pathways, caspase-4-mediated apoptosis is also induced by the unfolded protein response signaling pathway when endoplasmic reticulum stress involved in neurodegenerative disease including AD is prolonged [65].

I-6. Out Line of the Thesis

The thesis includes the investigation of intracellular events occurs in the apoptotic processes induced by oligomeric species of Aβ42. The initial part consists of the study of the conditions in which potential activation of caspases occurs, and elucidation of the related cell death mechanism under the condition. The second part presents a new interaction mechanism of Aβ42 peptide with a protein involved in programmed cell death process. And the last part deals with the purification of a cell penetrating version of Aβ42 that is, TAT- Aβ42 and comparative study of TAT- Aβ42, wild type Aβ42 and FLAG- Aβ42 in terms of cell death and cell penetration characteristics. The rational of these studies is

summarized below:

1. The mechanism and role of apoptotic pathway induced by Aβ42 oligomeric species has been elucidated. Activation of intrinsic and extrinsic apoptotic pathway has been checked and found that only intrinsic apoptotic pathway has been activated by oligomeric species of Aβ42. Then the effects of this activated intrinsic apoptotic pathway have been analyzed.
2. Interaction of Aβ42 with caspases was screened by confocal microscopy. A novel interaction between Aβ42 and caspase-6 has been outlined and the consequences of the interaction have been analyzed.
3. Cell penetrating TAT- Aβ42 was expressed and purified and characterized in terms of cell death and cell penetration ability by comparing with wild type Aβ42 and FLAG- Aβ42.

II. Activation of intrinsic apoptotic pathway by amyloid β

Abstract

Amyloid-β (Aβ), a main component of the senile plaque detected in Alzheimer's disease, induces cell death. Apoptotic pathway accompanying caspase activation is known to be involved in the death process. However, the role of apoptosis in the cell death was questionable, as limited activation of caspases in Aβ-treated cells frequently observed and also found that Aβ peptide could suppress the intrinsic apoptosis pathway. Here we sought conditions in which caspases are potently activated in Aβ-induced cell death and to explore related death pathways under the condition. Single treatments of Aβ42 to cells for up to 48 h barely induce caspase activation. However, when cells were treated with Aβ42 twice for 2 h and following 22 h (2+22 h) or more, caspase-9-activating protein complex apoptosome was found to be formed and caspases could be activated, implying activation of intrinsic apoptosis pathway. 30-kDa and 41/43-kDa fragments derived from procaspase-8 were recognized in the early and later stage of Aβ treatment, respectively. Formation of DISC, caspase-8-activating death inducing signaling complex was absent in the 2+22 h sample, indicating no involvement of extrinsic apoptotic pathway in the process. The fragments of caspase-8 are all found to be produced through intrinsic pathway. We suggest that intrinsic pathway is the main apoptosis pathway in Aβ-treated cells.

II-1. INTRODUCTION

Amyloid β (Aβ) is 36-43 amino acid-long peptides to elicit the neurodegenerative Alzheimer's disease (AD) [66]. The peptide is generated by proteolytic cleavage of the amyloid precursor protein by α-, β- and γ- secretases [4, 67]. Monomeric Aβ is prone to change its conformation to β-sheet-rich intermediate structures. The intermediates interact with each other to form multimeric aggregates such as oligomers, protofibrils and fibrils [19, 68, 69]. The aggregated Aβ progressively deposits in brain parenchyma and cerebral blood vessels [70]. The soluble Aβ oligomers and protofibrils have been found to be more toxic than the fibrils, suggesting that the oligomeric aggregates would be the main factor for AD [19, 71].

Essential role of apoptosis in eliciting Aβ cytotoxicity has been proposed, because caspases are activated in cells treated with the peptide [72-75]. Caspase, a hallmark enzyme of apoptosis, is synthesized as a zymogen form which is activated by apoptotic signal. Caspase-8 is processed and catalytically activated through receptor-mediated apoptosis, or extrinsic apoptosis in which the death-inducing signaling complex (DISC) is form [76]. On the other hand, chemical-induced apoptosis or caspase-dependent intrinsic apoptosis leads to activation of caspase-9 which is associated with cytochrome c released from the mitochondria, dATP and an adaptor protein Apaf-1 to form mutiprotein complex called apoptosome [75-77]. Once activated, caspase-8 and -9 then process effector caspases, including caspase-3, -6 and -7 which subsequently transduce the death signal by cleaving other proteins [60, 61].

Binding of Aβ to receptors such as death receptor or p75 neurotrophin receptor can trigger the extrinsic pathway [45, 46], while impaired autophagic degradation of the damaged mitochondria during aging [78] may lead to the accumulation of Aβ in the mitochondrial membrane in neurons and following release of cytochrome c [78, 79]

which can trigger the caspase cascade of the intrinsic pathway [78]. On the other hand, caspase-4-mediated apoptosis is also induced by the unfolded protein response signaling pathway when endoplasmic reticulum stress is prolonged [65]. The differential activation of each pathway depends on proteins or factors that interact with Aβ [25, 80] and the conformational states of Aβ (oligomer vs. fibril) [75, 81, 82].

Although a major role of apoptosis in Aβ-induced cell death is evident, we often found that caspase activation was not potent in Aβ-treated cells [83], and also see "Result". We recently found that caspase activation and cell death induced by staurosporine (STS), employed to induce the intrinsic mitochondria-dependent apoptotic pathway, was significantly reduced by Aβ42 [52]. The inhibitory effect of Aβ42 on the apoptotic pathway is associated with its interaction with procaspase-9 and consequent inhibition of Apaf-1 apoptosome assembly. It is also possible that Aβ42 interacts with other proteins involved in apoptosis and disturbs their function, resulting in the low levels of caspase activation, as the peptide found to interact with many proteins [84, 85]. However, on the basis of reports regarding Aβ-induced apoptosis we speculate that the inhibitory effect can be overcome such that caspase can be potently activated. In the current study, we probed apoptosis pathways under the experimental condition leading to robust caspase activation in Aβ-treated cells.

II-2. MATERIALS AND METHODS

Materials

Fetal Bovine serum (FBS) was purchased from Life Technology Inc. (Grand Island, USA). Dulbecco's modified Eagles medium, high glucose (DMEM/HG) was obtained from Welgene (Daegu, Korea). Caspase-9, Caspase-8, Caspase-6 and Caspase-3 substrates, N-acetyl Leu-Glu-His-Asp-amino methyl coumarin (Ac-LEHD-AMC), Ac-IETD-AMC, Ac-VEID-AMC and Ac-DEVD-AMC, respectively, were from A.G. Scientific Inc. (San Diego, USA). Ni-NTA column were purchased from Amersham Biosciences (Piscataway, USA). Western blotting detection kit (WEST-ZOL PLUS) from iNtron Biotechnology (Gyeonggi-do, Korea). Phosphate buffer saline (PBS) purchased from Amresco (solon, USA). Anti-caspase-9, anti-caspase-3, anti-lamin-A/C, anti-lamin B and anti-β-actin from Santa Cruz Biotechnology (California, USA), anti-caspase-8 from Cell Signaling Technology (Massachusetts, USA), anti-DFF45 from BD Transduction Laboratory (San Diego, USA), anti-FADD from AbFrontier and anti-Bid developed in laboratory. Polyclonal antibody anti-caspase-9(p10) obtained from Santa Cruz Biotechnology, Urea was from USB chemicals, Acetonitrile from Merck (Darmstadt, Germany). All other chemicals obtained from Sigma (St. Louis, USA), unless otherwise stated.

Preparation of Aβ peptide

The purified peptide was solubilized in 100% 1,1,1,3,3,3,-hexafluoro-2-propanol, and dried under nitrogen flow and subsequently, under vacuum for 30 min. The peptide aliquots were stored at –20 °C until use. Immediately before use, the peptide was dissolved in 0.1% NH_4OH at a concentration of 2 mg/ml followed by bath sonication for 10 min in ice cold water. The solution was diluted at the desired concentration with cell culture media without FBS. Aβ42 oligomers were prepared as described earlier [86] with little modification. Briefly, peptides were diluted in cell culture media without FBS at 100 μM concentration, vortexed for 30 seconds and incubated at 4^{o}C for 12 h. The peptide solution then diluted to the desired concentrations with cell culture media without FBS. To make fibrils, Aβ42 (100 μM) was incubated in presence of 0.02% sodium azide in PBS at 37 ^{o}C for 4 days

Measurement of Caspase activity

Caspase activity was measured as described earlier [56]. Briefly, treated cells were washed twice with ice-cold phosphate-buffer saline (PBS). Then, 40 μl of buffer containing 20 mM HEPES-NaOH, pH 7.0, 1mM EDTA, 1mM EGTA, 20mM NaCl, 0.25% Triton X-100, 1mM dithiothreitol (DTT), 1mM phenylmethanesulphonylchloride (PMSF), 10 μg/ml leupeptin, 5 μg/ml pepstatin A, 2 μg/ml aprotinin, 25 μg/ml ALLN was added into each well and incubated on ice for 20 min. The cell extracts were dispersed intermittently with Gilson pipette. Caspase assay

buffer (final 20mM HEPES-NaOH, pH 7.0, 20mM NaCl, 1.5 mM $MgCl_2$, 1mM EDTA, 1mM EGTA and 10mM DTT) was added and the release of AMC was monitored for 2h in 2 minute interval with respective caspase substrates at excitation and emission wavelengths of 360 nm and 480 nm respectively, using microplate sepectrofluorometer (Molecular Devices, CA, USA). The results were expressed as a slope of total readings versus time.

Cell Culture and Cell death Assay

Human epithelial HeLa cells were cultured in DMEM (High glucose) medium supplemented with 10% (v/v) FBS and 1% antibiotics at 37 °C under 5% CO_2.

For MTT cytotoxicity assay, cells were plated at a density of 15,000 cells/well in 96-well plates (Nunc, Denmark) and cultured for 24 h followed by serum deprivation for another 12 h. Cells were exposed to the Aβ preparation for appropriate time and the viability was assessed by 3-(4,5-dimethylthiazol-2-yl)-2,5-di-phenyltetrazolium bromide formazan (MTT) reduction test. Briefly, 20 μl of 5 mg/ml MTT solution in PBS was added to each well, rapped with aluminum foil and incubated for 2 h. Then 100 μl of solubilization buffer [20% SDS solution in 50% (v/v) DMF (pH 4.7)] was added. After 12-16 h of incubation, absorbance was recorded at 570 nm using a micro plate reader KisanBio plate reader (KisanBio, Seoul, South Korea).

For Alamar blue assay also same cell culture and treatment method was followed. After treatment 10 μl of alamar blue (Life technologies) was added directly to the cells and incubated for 4-16 h, absorbance was recorded at 570 nm using a micro plate reader Spectra Max 190 (Molecular Devices, CA, USA).

Western blot analysis

Cells were harvested, washed with ice-cold PBS for at least twice and resuspended in lysis buffer containing, (50 mM Tris-HCL, pH 8.0, 150 mM NaCl, 1% Triton X-100, 5mM EDTA, 5mM EGTA, 1mM PMSF, 10 μg/ml leupeptin, 2 μg/ml pepstatin A and 2 μg/m aprotinin) for 20 min on ice. The extract was obtained by centrifugation at 13,000 rpm at 4^{o}C for 30 min. The amount of protein was measured through Bradford assay. Equal amounts of proteins were separated on 12–15 % SDS-PAGE and transferred on to a PVDF membrane. The membrane was immunoprobed with primary antibodies and horseradish peroxidase-conjugated secondary antibodies. The blots were visualized using West-Zol plus reagent (iNtron Biotechnology Inc., Seoul, Korea) in a Chemiluminescent detection system (Supernova 1800).

Analysis of Cyto c release

Cells were harvested, washed with ice-cold PBS and resuspended in digitonin buffer (75 mM NaCl, 1 mM NaH2PO4, 8 mM Na2HPO4, 250 mM sucrose, 190 μg/ml digitonin). After 5 min on ice, the cells were spun for 5 min at 14,000 rpm at 4°C in a microcentrifuge. Supernatants

were transferred to fresh tubes and the pellets were resuspended in buffer containing 25 mM Tris-HCl, pH 8.0, and 1% Triton X-100. Equal amount of proteins from each sample were subjected to sodium dodecylsulfate-polyacrylamide gel electrophoresis (SDS-PAGE) and western immunoblot assay as described before [56].

Size exclusion column chromatography (SEC) for monitoring apoptosome and DISC formation

For analysis of apoptosome assembly and death inducing signaling complex (DISC) assembly, cell extracts prepared from the treated cells were subjected to SEC following the procedure described earlier [56]. Briefly, 0.9-2 mg cell extract was loaded onto a Superose 6 HR (10/30) column (Amersham pharmacia biotech, Uppsala, Sweden) and 0.5 ml fractions were collected at a flow rate of 0.2 ml/min. Proteins in the fractions were analyzed by western blot analysis. The column was calibrated with calibration kits that included thyroglobulin (669 kDa), ferritin (440 kDa), catalase (232 kDa), and aldolase (158 kDa).

Preparation of cell extract and cell free system

After harvesting, the cells were washed twice with ice-cold PBS, resuspended in buffer consists of (20 mM HEPES-KOH, pH 7.5, 0.5 mM EDTA, 0.5 mM EGTA, 10 mM KCl, 1mM β-merceptoethanol, 0.1 mM PMSF, 10 μg/ml leupeptin, 5 μg/ml pepstatin A, 2 μg/ml aprotinin, 25 μg/ml ALLN) and dounce-homogenized with 40-50 strokes. Then the

supernatant was obtained by centrifuging at 13000 rpm for 1 h and used immediately.

In vitro apoptosis was induced by incubating the prepared HeLa cell extract (100 μg) with 1 mM dATP and 1- 10 μM cytochrome c in buffer containing 20 mM HEPES-NaoH, pH 7.0, 20 mM NaCl, 1 mM EDTA, 1mM EGTA, 1.5 mM $MgCl_2$, 10 mM DTT for the indicated time period at 30˚ C. The reaction mixture was then resolved with 12-15 % SDS-PAGE and subjected to western blot analysis.

Construction and purification of caspases

The human caspase-8 and caspase-8 double mutants were cloned in bacterial expression pET15b vectors (Novagen), and to generate the mutant version of caspase-8 (DM), point mutations were done using DpnI mediated site directed mutagenesis (New England Biolabs) by PCR. The primers used for double mutant are: D374A (sense 5′- ATACCTGTTGAGACTGCTTCAGAGGAGCAA -3′, anti-sense 5′- TTGCTCCTCTGAAGCAGTCTCAACAGGTAT -3′) and D384A (sense 5′- TATTTAGAAATGGCTTTATCATCACCTCAA -3′, anti-sense 5′- TTGAGGTGATGATAAAGCCATTTCTAAATA -3′). The underlined sequences refer to incorporated alanine sequence in each case. The mutated plasmid was confirmed by sequencing both strands. Then the recombinant caspase was expressed in BL21 pLys *Escherichia coli* strain as N-terminal histidine tag. Protein was purified by two successive chromatographic procedures. Initially, bacterial cell lysates from 2 L

culture were prepared by sonication and centrifugation 20000 rpm for 1 h in lysis buffer (20 mM Tris-HCl, pH 8.0, 10 mM NaCl, 0.1 mM PMSF, 0.1 mM EDTA, 1 mM DTT). The supernatant was loaded onto a Ni^{2+}-NTA column (Qiagen). The column was washed with two column volume of washing buffer (20 mM Tris-HCl, pH 8.0, 10 mM NaCl, 1 mM beta-ME, 10 % glycerol) and eluted with elution buffer (20 mM Tris-HCl, pH 8.0, 10 mM NaCl, 1 mM beta-ME, 10 % glycerol and 250 mM imidazole). The active fractions were then loaded onto a HiTrapQ sepharose column (Amersham Pharmacia Biotech) equilibrated with equilibration buffer (20 mM HEPES-NaOH, pH 7.5, 10 mM NaCl, 0.1 mM EDTA, 1 mM DTT, 10 % glycerol). The protein was then eluted with 1-400 mM NaCl gradient. The concentration of the purified protein was then measured and aliquots were saved at -80˚ C before use.

The caspase assay was performed by using fluorogenic substrate Ac-IETD-amc at 30˚ C by monitoring the release of amc at excitation and emission wavelengths of 360 nm and 480 nm respectively, with a micro plate spectrofluorometer (Spectramax Gemini, Molecular Devices). The catalytic parameters were calculated using Michaelis-Menten equation:

$$V_0 = \frac{V_{\max}[S]}{(K_M + [S])} \quad \text{..... (1)}$$

$$V_{\max} = k_{cat} \,.\, [\mathrm{E}]_{\mathrm{T}} \quad \text{..... (2)}$$

Where, V_0 is the initial velocity, [S] is substrate concentration, and $[\mathrm{E}]_{\mathrm{T}}$ is the total amount of enzyme used in the reaction.

II-3. RESULTS

Single treatment of Aβ42 induce limited activation of caspase-3, -8, and -9

Although many reports including ours indicate the involvement of apoptosis and accompanying caspase activation in Aβ-induced cell death [72-75, 83], we have often observed low activities of caspases as shown in Fig. 1. We evaluated the activity of caspase-3, -8 and -9 which participate in intrinsic and extrinsic pathways, two major caspase dependent apoptotic processes. The activity was measured using 3 different synthetic substrates (DEVD-AMC, IETD-AMC, and LEHD-AMC) for each caspase. The cells were incubated with up to 40 μM of Aβ42 for as long as 48 h (Fig. 1). In the investigation, we employed human epithelial HeLa cells which showed relatively higher caspase activity than other cell lines such as human neuroblastoma SH-SY5Y cells in which death occurred too easily with Aβ treatment and the levels of activated caspase were often inconsistent (data not shown). And oligomeric preparation of Aβ42 was mainly used for the experiments instead of monomeric or fibrillar peptide, otherwise indicated, because it was reported in earlier studies and our laboratory to be superior to the monomer or fibrillar form in inducing caspase activity and cell death [19, 71].

Some levels of caspase activities with the synthetic substrates were detected in Aβ42-treated cells, especially in 48 h-incubation samples (Fig. 1A-1C). However, we are not convinced that this was derived from Aβ42-induced damage, because no Aβ42-concentration dependency of the activity was observed and the activity could be due to the background activities which might be increased by cell division during the treatment time. It is also possible that the serum deprivation of the cells before Aβ42 treatment may cause the increase of background activity. Thus, it is questionable whether the activity is due to Aβ42 or to

other unknown factors. Furthermore, the activity levels were lesser by several times than those induced by other damaging agent such as STS [83].

The caspase activation was further explored in the Aβ42-treated cells, using the immunoblot assay. Cleaved fragments (see Fig. 2) were expected to be seen for each caspase if it is activated. No such fragments were detected in the immunoblotting assay (Fig. 1D). DFF45 and Bid, substrates of caspase-3 and -8 respectively, were not reduced, either (Fig. 1D). Altogether, there is no evidence to support the activation of caspase in the cells treated with Aβ42 under the experimental condition used above.

Aβ42 cytotoxicity was examined to confirm the low level of caspase activation is not due to a possible problem of the peptide preparation. The cell death was mainly assessed by the MTT [52]. However, soluble Aβ can lead to a decrease in MTT formazan production in the absence of overt cell death when cells are incubated for longer time. Thus, alamarBlue assay was also performed to complement the cell death experiments [63]. MTT formazan was reduced in 24-h and 48-h incubation samples in an Aβ42-dose dependent manner (Fig. 1E). AlamarBlue reduction was consistently observed in the 48-h sample, although the levels were less than those of MTT assay (Fig. 1E). These results indicate that cell death occurred in the 24 and 48 h samples. Thus, we concluded that Aβ42 used here was cytotoxic. On the other hand, it is questionable if cell death occurred in 12-h samples which showed decrease of the MTT formazan, but no Aβ42-dose dependency. Furthermore, the levels of cell death in the sample were barely decreased in the alamarBlue assay.

Previously, it was reported that Aβ fibrils induced extrinsic apoptosis which results in activation of caspase-8 and subsequently, caspase-3 [75]. In the current study, the caspase-3-like DEVDase activity was not detected in fibrillar Aβ42-treated cells (Fig. 1A). MTT formazan were reduced in cells treated with the fibrillar form of Aβ42, but it was

not Aβ42-dose dependent (Fig. 1E). It seems that non-specific reduction of MTT formazan caused the ambiguous results. In alamarBlue assay for the same samples, Aβ-dose-dependent reduction was clearly seen, suggesting that Aβ42-dose dependent cell death occurred. Altogether, these data indicate that the fibrillary form of Aβ42 led to cell death in which caspase-dependent apoptosis plays little role.

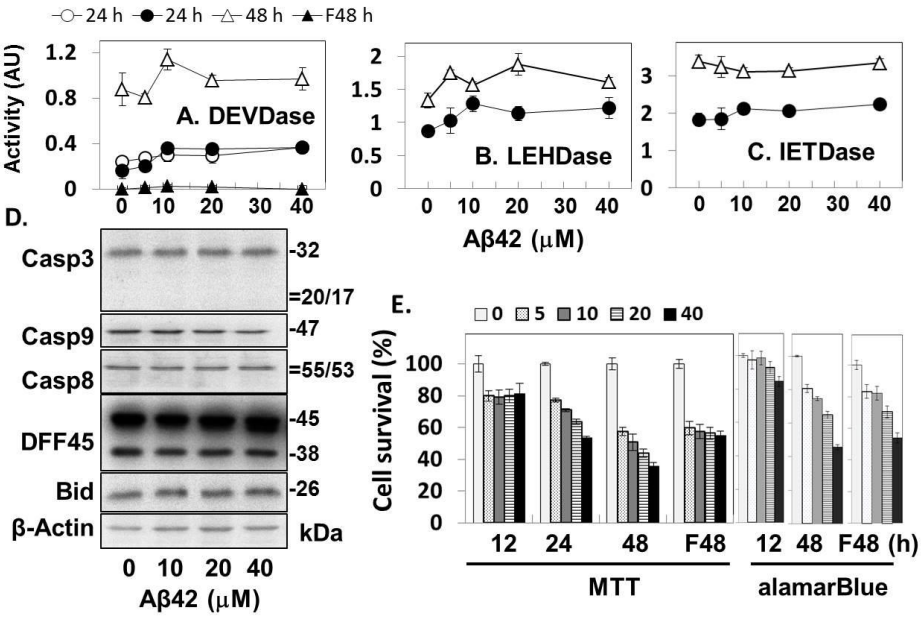

Fig. 1. Effects of single treatment of $A\beta_{42}$ oligomeric species on activation of caspases, processing of caspases and its substrates and cell death in HeLa cells. (**A-C**)Cells ($2x10^4$ /100 μl of culture media) were treated with oligomerized $A\beta_{42}$ at the indicated concentrations and time. The activities of Caspases – 3, -9 and -8 of the cell extracts were measured with their respective synthetic substrates (10 μM DEVD-AMC for caspase-3, 50 μM LEHD-AMC for caspase-9 and 50 μM IETD-AMC for caspase-8). (**D**) Immunoblot analysis of caspase and its substrates. HeLa cells ($2x10^4$ cells/100ul of culture media) treated with oligomeric $A\beta_{42}$ for 48 h at the indicated concentrations. Total cell extracts were prepared and assessed for processing of caspase-3, -9, -8 and its substrates DFF45 and Bid. Actin was employed as loading control. (**E**) to check the effect of $A\beta_{42}$ oligomeric and fibrillar species of cytotoxicity, HeLa cells were plated at a density of $2x10^4$ cells per well and treated with oligomeric and fibrillar $A\beta_{42}$ at the indicated concentration and time point, cell viability was measured by MTT reduction assay and alamrBlue assay.

Double treatment of Aβ induces potent caspase activation.

Next, we sought conditions under which caspases are potently activated and then probed apoptosis pathways accompanying caspase activation under the condition in Aβ42-treated cells. To find those conditions, we tested "double treatment" method in which Aβ42 peptide was sequentially administered to cells twice, referring to a report that nucleation-dependent polymerization is essential for Aβ-mediated cell death [87, 88]. We inferred that the polymerization could give differential or stronger signal to activate caspase. In the previous study, cells were treated with fibrillar form of Aβ42 for 1 h and followed by the treatment of soluble Aβ42. Here we use only soluble oligomeric Aβ42 to facilitate the quantitation of peptide amount and the pretreatment time was determined after testing different time points. Based on the time points tested, cells were initially treated for 2 h with the indicated concentration of oligomeric Aβ42 which then was removed at the end of incubation and subsequently, were further incubated with new preparation of oligomeric Aβ42 peptide at the same concentration for 10 (2+10 h sample), 22 h (2+22 h), 34 h (2+34 h) or 46 h (2+46 h sample).

The 2+22 h and longer incubation samples showed caspase-3-like DEVDase activity in an Aβ42-dose dependent manner (Fig. 2A). ~20 kDa processed fragment of caspase-3 was detected in the 2+22 h and 2+34 h samples treated with the high concentrations of Aβ42, and fully processed ~17 kDa fragment additionally recognized in the 2+46 h samples (Fig. 2D). Although the intensity of processed fragment was strongest in 2+34 h and additional ~17 kDa is present in 2+46 h samples (Fig. 2D), those DEVDase activities were similar with that of 2+22 h sample (Fig. 2A), indicating that correlation of the activity and the processed fragments is not clear. The product fragment of or decrease of DFF45, substrates of caspase-3, were seen (Fig. 2D), confirming the catalytic activation of caspase-3.

Caspase-9-like LEHDase activity was the greatest in the 2+22 h

sample in which also showed Aβ42-dose dependency, and it was decreased in the longer incubation samples (Fig. 2B). Procaspase-9 decrease was clearly shown in 2+22 h or the longer incubation samples treated with the high Aβ42 doses (Fig. 2D). Although ~35/37 kDa cleaved products were barely seen for the enzyme, the fragments were recognized in the analysis of apoptosome (see Fig. 3C). Moreover, the processing of procaspase-3, the substrate of caspase-9, (Fig. 2D) implies catalytic activation of caspase-9. Altogether, these data support activation of caspase-9.

Caspase-8-like IETDase activity was the highest in the same 2+22 h sample, but the correlation of Aβ42-dose and the activity was weak (Fig. 2C). Procaspase-8 was processed in 2+22 h or later samples, but two different types of fragments are observed (Fig. 2D). In 2+22 h samples, ~30 kDa fragment (p30) was mainly detected, while typical 41/43 kDa fragments (p41/43) were recognized in 2+46 h samples. p30 is a fragment of procaspase-8 lacking the prodomain, while p41/43 contains the prodomain and the large domain that becomes large subunit when caspase-8 is fully matured [89]. Thus, the cleavage sites to form the two different fragments are distinct [89]. We further characterized the fragments in the following exploration (see below). The immunoblot signal intensity of Bid, substrate of caspase-8, was rather consistent regardless of the incubation time and dose of Aβ42. Thus, it seems that the catalytic activation of caspase was uncertain in the samples, although a part of it is processed into two different types of fragments.

For a reference for the cytotoxicity of Aβ42 peptide preparation, cell death was assessed in the double treatment samples. All showed Aβ42-dose dependent cell death evaluated by the two methods (Fig. 2E). The levels of cell death evaluated by MTT formazan reduction were generally more than those of alamarBlue assay (2+22 h and 2+46 h samples of MTT vs those of alamarBlue) as in the single treatment samples (Fig. 1E). Reduction of the values was slightly higher in the double treatment sample than in the equivalent single treatment sample

(i.e. 2+22 h vs 24 h). Roughly speaking, we could not detect prominent differences in the single and double treatment samples in induction of cell death.

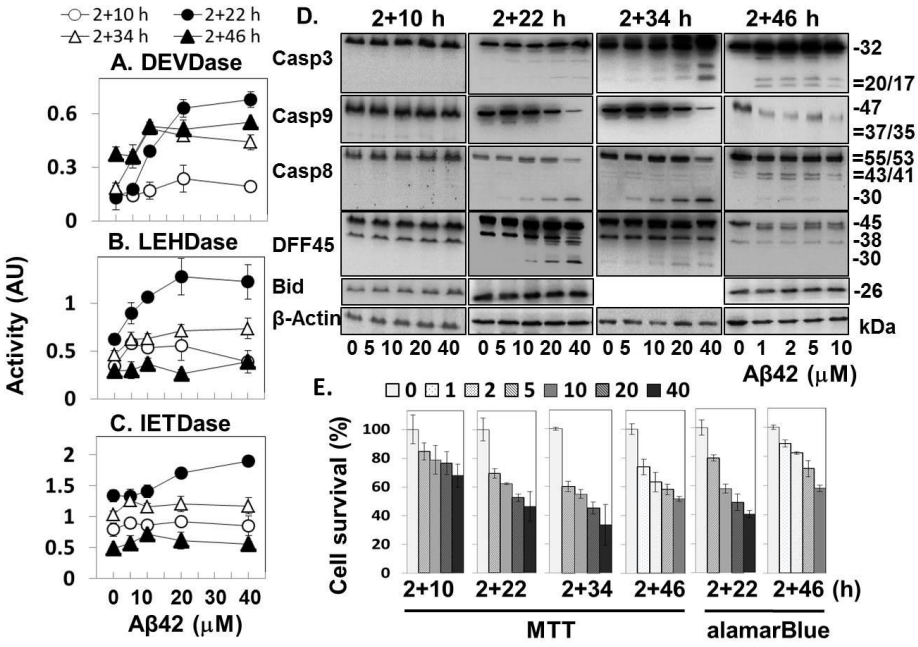

Fig. 2. Effects of double treatment of $A\beta_{42}$ oligomeric species on activation and processing of caspases and its substrates, and cell death in HeLa cells. (**A-C**)Cells ($2x10^4$ /100 μl of culture media) were treated with oligomerized $A\beta_{42}$ at the indicated concentrations and time. The activities of Caspases – 3, -9 and -8 of the cell extracts were measured with their respective synthetic substrates (10 μM DEVD-AMC for caspase-3, 50 μM LEHD-AMC for caspase-9 and 50 μM IETD-AMC for caspase-8). **(D)** Total cell extract were prepared and assessed for processing of caspase-3, -9, -8 and its substrates DFF45 and Bid by western

blotting. HeLa cells were treated for 2+10h but no caspases and its substrates were found to be processed. In case of 2+22h double treatment, caspase-9, -3 and the substrate for caspase-3, DFF45 were processed. Caspase -8 was found to be processed in a unique manner, only p30 processed fraction was observed but neither the p43/41 nor the p18/12 fractions were observed and the substrate Bid was not processed, p30 fraction may be the intermediate stage of caspase-8 processing as longer period double treatment resulted in the formation of the other fractions. With longer period of incubation 2+34h and 2+46h the cleavage of caspase-3, -9, -8 and the substrate of caspase-3 DFF45 was more prominent but Bid was not cleaved even with 2+46h incubation. (**E**) To check the effect of $A\beta_{42}$ oligomeric species of cytotoxicity HeLa cells were plated at a density of $2x10^4$ cells per well and treated with oligomeric $A\beta_{42}$ at the indicated concentration and time point, cell viability was measured by MTT reduction assay and alamarBlue assay.

Cytochrome c release from the mitochondria and formation of the Apaf-1 apoptosome

On the basis of catalytic activity and processing of caspase, it was concluded that intrinsic apoptosis pathway was activated in the Aβ42-doubly treated cells. To confirm activation of the pathway cytochrome c release from the mitochondria were probed in the 2+22 h samples which showed potent activation and processing of caspase-3 and reduction of procaspase-9 (Fig. 2A-D). Cytochrome c was detected in the samples treated with 20 and 40 μM Aβ42, indicating the release (Fig. 3A). Next, formation of apoptosome, a hallmark of the intrinsic pathway, was examined in the 2+22 h samples treated with 20 μM Aβ42. Apaf-1 and caspase-9 were recognized only in the later fractions (>#25) in the analysis of the control sample prepared from Aβ42-non-treated cells by SEC (Fig. 3B), while those proteins were detected in the earlier fractions (~#15-#23) in the 2+22 h sample (Fig. 3C). These data clearly indicate the formation of apoptosome in the sample. It is noted that 35/37 kDa fragments of caspase-9 which were not detected above (Fig. 2D) were seen in the western blotting analysis followed by SEC (Fig. 3C). It was recognized in this experiment probably because the protein was concentrated during the chromatography.

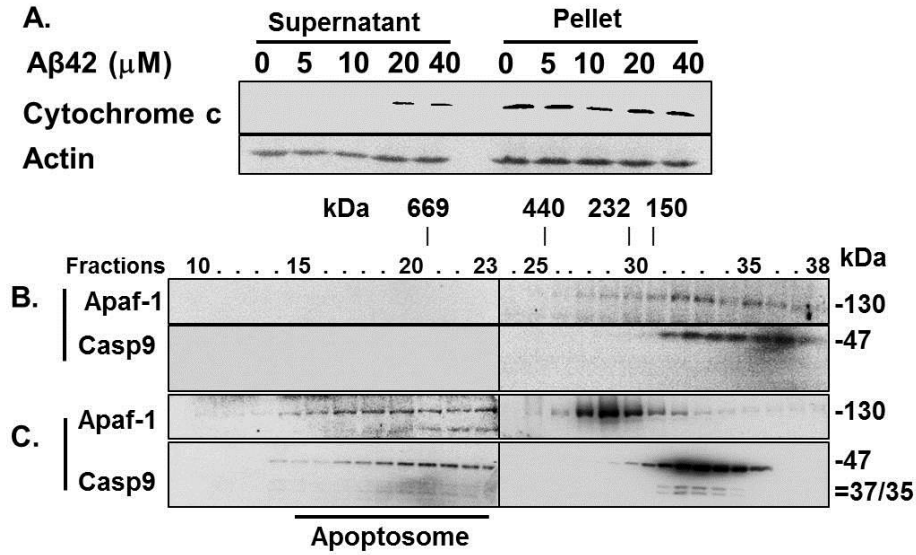

Fig. 3. Double treatment of Aβ_{42} oligomeric species induce cytochrome c realese and the formation of Apaf-1 apoptososme in HeLa cells. (**A**) After HeLa cells were treated with oligomerized Aβ_{42} at the indicated concentrations for 2+22h and the release of cytochrome c was assessed by immunoblot analysis. Supernatant and pellet in cytochrome c release indicate soluble and precipitated parts of the cell extracts respectively. Actin was loaded as loading control. (**B** and **C**) HeLa cells were incubated without or with 20μM oligomerized Aβ_{42} for 2+22h. The extract prepared from the cells (0.8 ~ 1.0 mg) was fractionated by gel filtration chromatography. The fractions were analyzed by immunobloting for Apaf-1 and caspase -9. The standard molecular markers are indicated above the scale with elution fractions.

DISC is not formed in Aβ42-treated cells

The formation of DISC was also probed. Caspase-8 and FADD proteins were detected only in the later fractions (>#22) in the analysis of the control cells by SEC, while ~#14-#21 fractions contained the two proteins in a positive control sample prepared from cells treated with actinomycin-D followed by TNF-α (Fig. 4A and 4B), confirming the formation of DISC. The two proteins were detected in the later fractions (>#22) in the 2+22 h and 2+46 h samples treated with 20 μM Aβ42 (Fig. 4C and 4D). Based on the data, we concluded that DISC was not formed in those samples. However, processed fragment of caspase-8 was recognized. In the 2+22 h sample p30 was seen (Fig. 4C), while p41/43 was also detected in the 2+46 h sample (Fig. 4D). These data indicate that formation of p30 fragment of caspase-8 precedes that of p41/43 fragment, consistent with those of Fig. 2D,

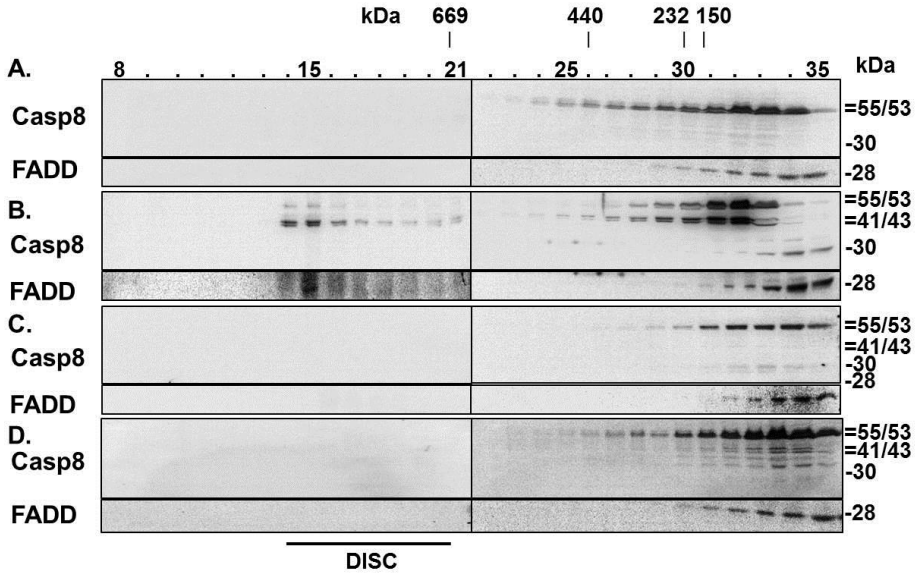

Fig. 4. Effects of $A\beta_{42}$ oligomeric species double treatment DISC assembly in HeLa cells. (A, C and **D**) HeLa cells were incubated without or with 40 μM oligomeric $A\beta_{42}$ for 2+22h and 2+46h respectively, cell extracts prepared from cells (1.0 ~ 1.2 mg) were fractionated by gel filtration chromatography. The fractions were analyzed by immunobloting for caspase-8 and FADD. Only p30 processed fraction was observed but neither the p43/41 nor the p18/12 fractions were observed, p30 fraction may be the intermediate stage of caspase-8 processing as longer period (2+46h) double treatment resulted in the formation of the other fractions. FADD was not detected in any time point with $A\beta_{42}$ treated cell extract. (**B**) HeLa cells were treated with 100ug/ml of Actinomycin D for 2h and then treated with 50nM of TNFα for 24hr. Cell extracts prepared from cells (1.0 ~ 1.2 mg) were fractionated by gel filtration chromatography. The fractions were analyzed by immunobloting for caspase-8 and FADD. Processed caspase-8 and FADD was detected in the earlier fractions which indicate the formation of DISC.

p30 and p41/43 fragments of caspase-8 fragment is formed by caspase-3 and -6.

Because DISC was not formed in the 2+22 samples, we considered intrinsic apoptotic pathway for the induction of formation of the caspase-8 fragments, because caspase-3 and -6 activated in the pathway are also known to induce the fragmentation [90, 91]. The intrinsic apoptosis process was reconstituted in a cell-free experiment in which cell extracts was incubated with dATP and cytochrome c that results in formation of the Apaf-1 apoptosome [52]. As expected, caspase-8 and its substrate Bid was processed, but only p41/43 were detected (the second lane of Fig. 5A). The p30 fragment was seen in the following experiments in which lower dose of cytochrome c was used and caspase-8 processing was not complete (see lanes 3-7 of Fig. 5A), implying that p30 might exist only in the early stage of apoptosis, consistent with the results of Fig. 2D. The apoptosome is a sort of holoenzyme of caspase-9 that leads to activation of caspase-3 and subsequently caspase-6 [92]. Purified caspase-3 could induce the formation of the p30 fragments (Fig. 5B), while caspase-6 induced only the formation of p41/43 fragments (Fig. 5C). Although physiological implication of the differential activity of the two caspases on caspase-8 processing remained to be pursued, they clearly showed that the fragmentation process of caspase-8 could occur through the intrinsic apoptotic pathway.

The levels of Bid were rather consistent under the condition in which caspase-8 was not completely processed (Fig. 5A-C). In fact, the condition seems to better reflect the real situation of samples shown in Fig. 2D, considering the level of Bid and processed caspase-8. Bid processing is essential to strengthen the apoptotic signal in type II cells. It can be hypothesized that the low levels of caspase activation in Aβ42-treated cells may be attributed to the weak activation of the amplification loop.

For a reference, we determined catalytic activity of p30 for Bid. It was assessed by using prodomainless caspase-8 double mutant mimicking p30 (DM, see "Materials and methods", [93]). We also estimated the catalytic activity of enzymes containing p41/43 using enzymes containing the prodomainless equivalent of p41/43 (p18-10) for comparison (Fig. 6A). p18-10 could process procaspase-3 and Bid in the cell extracts as expected, while DM was inefficient in the process (Fig. 6B and 6C). Purified Bid was also cleaved by p18-10 to produce the products (Fig. 6D) which was not detected in the cell-free experiments (Fig. 6C). Consistently, DM could not cleave the purified Bid. k_{cat} of DM was ~800-fold lower than that of p18-10, indicating that the lower activity of DM is due to the slower catalytic velocity (Fig. 6E), consistent with the previous reports [93].

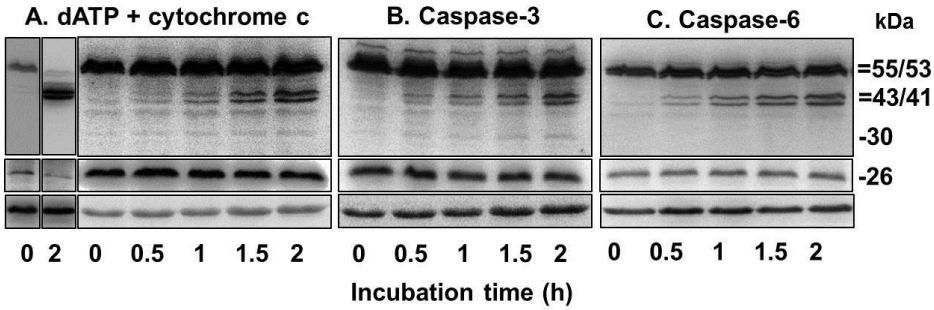

Fig. 5. Caspase-8 is processed by intrinsic apoptotic pathway. To find out the mechanism of caspase-8 processing **(A)** HeLa cell extract was prepared and incubated with cytochrome-c and dATP for the indicated time and immunoblotted for caspase-8 and bid cleavage. It was found that caspase-8 and bid were cleaved in case of high concentration of cytochrome-c (10 μM) (lane-2), but in case of 1 μM of cytochrome-c bid was not processed into truncated bid. Actin was employed as loading control. **(B** and **C)** HeLa cell extract was incubated with purified recombinant active caspase-3 and caspase-6 for indicated time period and probed for caspase-8 and bid processing by western blot. p30 fragment of caspase-8 was found only in the case of in vitro apoptosis and caspase-3 mediated cleavage. Actin was employed as loading control.

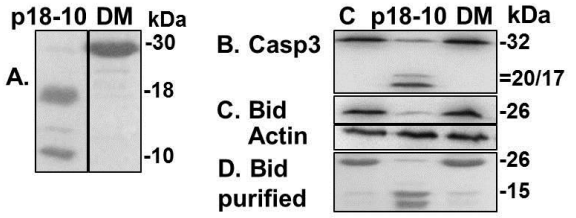

E.

Enzyme	p18-10	DM
K_M (mM)	29.86	28.78
k_{cat} s^{-1}	0.08	0.000098
k_{cat}/K_M ($M^{-1}S^{-1}$)	2680	3.4

Fig. 6. p30 fragment of Caspase-8 is not active but p18 and p12 fragments are active. (A) Recombinant active caspase-8 and caspase-8 double mutant (DM) was purified as described in the materials and method section and run for SDS-PAGE. Lane 1 purified active caspase-8 and lane 2 caspase-8 double mutant. **(B** and **C)** Procaspase-3 and bid processing by wild type caspase-8 and caspase-8 (DM) were checked.70 μg of HeLa cell extracts were incubated with 30 ng of wild type caspase-8 and caspase-8 (DM) for 1 h at 30˚C and the reaction mix was probed for procaspase-3 and bid processing by western blot. Actin was employed as loading control. **(D)** Effect of wild type caspase-8 and caspase-8 (DM) on purified recombinant bid processing. 1 μg of purified bid was incubated with equal amount of (30 ng) wild type and double mutant caspase-8 and incubated for 1 h at 30˚C. The reaction mix was separated by SDS gel electrophoresis. In all **(B, C** and **D)** cases caspase-8 (DM) was found to be inactive. **(E)** Catalytic parameters of purified recombinant wild type and DM caspase-8.

II-4. DISCUSSION

Previously we found that Aβ42 could suppress an apoptosis pathway by interacting with procaspase-9 [52]. However, accumulating data has implicated apoptotic process as a mechanistic feature of the cell death induced by Aβ42 [78, 94]. Although significant progress has been made in understanding the apoptotic pathway related with Aβ42 through extensive studies over decades, cytotoxic properties of Aβ42 and its mechanistic features have been difficult to assess because of variability in culture systems and methods associated with Aβ42 preparation and treatment [24]. In the current study, we sought a condition in which caspases are activated and explored the involvement of apoptosis pathways under the condition. We employed two different treatment ways with the peptide. In the cells treated with Aβ42 “once”, cell death evaluated by MTT and alamarBlue assay occurred in a dose-dependent manner (Fig. 1E). Cells treated with the peptide “twice” showed the similar levels of cell death. This result is inconsistent with the previous report showing that the double treatment of Aβ42 which leads to polymerization of the peptide was necessary to elicit the cell death [88]. Many reports including the present study, however, showed that the single treatment was sufficient to induce cell death.

Caspase activity was detected in the cells treated once with Aβ42 previously [72, 75]. Here, the activity was also detected in the cells singly treated with the peptide (Fig. 1A-C). However, Aβ42-dose-dependency was not seen and furthermore, the processed fragments of caspase were not detected (Fig. 1D). Actually, detection of processed fragment of caspase might not be absolute necessity to prove the activation of the enzyme, because undetectable amount of activated caspase can produce the catalytic activity evaluated with the synthetic substrates (data not shown). Thus, we think that a certain level of caspase activation occurred in the single-treatment sample, although it is questionable whether all

activity is elicited only by Aβ42. A part of the activation could be elicited by other factors. Moreover, we showed previously that apoptosome was not formed in Aβ42-treated cells, which was due to interaction of the peptide with procaspase-9 [52]. We conclude that caspase activation is not potent in the cells singly treated with Aβ42 and the single treatment was not adequate for the purpose of the current study to probe apoptotic pathway leading to caspase activation in Aβ42-treated cells.

The activation of caspase was clearer in cells doubly treated with Aβ42 (Fig. 2A-D). Aβ42-dose dependency was evidently seen and the processed fragments of caspase were detected. The Apaf-1 apoptosome was also formed in Aβ42-doubly treated cells (Fig. 3B), implying that Aβ42 induced the intrinsic pathway in cells. The suppressive effect of Aβ42 on the formation of apoptosome [52] seems to be overcome in the doubly treated cells. Although the mechanism for the necessity of double treatment of Aβ42 to induce robust activation of caspase is not understood yet, polymerization of the peptide [95] is likely to give a strong signal to activate the apoptotic pathway and related caspases.

Previously, Aβ42 fibrils could elicit the extrinsic apoptosis pathway which leads to activation of caspase-8 [75]. In the current study, we failed to detect any activation of caspase in cells treated with Aβ42 fibrils (Fig. 1D), although cell death occurred (Fig. 1E). Again the single treatment of Aβ42 was not efficient in inducing caspase activation regardless of the peptide's form. Fragmentation of caspase-8 to 30 kDa and 41/43 kDa was recognized in the cells doubly treated with Aβ42 oligomeric forms (Fig. 2D). The p41/43 is generally detected in the extrinsic apoptosis process by formation of DISC [96, 97]. But the protein complex was not observed in the cells, implying that p41/43 fragment may be formed by other pathway (Fig. 4C). The fragment can also be produced by the catalytic activity of caspase-3 and -6 [90, 92] that can be processed by the intrinsic pathway. Indeed, the generation of p41/43 was demonstrated in the cell-free experiment in which the intrinsic pathway was reconstituted by addition of dATP and cytochrome

c to the cell extracts (Fig. 5A). The direct addition of purified caspase-3 and -6 to the cell extracts also leads to the fragment production (Fig. 5B and 5C), further supporting the possibility that the intrinsic pathway is responsible for production of caspase-8 fragments.

Here we recognized p30 fragment of caspase-8 formation in Aβ42-treated cells. The caspase-8 fragment p30 was rarely shown in the previous reports. It was generated in cells treated with CD95 by formation of DISC and following autocatalytic process and was further processed to p18 and p10 fragments [89]. Here we firstly showed that p30 was formed in the cells doubly treated with Aβ42 without formation of DISC (Fig. 4C and 4D). It could be produced in the cell-free assay that reconstituted the intrinsic pathway (Fig. 5A and 5B), giving a potential role of the pathway in generation of the fragment. It is also intriguing that p30 fragment was produced only by caspase-3, not by caspase-6 in the cell-free experiments (Fig. 5B and 5C). p30 was produced in earlier stage of the treatment before formation p41/43 fragments (Fig. 2D), consistent with the previous suggestion that p30 can sensitize cells toward death receptor-induced apoptosis [89].

The death signal can be amplified via Bid cleavage in type II cells such as HeLa cells used here [98]. Although p41/43 fragments were formed, its substrate Bid was not processed (Fig. 2D), indicating that the amplification loop was not operated in the Aβ42-treated sample. The levels of caspase activation even in the doubly treated samples was not as high as that that induced by other damaging agents such as STS (data not shown). The weak activation caspase in Aβ42-treated cells can be attributed to the lack of the amplification loop.

In conclusion, we show that intrinsic apoptosis and accompanying caspase activation could be induced by double treatment of Aβ42 to cells. The double treatment seems to be necessary to overcome the inhibitory effect of Aβ42 on the intrinsic pathway. In fact, it is difficult to imagine that neuronal cells are exposed to the Aβ42 just once. Thus, the experimental condition with double or more treatment of

the peptide to cells might be near to the physiological conditions. Hopefully, a full characterization of the nature of the multiple treatment and related cell death pathway will provide novel insight into Aβ-associated pathology and control of AD.

III. Interaction of caspase-6 with amyloid β

Abstract

Amyloid-β (Aβ), a major component of the extracellular senile plaques implicated in the neurodegenerative Alzheimer's disease (AD), elicits apoptosis. However, we previously showed the peptide could suppress formation of the Apaf-1 apoptosome, a key machinery of the intrinsic apoptosis pathway, by interacting with procaspase-9. Here, we screened other caspases for a potential interaction with Aβ42 by analysis of images produced by confocal microscope study. Caspase-6 was found to interact with the peptide. In a subsequent study using size-exclusion chromatography followed by western blot analysis, the two proteins were recovered in the same fractions. Moreover, casepase-6 contained in the fractions could immunoprecipitate concomitantly with Aβ42, giving another evidence for the interaction. Though, caspase-6 was catalytically activated in the Aβ42-treated cells, Lamin A/C and B the substrates of the enzyme were cleaved in a completely different fashion. The sizes of the cleaved fragments of lamin proteins in the Aβ42-treated cells indicated that the lamins seemed to be fragmented by enzyme(s) other than caspase-6, implying that the enzyme was not functionally active in the cells. We suggest that the interaction of caspase-6 and Aβ42 negatively affected the intracellular function of the enzyme.

III-1. INTRODUCTION

Amyloid β (Aβ) peptide is a major component of the extracellular senile plaques implicated in the neurodegenerative Alzheimer's disease (AD) [66]. The peptide is 36-43 amino acid-long and is generated by proteolytic cleavage of the amyloid precursor protein by α-, β- and γ- secretases [4, 67]. Aβ peptide is prone to change its conformation to β-sheet-rich intermediate structures that interact with each other to form soluble aggregates such as oligomers, protofibrils and subsequently insoluble fibrils [19, 68, 69]. The aggregated Aβ progressively accumulates in brain parenchyma and cerebral blood vessels [70]. However, the depositing fibrils was less toxic than the soluble Aβ oligomers and protofibrils, suggesting that the oligomeric aggregates would be the main neurotoxic factor for eliciting AD [19, 71].

The etiology of AD and the mechanistic features of cell death induced by Aβ are not clearly understood, but involvement of apoptosis in the process has been proposed [72-75]. Several apoptotic pathways have been characterized. Binding of death ligands to receptor leads to receptor-mediated apoptosis, or extrinsic apoptosis which is characterized by the formation of the death-inducing signaling complex (DISC) [76]. Caspase-8 is activated as a result of the apoptosis pathway [76, 77]. On the other hand, chemical-induced apoptosis or caspase-dependent intrinsic apoptosis is elicited by mitochondrial damage that results in the release of cytochrome c which associates with procaspase-9, dATP and an adaptor protein Apaf-1 to form a mutiprotein complex called apoptosome [75-77]. Apoptosome complex functions as a holoenzyme of caspase-9 that catalytically activates effector caspases such as caspase-3, -6 and -7 which are responsible for most of the cleavage events observed during apoptosis. The proposal on the involvement of apoptosis in Aβ-induced cell death is based on activation of apoptosis-related proteins such as caspases. Aβ can damage mitochondria leading to cytochrome c

release which can trigger formation of apoptosome and activation of caspases [78, 79]. On the other hand, binding of Aβ to death receptor can elicit the extrinsic apoptosis pathway so that caspase-8 is activated [45, 46].

Although a critical role of apoptosis in Aβ-induced cell death is evident, we recently found that Aβ42 could suppress the activation of the intrinsic apoptosis pathway [52]. The inhibitory effect of Aβ42 on the apoptotic pathway is associated with its interaction with procaspase-9 and consequent inhibition of Apaf-1 apoptosome assembly. Currently, ~15 different caspases have been found and they all share homologous amino acid sequences with each other. Thus, it is possible that Aβ42 might interact with other caspases and affect function of the caspases positively or negatively. In the current study, we made an attempt to recognize caspases that interact with Aβ42 and explore the potential effect of interaction on the apoptosis pathway.

III-2. MATERIALS AND METHODS

Materials

Fetal Bovine serum (FBS) was purchased from Life Technology Inc. (Grand Island, USA). Dulbecco's modified Eagles medium, high glucose (DMEM/HG) was obtained from Welgene (Daegu, Korea). Caspase-9, Caspase-8, Caspase-6 and Caspase-3 substrates, N-acetyl Leu-Glu-His-Asp-amino methyl coumarin (Ac-LEHD-AMC), Ac-IETD-AMC, Ac-VEID-AMC and Ac-DEVD-AMC, respectively, were from A.G. Scientific Inc. (San Diego, USA). Ni-NTA column were purchased from Amersham Biosciences (Piscataway, USA). Western blotting detection kit (WEST-ZOL PLUS) from iNtron Biotechnology (Gyeonggi-do, Korea). Phosphate buffer saline (PBS) purchased from Amresco (solon, USA). Monoclonal anti-Aβ antibody 6E10 was acquired from Signet Laboratories (Dedham, USA), anti-amyloid oligomer polyclonal antibody A11 from Cheimicon International (USA) anti-lamin-A/C, anti-lamin B and anti-β-actin from Santa Cruz Biotechnology (California, USA). Anti-caspase-6 antibody that can detect small domain of caspase-6 was from BD Pharmingen (CA, USA) (named as AbA). Anti-caspase-6 antibody that recognizes the large domain of the enzyme was from Abfrontier (Seoul, Korea) (named as AbB). Anti-caspase-6 antibody used for the immunoprecipitation study recognized the small domain of caspase-6 and was from Santa Cruz Biotechnology (CA, USA) (named as AbC).

Cell Culture

Human epithelial HeLa cells were cultured in DMEM (High glucose) medium supplemented with 10% (v/v) FBS and 100 units of penicillin and 100 μg/ml streptomycin at 37 °C under 5% CO_2. The cells were seeded at 2000 cell/100 μl of culture media and cultured for 24 h. Then, serum deprivation was carried out for another 12 h and treatment was done according to the mentioned time point.

Preparation of Aβ peptide

The purified peptide was solubilized in 100% 1,1,1,3,3,3,-hexafluoro-2-propanol, and dried under nitrogen flow and subsequently, under vacuum for 30 min. The peptide aliquots were stored at –20 °C until use. Immediately before use, the peptide was dissolved in 0.1% NH_4OH at a concentration of 2 mg/ml followed by bath sonication for 10 min. The solution was diluted at the desired concentration with cell culture media without FBS. Aβ42 oligomers were prepared as described earlier [86] with little modification. Briefly, peptides were diluted in cell culture media at 100 μM concentration, vortexed for 30 seconds and incubated at 4^oC for 12 h. The peptide solution then diluted to the desired concentrations.

Confocal microscopy

HeLa cells were seeded in 6 well plate at 70% confluency, cultured for 24h and further incubated for 12h in serum free media and

then treated without or with 20 μM Aβ42 for 12 h. Treated cells were fixed in methanol at -20 ^{o}C and permeabilized by 0.3% Triton X-100. After blocking with 0.1% BSA overnight, primary mouse anti-amyloid beta (6E10), rabbit anti caspase-2, goat anti caspase-4, -6, -7 and -8 antibodies were added to each samples and incubated overnight at 4°C. After washing with PBS, Alexa-Flour-488 conjugated chicken anti mouse IgG, FITC conjugated goat anti-rabbit and Alexa-Fluor-543 conjugated rabbit anti-goat IgG antibodies antibodies (dilution, 1:200) were treated for 2h at room temperature followed by PBS washing. Nuclei were stained with Hoechst and confocal images were obtained with Carl Zeiss LSM510 microscope (Jena, Germany) using vendor provided software (LSM 510).

Size exclusion column chromatography (SEC) for monitoring protein-protein interaction

For analysis of interaction of capsae-6 with $A\beta_{42}$, cell extracts prepared from the treated cells were subjected to SEC following the procedure described earlier [56]. Briefly, 0.9-2 mg cell extract was loaded onto a Superose 6 HR (10/30) column (Amersham pharmacia biotech, Uppsala, Sweden) and 0.5 ml fractions were collected at a flow rate of 0.2 ml/min. Proteins in the fractions were analyzed by western blot analysis. For checking the interaction of $A\beta_{42}$ with caspase-6 in the cell free system, HeLa cell extracts was prepared (1 mg) and incubated with freshly prepared 20 μM of purified $A\beta_{42}$ at 37˚ C for 2 h and the reaction

mixture was separated by SEC and analyzed by western blot.

Interaction of purified caspase-6 (active) with Aβ42 was also analyzed by SEC. 10 μg of each protein incubated with or without 20 μM Aβ42 for 1 h at 30°C was fractionated as above and the collected fractions were analyzed by immunoblot analysis for caspase-6 and Aβ. In both cases, the column was calibrated with calibration kits that included thyroglobulin (669 kDa), ferritin (440 kDa), catalase (232 kDa), and aldolase (158 kDa).

Immunoprecipitation

After size exclusion chromatography, the desired fractions were pooled together and protein concentration was measured. Then the indicated antibodies were added to 100-500 μg of protein (final volume 1 ml) and incubated at 4˚ C overnight with rotor agitation. Next, 40 μl of protein A sepharose beads (Amersham Biosciences, Uppsala, Sweden) were added to each sample and incubated at 4˚ C for 2 h. Beads were precipitated by centrifuging at 13000 rpm at 4˚ C for 5 min and washed 3 times with PBS. 15 μl 2X SDS gel loading buffer was added to the beads, boiled for 5 min and centrifuged at 13000 rpm for 10 min. The obtained supernatants were then analyzed by SDS-PAGE and immunoblotting.

For purified caspase-9 and wild type $A\beta_{42}$, 10 μg of purified active caspase-6 was incubated with 20 μM of $A\beta_{42}$ for 2 h at 30˚ C. Then the antibodies were added to the reaction mixture and kept at 4˚ C for

overnight and analyzed by SDS-PAGE and analyzed by western blot analysis.

Measurement of Caspase activity

Caspase activity was measured as described earlier [56]. Briefly, treated cells were washed twice with ice-cold phosphate-buffer saline (PBS). Then, 40 μl of buffer containing 20 mM HEPES-NaOH, pH 7.0, 1mM EDTA, 1mM EGTA, 20mM NaCl, 0.25% Triton X-100, 1mM dithiothreitol (DTT), 1mM phenylmethanesulphonylchloride (PMSF), 10 μg/ml leupeptin, 5 μg/ml pepstatin A, 2 μg/ml aprotinin, 25 μg/ml ALLN was added into each well and incubated on ice for 20 min. Caspase assay buffer (final 20mM HEPES-NaOH, pH 7.0, 20mM NaCl, 1.5 mM $MgCl_2$, 1mM EDTA, 1mM EGTA and 10mM DTT) was added and the release of AMC was monitored for 2h in 2 minute interval with respective caspase substrates at excitation and emission wavelengths of 360 nm and 480 nm respectively, using microplate sepectrofluorometer (Molecular Devices, CA, USA). The results were expressed as a slope of total readings versus time.

Western blotting

Cells were harvested, washed with ice-cold PBS for at least twice and resuspended in lysis buffer B (50 mM Tris-HCL, pH 8.0, 150 mM NaCl, 1% Triton X-100, 5mM EDTA, 5mM EGTA, 1mM PMSF, 10 μg/ml leupeptin, 2 μg/ml pepstatin A and 2 μg/m aprotinin) for 20 min on

ice. The extract was obtained by centrifugation at 13,000 rpm at 4^{o}C for 30 min. The amount of protein was measured through Bradford assay. Equal amounts of proteins were separated on 12–15 % SDS-PAGE and transferred on to a PVDF membrane. The membrane was immunoprobed with primary antibodies and horseradish peroxidase-conjugated secondary antibodies. The blots were visualized using West-Zol plus reagent (iNtron Biotechnology Inc., Seoul, Korea) in Chemiluminescent detection system (Supernova 1800).

Purification of caspase-6

The human caspase-6 was cloned in bacterial expression pET28b vectors (Novagen). Then the recombinant caspase was expressed in BL21 pLys *Escherichia coli* strain as N-terminal histidine tag. Protein was purified by two successive chromatographic procedures. Initially, bacterial cell lysates from 2 L culture were prepared by sonication and centrifugation 20000 rpm for 1 h in lysis buffer (20 mM Tris-HCl, pH 8.0, 10 mM NaCl, 0.1 mM PMSF, 0.1 mM EDTA, 1 mM DTT). The supernatant was loaded onto a Ni^{2+}-NTA column (Qiagen). The column was washed with two column volume of washing buffer (20 mM Tris-HCl, pH 8.0, 10 mM NaCl, 1 mM beta-ME, 10 % glycerol) and eluted with elution buffer (20 mM Tris-HCl, pH 8.0, 10 mM NaCl, 1 mM beta-ME, 10 % glycerol and 250 mM imidazole). The active fractions were then loaded onto a HiTrapQ sepharose column (Amersham Pharmacia Biotech) equilibrated with equilibration buffer (20 mM HEPES-NaOH, pH 7.5, 10 mM NaCl, 0.1 mM EDTA, 1 mM DTT, 10 % glycerol). The

protein was then eluted with 1-400 mM NaCl gradient. The concentration of the purified protein was then measured and aliquots were saved at -80˚C before use.

III-4. RESULTS AND DISCUSSION

Confocal image analysis of Aβ42-treated cells to probe interaction of Aβ42 and caspase

We explored the interaction of Aβ42 with the selected caspases using confocal microscope image analysis. Previously, procaspase-9 was proven to interact with the peptides. In the current study, we probed caspase-2, -4, -6, -7 and -8. We chose them, because they are known to play a critical role in the intrinsic and extrinsic apoptosis pathway and one aim of this study was characterization of the potential interaction in relation to the apoptosis pathway. Probing of caspase-3 was omitted because the previous study indicated that it did not interact with Aβ42 [52]. In the current investigation, we employed human epithelial HeLa cells which showed relatively high resistance to Aβ42 damage than other cell lines such as human neuroblastoma SH-SY5Y cells in which death occurred too easily with Aβ treatment (data not shown). And oligomeric preparation of Aβ42 was mainly used for the experiments instead of monomeric or fibrillar peptide, otherwise indicated, because it was superior to the monomer or fibrillar form in entering into the cells [19, 71].

We analyzed the images of cells treated with Aβ42 for the peptide and each caspase. The interaction was determined by revealing the yellow-colored spots in the merged images. Among the tested caspases, prominent yellow spots were recognized in caspase-6 samples,

while they were rarely seen in other caspase test group (Fig. 7). In the current study, we focused on exploration of caspase-6 and its potential interaction with Aβ42. We used 3 different antibodies against caspase-6 for this and following experiments (see "Materials and methods").

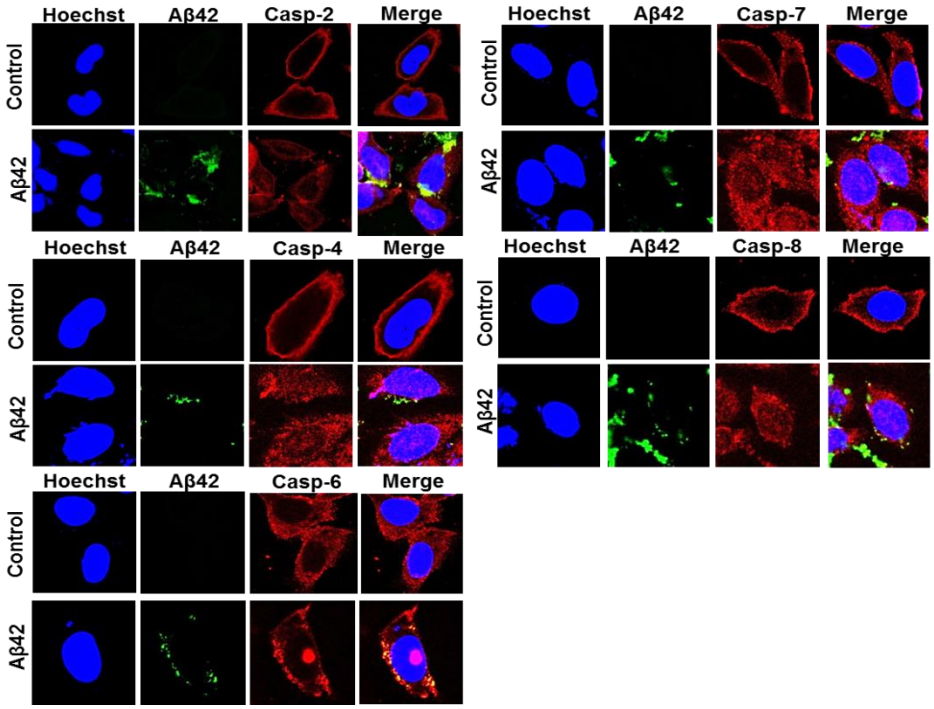

Fig. 7. Aβ42 binds Caspase-6 but not with Caspase -2, -4, -7 and -8. HeLa cells were cultured and treated with 20 μM Aβ42 for 12h. Cells were fixed and permeabilized by methanol and triton x-100. Primary mouse anti amyloid beta (6E10) and rabbit anti caspase-2, goat anti caspase-4, -6, -7 and -8 antibodies in addition to secondary anti-mouse IgG-FITC and anti-rabbit or anti-goat IgG rhodamine antibodies were used to detect intracellular Aβ (green) and caspases (red). Nuclei were seen with the nucleic acid flurochrome Hoechst and images were visualized using a confocal microscope.(LSM 510, Carl Zeiss)

Probing interaction of Aβ42 and caspase-6 by SEC

Immunoblotting analysis can produce frequently false positive results which are partly due to less specific antibodies. In the above confocal studies, caspase-6 was recognized as an Aβ42-interacting protein, but proteins other than caspase-6 were also detected in the western blot analysis as shown in Fig. 8A and Fig. 10C. We made extensive efforts to find more specific anti-caspase-6 antibodies for the confocal and the following studies, but it was not successful (see also Fig. 10C). To reduce this limitation and confirm the interaction, we further investigated the interaction of caspase-6 and Aβ42 using SEC followed by western blotting analysis. It was expected that the two proteins are recognized in the same SEC fractions if they interact with each other. Initially, cell extracts prepared from Aβ42-non-treated cells were analyzed to probe the elution pattern of caspase-6. ~34 kDa band corresponding to procaspase-6 was recognized in fractions #33-#37 (Fig. 8A). In addition to them, other bands were also seen in other fractions among which the fractions around #22 contained the most prominent signals. They were not related with caspase-6, considering the size and the result using purified caspase-6 in which the bands were not seen (Fig. 8E).

Aβ42 peptide was also subjected to SEC and the peptide of the fractions was visualized by western immunoblot analysis using 6E10 and A11 antibodies which bind to different structural species of Aβ [19]. ~9 kDa peptide was detected in #17-25 fractions with 6E10, while ~25 kDa bands was recognized in #14 fraction with A11 (Fig. 8B). Those should

be dimer and oligomers respectively, because the monomeric Aβ42 is 4~5 kDa. However, the sizes of each species estimated by comparison of the molecular weight standard markers of SEC were much bigger, implying that those seen on gels might be an SDS-resistant core of bigger oligomeric species. Monomeric forms of Aβ42 were also detected in the later (>#42) fractions which were not shown here to focus on the caspase-6 containing fractions.

The similar elution pattern of caspase-6 was shown in the fractionation of cell extracts prepared from Aβ42-treated cells by SEC (Fig. 8C). In the analysis of the same cell extracts for Aβ42, only very faint bands estimated as ~9 kDa were detected by western blot analysis with 6E10 antibody in fractions #36-#39, parts of which are caspase-6-containing fractions (Fig. 8C). On the other hand, in the western blot analysis with A11 antibody, protein bands estimated ~25 kDa were recognized in fractions #36-#38 (Fig. 8C). The cell-free experiments using cell extracts and Aβ42 peptide directly added to them also showed the similar ~9 and ~25 kDa bands in the western blot analysis with 6E10 and A11, respectively (Fig. 8D). Similarly, other cell-free experiments using purified caspase-6 and Aβ42 peptide revealed the two protein bands with the same experiments (Fig. 8D), consistent with above results. Altogether, these data suggest a potential interaction of caspase-6 and at least two structural species of Aβ42, though characterization of ~9 kDa and ~25 kDa species remains to be explored.

It is noted that the two bands were also detected in the early

fractions both in the cell-based and cell-free experiments. Those seem to be derived from oligomerized Aβ42 or the peptide that interacts with other cellular proteins, for those were not detected in experiments employing the purified caspase-6 (Fig. 8E). For this western blot analysis, we used AbA which could detect the small domain of caspase-6 (p11) and procaspase-6. However, p11 was very difficult to detect in samples prepared from cells (Fig. 8A, 8C, 8D and Fig. 10C). Only it was recognized in purified caspase-6 (Fig. 8E).

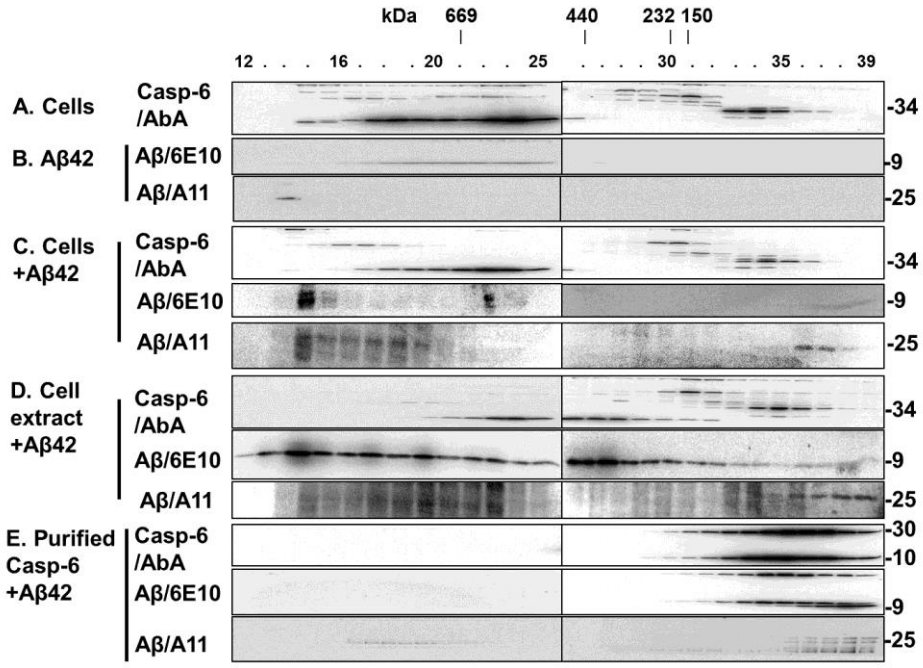

Fig. 8. Aβ42 interacts with Caspase-6. (A, B) HeLa cells were incubated in the absence or presence of 20 μM oligomerized $A\beta_{42}$ for 2+22 h respectively. The extract prepared from the cells (1 ~ 1.5 mg) was fractionated by gel filtration chromatographyas described previously. The fractions were analyzed by immunobloting for caspase-6 and $A\beta_{42}$. The standard molecular markers are indicated above the scale with elution fractions. **(C)** HeLa cell extracts were prepared (1 ~ 1.5 mg) and incubated with 20 μM of $A\beta_{42}$ for 2 h at 30˚C and the reaction mixture was fractionated by gel filtration and analyzed by western blot analysis for caspase-6 and $A\beta_{42}$. **(D)** 10 μg of purified recombinant active caspase-6 was incubated with 20 μM of $A\beta_{42}$ for 2 h at 30˚ C and the reaction mixture was separated and analyzed for caspase-6 and $A\beta_{42}$ as above. **(E)** 20 μM of purified $A\beta_{42}$ was incubated at 30˚C for 2 h and fractionated by gel filtration and probed for $A\beta_{42}$ by western blot analysis.

Probing interaction of Aβ42 and caspase-6 by immunoprecipitation

Immunoprecipitation method was further employed to confirm the interaction (see below). Proteins in the SEC fractions #33-37 of samples shown in Fig. 2B were analyzed for probing the interaction of caspase-6 and Aβ42. We used the fractions instead of cell extract prepared from Aβ42-treated cells, because cells contained many other proteins that could be detected by the antibodies against caspase-6 used here. The immunoprecipitation was performed using AbC, because the other two antibodies (AbA and AbB) were not recommended by the manufacturer for the study. Aβ42 was detected in fractions precipitated with AbC (Fig. 3A), indicating the binding of the peptide to caspase-6. The Aβ42 bands recognized by 6E10 and A11 have sizes different from those in the SEC experiments of Fig. 2 (Fig. 9A). This is probably because the samples were incubated for long time (>12 h) for the immunoprecipitation study and Aβ42 might aggregate during the precipitation procedure. We could not performed the immunoprecipitation with the Aβ antibodies, because of their inability for the experiments. For a reference, purified caspase-6 was incubated with Aβ42 peptide and the reaction mixture was subjected to the same immunoprecipitation study. 6E10 was applicable for this purified caspase-6 experiments. Aβ42 immunoprecipitated with caspase-6 and vice versa (Fig. 9B). Altogether, these all data strongly suggest the binding of Aβ42 to caspase-6.

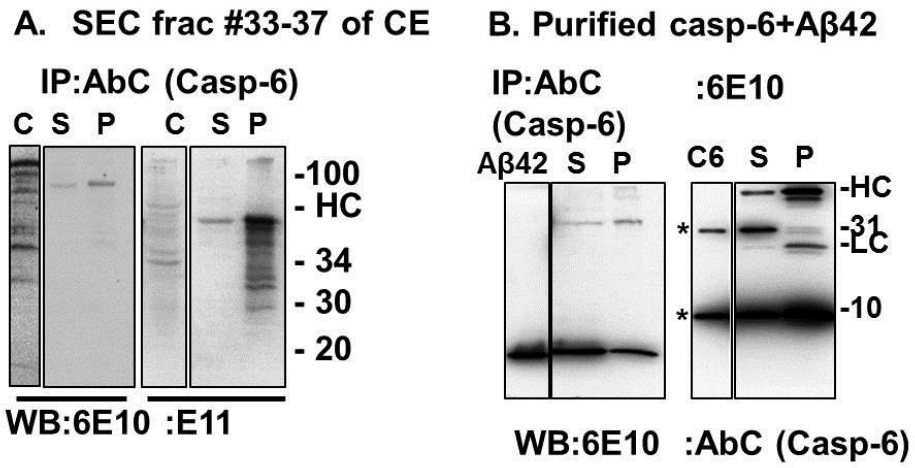

Fig. 9. Immunoprecipitation analysis of the interaction between Aβ42 and Caspase-6. (A) After treating the HeLa cells with 20 μM of $A\beta_{42}$ for 2+22 h, cell extracts were prepared and separated by gel filtration chromatography. Fraction 33-37 as indicated in Fig: 12 were pooled and immunoprecipitated with caspase-6 antibody (Santa Cruz: sc-1232) and probed for $A\beta_{42}$ with 6E10 and A11 antibody. Pooled fractions were loaded as control denoted with C. **(C)** Purified caspase-6 and 20 μM of $A\beta_{42}$ were incubated for 2 h at 30˚ C and immunoprecipated with caspase-6 and 6E10 ($A\beta_{42}$) antibody and western bloted for $A\beta_{42}$ and caspase-6 respectively. Purified $A\beta_{42}$ and caspase-6 (marked with *) was loaded as control.

Activation of caspase-6 and cleavage of lamin A and B

In the above experiments, we used cells in which caspase-6 was potently activated to probe a potential effect of the interaction of caspase-6 and Aβ42 on intracellular function of the caspase. Several different concentrations of Aβ42 and different treatment methods were tested. The "single" treatment of Aβ42 to cells for up to 48 h resulted in a certain levels of activation of caspase-6 that was evaluated by a synthetic substrate VEID-AMC (Fig. 10A). However, it was questionable if the activity was derived from solely Aβ42 treatment, because there was a weak dependency of the activity on concentration of Aβ42. The Aβ42-dose dependency was seen relatively prominently in cells treated twice with Aβ42 (Fig. 10B). Among the "double" treatment conditions, the 2 h pretreatment and subsequent 22 h (2+22 h) treatment induced the most potent activation (Fig. 10B). The 2+22 h samples were employed throughout the current study, because of the prominent activation of caspase-6. We further probed the processing of caspase-6 using western blot analysis. As experiments of Fig. 10, AbA was used initially in the analysis. Although it was difficult to detect the p11, decrease of procspase-6 was clearly seen in the 2+22 h samples with high dose of Aβ42 (20 and 40 μM) (the left panel of Fig. 10C). The same western blot analysis was performed with other anti-caspase-6 antibody, AbB which recognizes the large subunit of the enzyme. ~23 kDa proteins corresponding to the large domain of caspase-6 were clearly seen in the same samples as above (the right panel of Fig. 10C). Altogether, these all data indicated that caspase-6 is activated in the 2+22 h samples treated with Aβ42 at 20 and 40 μM.

We next probed the processing of lamin A/C and B, substrates of catalytically active caspase-6, to know if the enzyme properly functioned inside of cells. While no fragmentation of lamin proteins was observed in cells treated with Aβ42 for 48 h or 2+10 h (Fig. 11A and 11B), the fragmentation was detected in 2+22 h and 2+34 h samples (Fig. 11C and

11D). The detected ~46 kDa lamin A fragment and ~21 kDa lamin B fragment, however, should not be generated by the action of caspase-6, because it produces ~28 kDa lamin A fragment and ~46 kDa lamin B fragment (Fig. 11F). For comparison, caspase-6-dependent fragmentations of lamins were clearly seen in STS-treated cells (Fig. 11E). Thus, it seems that caspase-6 is catalytically active in Aβ42-treated cells, but is not functionally active. Hopefully, understanding the mechanistic details of the caspase-6 in the Aβ42-treated cells will provide novel insight into Aβ-associated pathology and control of AD.

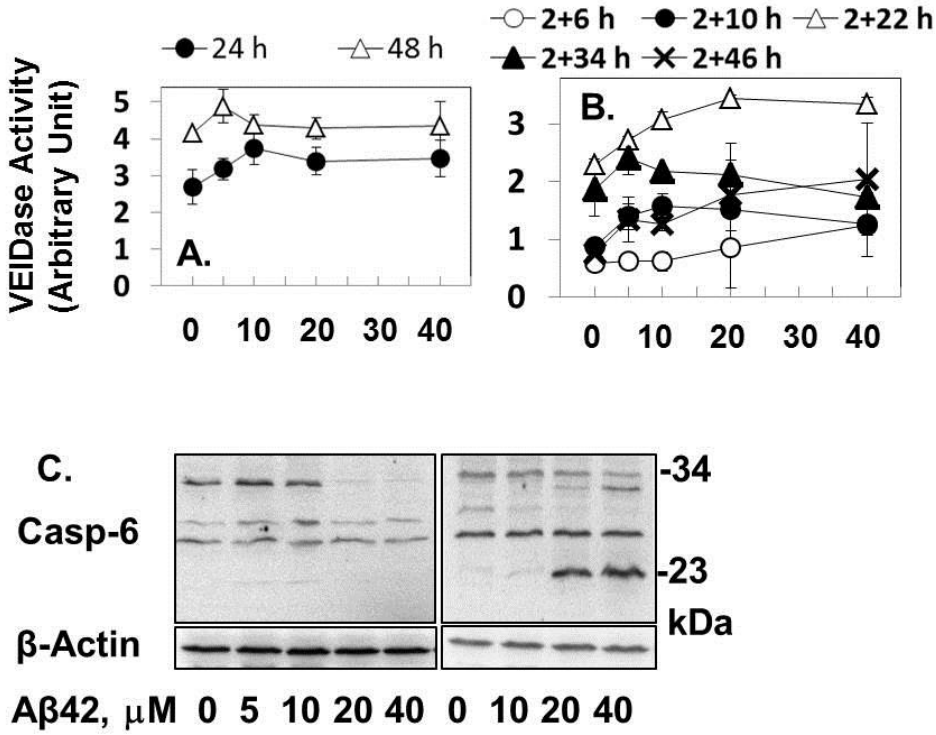

Fig. 10. Double treatment but not single treatment of $A\beta_{42}$ oligmeric species induces caspase-6 activity and cleavage. (A,B) HeLa cells ($2x10^4$ /100 μl of culture media) were treated with oligomerized $A\beta_{42}$ at the indicated concentrations and time. Caspase-6 activity was measured using its synthetic substrate VEID-AMC (50μM). **(C)** HeLa cells ($8x10^5$) were treated with indicated concentration of $A\beta_{42}$ for 2+22 h, total cell lysate were prepared and caspase-6 cleavage was checked by immunoblot analysis with mouse anti-human caspase-6 monoclonal antibody (BD Pharmingen) and rabbit anti-caspase-6 polyclonal antibody (Ab Frontier). Actin was loaded as loading control.

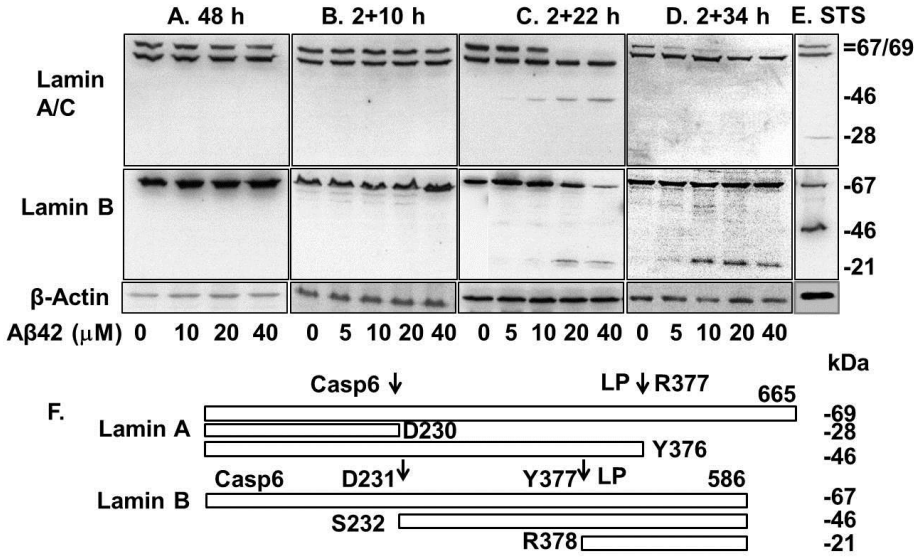

Fig. 11. Time and concentration dependent cleavage of Lamin A and B by $A\beta_{42}$. **(A - D)** HeLa cells ($8x10^5$) were treated with indicated concentration of $A\beta_{42}$ for the indicated time periods, total cell lysate were prepared and analyzed for the cleavage of Lamin A/C and B by immunoblot (antibody for Lamin A/C was raised against N-terminus of human Lamin A/C and for Lamin B was raised against C-terminus of human Lamin B1). Actin was employed as loading control. **(E)** HeLa cells were treated with 5μM of STS for 6 h and after preparation of whole cell lysate probed for the cleavage of Lamin A/C and B by western blot. Actin was loaded as control. **(F)** Schematic drawing of Lamin A and B cleaving sites by caspase-6 and Lamin protease. The predicted sizes of the cleavage fragments are indicated.

IV. Purification and characterization of cell penetrating TAT-Aβ$_{42}$

IV-1. INTRODUCTION

Amyloid beta plaques consisting of fibrillar aggregates of amyloid beta Aβ peptides are the pathological hallmark of Alzheimer's disease. But the detail mechanism of Aβ aggregation, the nature of the toxic species, and the cellular pathway of Aβ induced toxicity is yet to be revealed. It has been proposed that the soluble oligomers as well as the fibrillar aggregates are responsible for the neuronal toxicity. Substantial evidence suggests that, intracellular accumulations Aβ is required to show the toxicity prior to extracellular deposition. Intracellular accumulations is reported to be occurred either by endogenous production of Aβ by some organelles e.g. lysosome, Golgi apparatus, endoplasmic reticulum etc., or by reuptake of extracellular Aβ by endocytosis. Long term expression of APP in rat culture has been shown to induce apoptosis [99]. Presence of intracellular Aβ dimers in primary human neurons and in neuronal cell lines, and accumulation of intracellular Aβ in FAD expressing mice and its correlation to accelerated toxicity clearly implicate the role of intracellular Aβ in neuronal loss [100, 101]. The interaction of amyloid beta with intracellular proteins and the implications of this interaction are also reported [52]. Aβ has been found to bind with a number of receptors or receptor related proteins such

as N-methyl-D-aspartic acid (NMDA) receptor [26], low-density receptor associated protein-1 [27], the α7 nicotinic acetyl choline receptor [28], the p75 neurotrophin receptor [29], and the receptor for advanced glycation endproducts [30]. However, due to lack of specificity of Aβ antibody, sometimes it is difficult to know the exact mechanism of these interactions and their implications on cell cytotoxicity. For the investigation of these mechanisms proposed, large amount of pure Aβ peptides and diverse mutants of Aβ are required. Therefore, cell penetrating version of $A\beta_{42}$, which is the major component of the senile plaques, could be a one interesting option to understand the role of intracellular Aβ in cytotoxicity and to identify Aβ- interacting protein. Cell penetrating version of $A\beta_{42}$ has its advantage over transgenic models, overexpression of APP and expression of cDNA coding Aβ sequence.

The major challenges in expressing this cell penetrating version of $A\beta_{42}$ in *Escherichia coli* is its toxicity towards the bacterial cells, poor expression, inclusion body forming and solubility problem. To overcome these difficulties, the peptide was co-expressed with a fusion protein such as maltose binding protein (MBP), thioredoxin (TRX), transcription pausing factor L (NusA), glutathione-S-transferase [102-104]. The fusion protein technology is beneficial both for high yield and purity, but in most cases, the insoluble inclusion bodies are solubilized by adding strong denaturant such as urea to prevent the aggregation by inhibiting inter and intra molecular interaction. Cleavage of fusion protein in presence of urea is also beneficial in two ways, first, it inhibits the

precipitation of fusion protein before cleavage and second, urea prevents the aggregation of cleaved peptide which is a common phenomenon in aggregation prone peptide. Recently, use of ubiquitin in fusion protein technology has gained considerable interest. Ubiquitin fusion offers efficient cleavage of target by highly specific and robust deubiqutylating enzyme, Usp2-cc. In this study, a recombinant fusion method was used to produce TAT- $A\beta_{42}$. The fusion protein consists of a co-chaperone GroES connected by ubiquitin and then the TAT- $A\beta_{42}$.

IV-2. MATERIALS AND METHODS

Construction and purification of TAT tagged amyloid beta peptides

Genes encoding GroES was PCR amplified (antisense primer, 5'- AAG TCC GCT CTA TTC TTG ATG CGG ATC CCG-3'; sense primer, 5'- GGA ATT CCA TAT GAA TAT TCG TCC ATT GCA -3') using *E. coli* DH5α genomic DNA as template and cloned in *Nde1* and *BamH1* sites of pET28b expression system (Novagen). Ubiquitin gene (kindly provided by Rohan T. Baker) was subcloned in *NdeI/BamHI* sites of a vector containing amyloid beta42 ($A\beta_{42}$). Thereafter, *BamHI* site between ubiquitin and $A\beta_{42}$ were destroyed by site directed mutagenesis to facilitate further cloning. Ubiquitin - $A\beta_{42}$ was PCR amplified (sense 5'- CGC GGA TCC CAG ATC TTT GTG AAG AC -3'; antisense 5'- CCG CTC GAG TCA CGC

TAT GAC AAC ACC GCC -3') and cloned between *BamHI* and *XhoI* sites following C-terminus GroES. TAT tagged Ab42 construct was prepared by inserting TAT sequence between ubiquitin and Ab42 sequence using antisense primer 5'- GGA ATT CTG CAT CGC CAC GAC GCT GAC GAC GTT TTT TAC GGC CTC CAC CGC GGA GGC GCA A -3' and sense primer 5'- CGC GGA TCC CAG ATC TTT GTG AAG AC-3').

Expression of GroES-Ub-TAT-Aβ_{42} fusion protein

The fusion protein was overexpressed as inclusion bodies in *E.coli* BL21 (DE3) pLysS cells. The protocol used as follows: a single colony was inoculated into 50 ml of LB media supplemented with kanamycin to a final concentration of 30 μg/ml and culture for overnight at 37˚ C. The next day, the 50 ml seed culture was transferred into 1L of LB media supplemented with kanamycin with a final concentration of 30 μg/ml and incubated at 37˚ C until the OD_{600} reaches to 0.6 – 0.8. Isopropyl-β- D- thiogalactopyranoside (IPTG) was the added to 0.4 mM concentration for induction. The culture was additionally grown for 4 h and the cells were harvested by centrifuging at 4000 rpm for 10 min at 4˚ C. The cells were then washed with buffer (20ml/1L of culture) containing 50 mM Tris-HCl (pH 8.0), 150 mM NaCl and 5 mM EDTA, collected in 50 ml conical tube and again centrifuged at 4000 rpm for 10 min. The pellets were either used for next step purification or stored at -20˚ C.

Cell lysis and preparation of inclusion bodies

The cell pellet was re-suspended in 20 ml (for 1 L culture) in lysis buffer (50 mM Tris-HCl pH 8.0, 150 mM NaCl, 5 mM EDTA, 0.5% triton X – 100, 1 mM DTT, 0.1 mM PMSF) and kept in ice for 30 min and lysed by sonication at ice cold temperature. The cell extract was then centrifuged at 20000 rpm for 30 min and the supernatant discarded. The pellets were washed 3 times by re-suspending in washing buffer I (50 mM Tris-HCl pH 8.0, 150 mM NaCl. 5 mM EDTA, 0.5% triton X – 100, 1 mM DTT) for 3 times followed by washing with washing buffer II (50 mM Tris-HCl pH 8.0, 150 mM NaCl, 5 mM EDTA, 1 mM DTT) for 2 times. Each time the inclusion bodies were collected by centrifuging at 20000 rpm for 30 min.

Solubilization and digestion of GroES-Ub-TAT-Aβ_{42} fusion protein with Usp2cc enzyme

The extensively washed inclusion bodies were solubilized in 20 ml of solubilization buffer (50 mM Tris-HCl pH 8.0, 150 mM NaCl, 1 mM DTT and 6 M urea) for 1 L of culture and kept at room temperature for 30 min. The soluble proteins were collected by centrifuging at 18000 rpm for 30 min; concentration was measured and adjusted to a final concentration of 9 mg/ml to facilitate the digestion. For digestion, the protein sample was diluted 2 times with buffer (50 mM Tris-HCl pH 8.0,

150 mM NaCl, 1 mM DTT) to maintain the final concentration of urea 3 M to avoid precipitation of fusion protein and to maintain the Usp2cc activity. The digestion reaction was carried with an enzyme : substrate molar ratio 1:100 for 3 h at 37˚ C. After digestion, the sample was sonicated on water bath for 10 min and centrifuged at 18000 rpm for 30 min and the supernatant was collected for next step purification.

HPLC purification of TAT-$A\beta_{42}$ peptide on polymer based column

The reverse phase polymer column was equilibrated with 3 column volume of HPLC buffer A (10 mM Ammonium acetate, pH 10 in 2% acetonitrile) and the sample was injected onto the column. The bound peptide was then eluted with linear gradient of HPLC buffer B (70% acetonitrile) with a flow rate of 10 ml/min. TAT- $A\beta_{42}$ was eluted as a single peak at 30-35% of buffer B. The TAT- $A\beta_{42}$ containing fraction was collected and lyophilized in 50 ml conical tube with Para film cover (~ 48 h).

Preparation of TAT- $A\beta_{42}$ peptides

The purified peptide was solubilized in 100% 1,1,1,3,3,3,-hexafluoro-2-propanol, and dried under nitrogen flow and subsequently, under vacuum for 30 min. The peptide aliquots were stored at –20 °C until use. Immediately before use, the peptide was dissolved in 0.1%

NH4OH at a concentration of 2 mg/ml followed by bath sonication for 10 min. The solution was diluted at the desired concentration with cell culture media without FBS.

Cell culture and cytotoxicity Assay

Human epithelial HeLa cells were cultured in DMEM (High glucose) medium supplemented with 10% (v/v) FBS and 1% antibiotics at 37 °C under 5% CO2.

For MTT cytotoxicity assay, cells were plated at a density of 15,000 cells/well in 96-well plates (Nunc, Denmark) and cultured for 24 h followed by serum deprivation for another 12 h. Cells were exposed to the Aβ preparation for 24 h and the viability was assessed by 3-(4,5-dimethylthiazol-2-yl)-2,5-di-phenyltetrazolium bromide (MTT) reduction test. Briefly, 20 μl of 5 mg/ml MTT solution in PBS was added to each well and incubated for 2 h. Then 100 μl of solubilization buffer [20% SDS solution in 50% (v/v) DMF (pH 4.7)] was added. After 12-16 h of incubation, absorbance was recorded at 570 nm using a micro plate reader KisanBio plate reader (KisanBio, Seoul, South Korea).

Immunocytochemistry to check the entry of $A\beta_{42}$ species inside the cells

HeLa cells were seeded in 6 well plate at 70% confluency, cultured for 24h and further incubated for 12h in serum free media and then treated without or with 5 μM of indicated $A\beta_{42}$ for 24 h. Treated cells were fixed in methanol at -20˚ C and permeabilized by 0.3% Triton X-100. After blocking with 0.1% BSA overnight, primary mouse anti-amyloid beta (6E10), mouse anti-HIV1 tat (N3), mouse anti-FLAG (M2) and rabbit anti caspase-9 antibodies were added to each samples and incubated overnight at 4°C. After washing with PBS, Alexa-Flour-488 conjugated chicken anti mouse IgG, FITC conjugated goat anti-rabbit antibodies (dilution, 1:200) were treated for 2h at room temperature followed by PBS washing. Nuclei were stained with Hoechst and confocal images were obtained with Carl Zeiss LSM510 microscope (Jena, Germany) using vendor provided software (LSM 510).

IV-3. RESULTS AND DISCUSSION

Overexpression of fusion protein and purification

After harvesting the cells by high speed centrifugation, the cells were lysed in lysis buffer and the supernatant solution and the precipitated pellets were checked for the expression and whether the fusion protein appeared in the supernatant or in the inclusion bodies in

SDS-PAGE gel (Lane 1-3 of Fig: 12B). As expected, a large protein band of approximate mass of 25 kDa, that of the fusion protein, was found in the pellets of the cell extracts (Lane: 3). Therefore, the supernatant was discarded and the inclusion bodies were used for further purification.

The pellets of the cell extract were washed extensively 3 times with washing buffer I (described in materials and methods) to remove the traces of other soluble proteins. Then the inclusion bodies were further washed with washing buffer II twice to eliminate the triton X-100 so that it does not interfere with Usp2cc digestion and HPLC purification. The inclusion bodies found after this washing step is mostly free of other contaminants (Lane 4 of Fig: 12B) as found in the SDS-PAGE gel electrophoresis. At this stage, the inclusion bodies were solubilized in 6 M urea and centrifuged in a high speed centrifugation at 18000 rpm to remove the small amount of insoluble proteins. The supernatant was collected, quantified for the protein concentration by Bradford assay and diluted twice to facilitate digestion by Usp2cc in 3 M of urea (Lane 5, Fig: 12B). Bellow this concentration of urea, the inclusion bodies tend to precipitate and over 3 M of urea concentration Usp2cc was found less effective in case of wild type $A\beta_{42}$. Following the cleavage reaction, the cleaved peptide was separated by using reverse phase HPLC polymer based column using the buffers systems mentioned in materials and method section. It is evident from the gel electrophoresis result (Lane 6, Fig: 12B) that the TAT-$A\beta_{42}$ we got finally is quite pure. Approximately 4.0 mg of TAT-$A\beta_{42}$ was obtained from 1 L of bacterial culture.

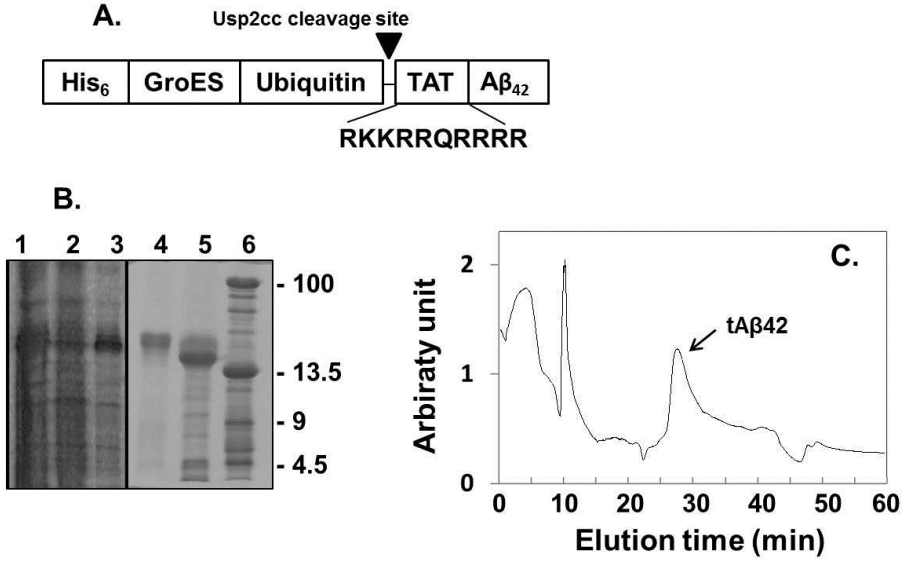

Fig. 12. Construction, Expression and purification of TAT- Aβ$_{42}$. (A) Schematic representation of the TAT- Aβ$_{42}$ construct. **(B)** SDS-PAGE analysis of overexpressed GroES-Ub-TAT- Aβ$_{42}$ fusion protein. Lanes: 1, Cell extracnts, 2, supernatant, 3, precipitant, 4, washed inclusion body of GroES-Ub-TAT- Aβ$_{42}$ fusion protein; 5, Fusion protein digested by Usp2-cc; 6, HPLC purified TAT- Aβ$_{42}$. **(C)** HPLC chromatogram shows elution profile of TAT- Aβ$_{42}$.

Toxicity of TAT, FLAG and wild type $A\beta_{42}$

The exact mechanism of toxicity by Aβ is not well defined till now. Although, the senile plaque consisting of Aβ is primarily extracellular, the role of this extracellular Aβ on cytotoxicity is also unknown to date, though many hypotheses have been proposed. Expression of Aβ inside the cells helps to reveal the role of intracellular accumulation of Aβ, but the consequences of large deposition of extracellular Aβ remains questionable. Moreover, transfection of Aβ plasmids may alter the membrane properties of the cells, which may interfere with the cytotoxicity rendered by Aβ. Considering these things, we treated the cells by three different kinds of Aβ, that is, a cell penetrating version of TAT- $A\beta_{42}$, FLAG- $A\beta_{42}$ which cannot enter into the cells revealed by confocal microscopy, and the wild type $A\beta_{42}$ as mentioned in the materials and methods section. The percentage of cell death induced by these three $A\beta_{42}$ varies significantly. As the data shows (Fig: 13), cell survival rate is the maximum with the cells treated by FLAG- $A\beta_{42}$. In the case of TAT- $A\beta_{42}$, the cell survival rate was the lowest even at very low concentration of TAT- $A\beta_{42}$, while the wild type $A\beta_{42}$ shows moderate cytotoxicity among the three different $A\beta_{42}$ species. The difference in the level of cytotoxicity induced by three groups of $A\beta_{42}$ can be described by the fact that, entry into the cell might be very crucial for $A\beta_{42}$ mediated cell death pathway.

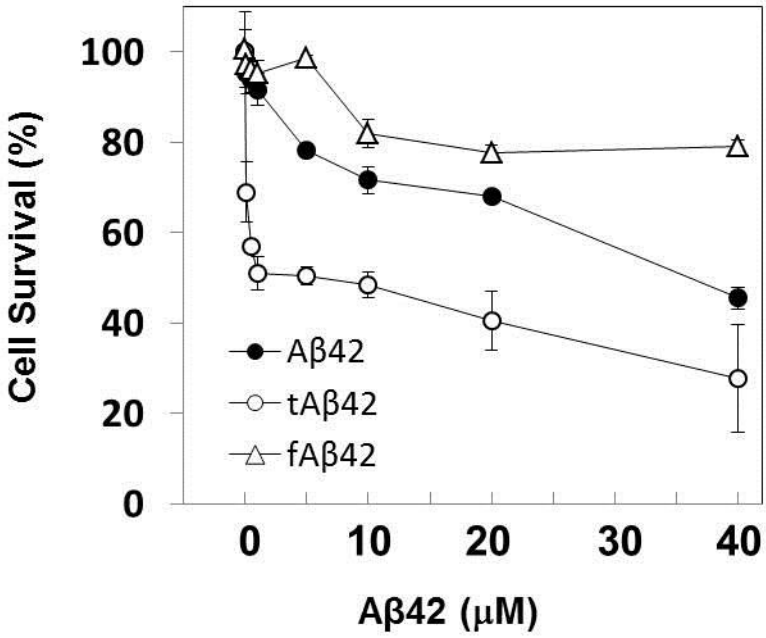

Fig. 13. Cytotoxicity of different species of $A\beta_{42}$ in HeLa cells. Cells were cultured (10000 cells/well) for 24 h and serum deprived for 24 h and then treated with mentioned species of $A\beta_{42}$ at indicated concentration for 24 h. Cytotoxicity was measured by MTT reduction assay. Triplicate experiments were performed and standard deviations were indicated as bars.

TAT- $A\beta_{42}$ preferentially enters into cells than wild type and FLAG- $A\beta_{42}$

It was found from confocal microscopy results that, FLAG- $A\beta_{42}$ was unable to enter into the cells, it accumulates outside the membrane. While, intra cellular accumulation of TAT- $A\beta_{42}$ was much higher than wild type $A\beta_{42}$. In the earlier study from our lab, it was shown that, $A\beta_{42}$ can bind to procaspase-9 and inhibit the caspase cascade initiated by intrinsic apoptotic pathway [52]. To confirm the binding ability of TAT-$A\beta_{42}$ with caspase-9, the interaction of all three groups of $A\beta_{42}$ was checked by concomitant antibody treatment for both Aβ antibodies (TAT, 6E10 and FLAG) and caspase-9 antibody. And the interaction was found very clearly (Fig: 14). The cause of higher cell death by TAT- $A\beta_{42}$ was further substantiated by this entrance into the cells.

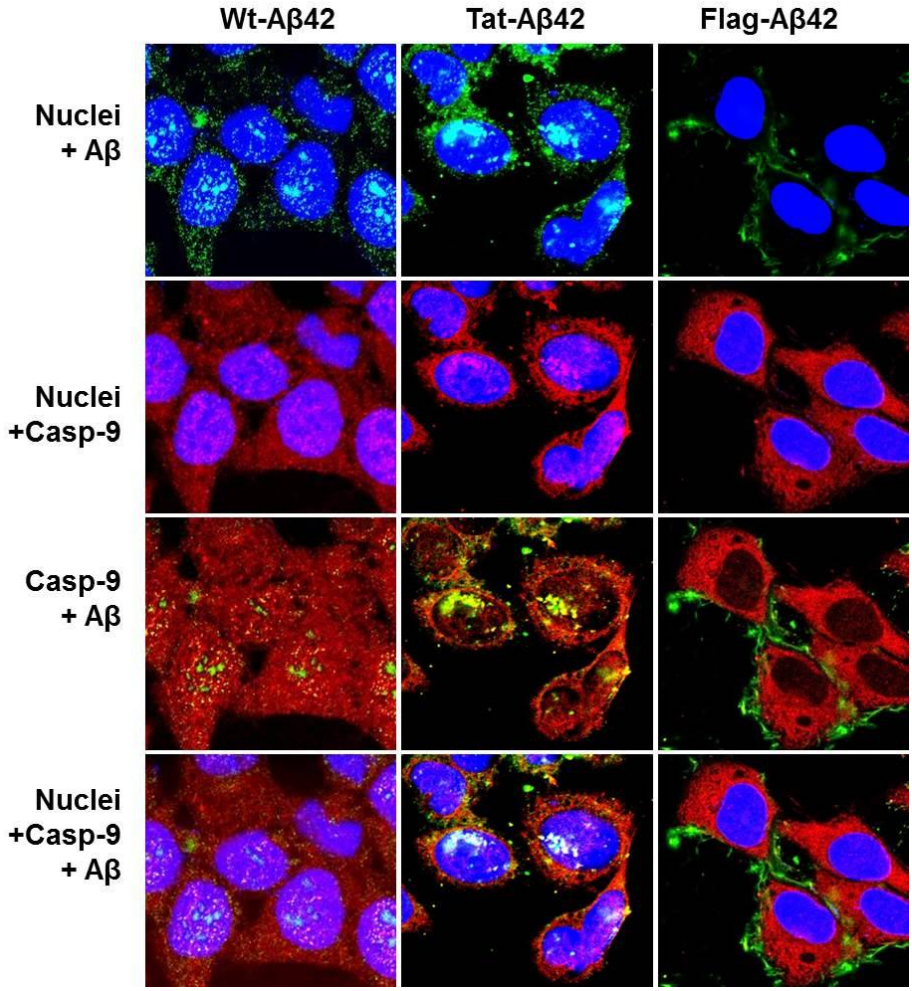

Fig. 14. Confocal microscopy analysis of different species of $A\beta_{42}$. HeLa cells were treated with 20 μM of wild type $A\beta_{42}$ and FLAG- $A\beta_{42}$ and 5 μM of TAT-$A\beta_{42}$ for 24 h. Cells were fixed and permeabilized by methanol and triton x-100. Primary mouse anti-amyloid beta (6E10), mouse anti- FLAG, mouse anti-TAT and rabbit anti-caspase-9 antibodies in addition to secondary anti-mouse IgG-FITC and

anti-rabbit IgG Rhodamine antibodies were used to detect intracellular Aβ (green) and caspase-9 (red) respectively. Nuclei were seen with the nucleic acid fluorochrome Hoechst and images were visualized using a confocal microscope. (LSM 510, Carl Zeiss).

FUTURE RESEARCH

Purification of TAT- $A\beta_{42}$ by Methanol Precipitation method

Purification of recombinant peptide always poses difficulties due to various factors such as: solubility problem, inclusion body formation, precipitation during purification which results in loss of biological activities. To overcome this problem, denaturant buffers e.g. urea or guanidine hydrochloride is used in the purification buffer systems. To remove this denaturant from the purified peptide sample is often problematic, either we have to go for dialysis which is a time consuming process or we have to go for another column chromatographic purification which may be both time consuming and costly. But, we can easily remove the denaturants from the peptide sample by precipitating with different organic solvents like ether, methanol, ethanol or iso-propyl alcohol and then solubilize the peptide in a suitable solvent. In this method, we also tried to precipitate TAT- $A\beta_{42}$ digested inclusion bodies with different solvents among which methanol was the most efficient to precipitate the peptide. The purification scheme is as bellow:

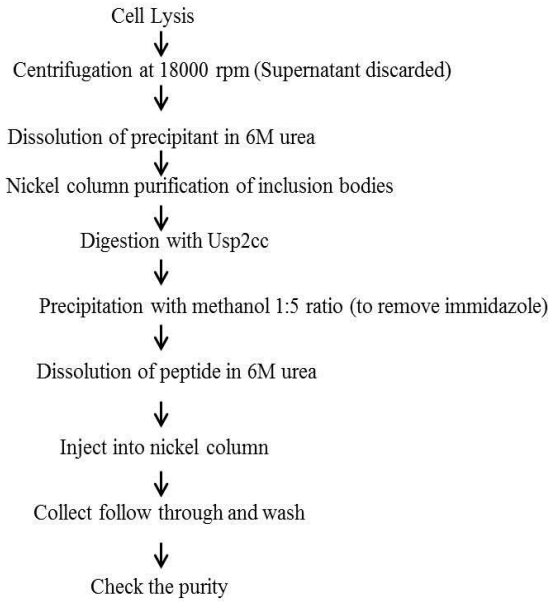

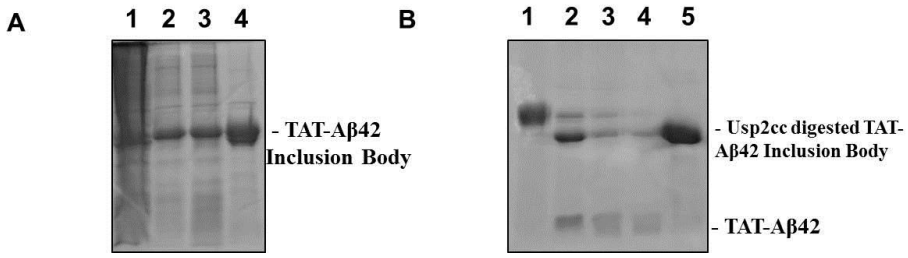

Figure. 15. Purification of TAT- $A\beta_{42}$ by precipitation method. (A) Purification of inclusion bodies by nickel column: lanes are as: 1- precipitant got after centrifugation of cell lysate, 2- follow through collected, 3- wash with washing buffer, 4- elution with imidazole. **(B)** Digestion and purification of TAT- $A\beta_{42}$. Lanes: 1- purified inclusion bodies, 2- inclusion bodies digested with Usp2cc enzyme, 3- follow through after nickel column injection, 4- wash after nickel column injection and 5- elution with imidazole.

V. REFERENCES

1. Selkoe, D.J., *Alzheimer's disease: genes, proteins, and therapy.* Physiol Rev, 2001. **81**(2): p. 741-66.

2. Suh, Y.H. and F. Checler, *Amyloid precursor protein, presenilins, and alpha-synuclein: molecular pathogenesis and pharmacological applications in Alzheimer's disease.* Pharmacol Rev, 2002. **54**(3): p. 469-525.

3. Goate, A., et al., *Segregation of a missense mutation in the amyloid precursor protein gene with familial Alzheimer's disease.* Nature, 1991. **349**(6311): p. 704-6.

4. Hardy, J. and D.J. Selkoe, *The amyloid hypothesis of Alzheimer's disease: progress and problems on the road to therapeutics.* Science, 2002. **297**(5580): p. 353-6.

5. Hardy, J.A. and G.A. Higgins, *Alzheimer's disease: the amyloid cascade hypothesis.* Science, 1992. **256**(5054): p. 184-5.

6. Cao, X. and T.C. Sudhof, *A transcriptionally [correction of transcriptively] active complex of APP with Fe65 and histone acetyltransferase Tip60.* Science, 2001. **293**(5527): p. 115-20.

7. Gao, Y. and S.W. Pimplikar, *The gamma -secretase-cleaved C-terminal fragment of amyloid precursor protein mediates signaling to the nucleus.* Proc Natl Acad Sci U S A, 2001. **98**(26): p. 14979-84.

8. Kimberly, W.T., et al., *The intracellular domain of the beta-amyloid precursor protein is stabilized by Fe65 and translocates to the nucleus in a notch-like manner.* J Biol Chem, 2001. **276**(43): p. 40288-92.

9. Deshpande, A., et al., *Different conformations of amyloid beta induce neurotoxicity by distinct mechanisms in human cortical neurons.* J Neurosci, 2006. **26**(22): p. 6011-8.

10. Koffie, R.M., et al., *Oligomeric amyloid beta associates with postsynaptic densities and correlates with excitatory synapse loss near senile plaques.* Proc Natl Acad Sci U S A, 2009. **106**(10): p. 4012-7.

11. Bitan, G., et al., *Amyloid beta -protein (Abeta) assembly: Abeta 40 and Abeta 42 oligomerize through distinct pathways.* Proc Natl Acad Sci U S A, 2003. **100**(1): p. 330-5.

12. Duering, M., et al., *Mean age of onset in familial Alzheimer's disease is determined by amyloid beta 42.* Neurobiol Aging, 2005. **26**(6): p. 785-8.

13. Shahnawaz, M., et al., *Wild-type, Flemish, and Dutch amyloid-beta exhibit different cytotoxicities depending on Abeta40 to Abeta42 interaction time and concentration ratio.* J Pept Sci, 2013. **19**(9): p. 545-53.

14. Bitan, G., S.S. Vollers, and D.B. Teplow, *Elucidation of primary structure elements controlling early amyloid beta-protein oligomerization.* J Biol Chem, 2003. **278**(37): p. 34882-9.

15. Klyubin, I., et al., *Amyloid beta protein dimer-containing human CSF disrupts synaptic plasticity: prevention by systemic passive immunization.* J Neurosci, 2008. **28**(16): p. 4231-7.

16. Shankar, G.M., et al., *Amyloid-beta protein dimers isolated directly from Alzheimer's brains impair synaptic plasticity and memory.* Nat Med, 2008. **14**(8): p. 837-42.

17. Naiki, H. and K. Nakakuki, *First-order kinetic model of Alzheimer's beta-amyloid fibril extension in vitro.* Lab Invest, 1996. **74**(2): p. 374-83.

18. Lambert, M.P., et al., *Diffusible, nonfibrillar ligands derived from Abeta1-42 are potent central nervous system neurotoxins.* Proc Natl Acad Sci U S A, 1998. **95**(11): p. 6448-53.

19. Kayed, R., et al., *Common structure of soluble amyloid oligomers implies common mechanism of pathogenesis.* Science, 2003. **300**(5618): p. 486-9.

20. O'Nuallain, B., et al., *Seeding specificity in amyloid growth induced by heterologous fibrils.* J Biol Chem, 2004. **279**(17): p. 17490-9.

21. Koo, E.H. and S.L. Squazzo, *Evidence that production and release of amyloid beta-protein involves the endocytic pathway.* J Biol Chem, 1994. **269**(26): p. 17386-9.

22. LaFerla, F.M., K.N. Green, and S. Oddo, *Intracellular amyloid-beta in Alzheimer's disease.* Nat Rev Neurosci, 2007. **8**(7): p. 499-509.

23. Bayer, T.A. and O. Wirths, *Intracellular accumulation of amyloid-Beta - a predictor for synaptic dysfunction and neuron loss in Alzheimer's disease.* Front Aging Neurosci, 2010. **2**: p. 8.

24. Small, D.H., S.S. Mok, and J.C. Bornstein, *Alzheimer's disease and Abeta toxicity: from top to bottom.* Nat Rev Neurosci, 2001. **2**(8): p. 595-8.

25. Verdier, Y. and B. Penke, *Binding sites of amyloid beta-peptide in cell plasma membrane and implications for Alzheimer's disease.* Curr Protein Pept Sci, 2004. **5**(1): p. 19-31.

26. Bi, X., et al., *Uptake and pathogenic effects of amyloid beta peptide 1-42 are enhanced by integrin antagonists and blocked by NMDA receptor antagonists.* Neuroscience, 2002. **112**(4): p. 827-40.

27. Deane, R., et al., *LRP/amyloid beta-peptide interaction mediates differential brain efflux of Abeta isoforms.* Neuron, 2004. **43**(3): p. 333-44.

28. Wang, H.Y., et al., *beta-Amyloid(1-42) binds to alpha7 nicotinic acetylcholine receptor with high affinity. Implications for Alzheimer's disease pathology.* J Biol Chem, 2000. **275**(8): p. 5626-32.

29. Yaar, M., et al., *Binding of beta-amyloid to the p75 neurotrophin receptor induces apoptosis. A possible mechanism for Alzheimer's disease.* J Clin Invest, 1997. **100**(9): p. 2333-40.

30. Du Yan, S., et al., *Amyloid-beta peptide-receptor for advanced glycation endproduct interaction elicits neuronal expression of macrophage-colony stimulating factor: a proinflammatory pathway in Alzheimer disease.* Proc Natl Acad Sci U S A, 1997. **94**(10): p. 5296-301.

31. Simakova, O. and N.J. Arispe, *The cell-selective neurotoxicity of the Alzheimer's Abeta peptide is determined by surface phosphatidylserine and cytosolic ATP levels. Membrane binding is required for Abeta toxicity.* J Neurosci, 2007. **27**(50): p. 13719-29.

32. Kanekiyo, T. and G. Bu, *Receptor-associated protein interacts with amyloid-beta peptide and promotes its cellular uptake.* J Biol Chem, 2009. **284**(48): p. 33352-9.

33. Kulandaivelu, U., et al., *Synthesis, antimicrobial and anticancer activity of new thiosemicarbazone derivatives.* Arch Pharm (Weinheim), 2011. **344**(2): p. 84-90.

34. Davis, C.H. and M.L. Berkowitz, *Structure of the amyloid-beta (1-42) monomer absorbed to model phospholipid bilayers: a molecular dynamics study.* J Phys Chem B, 2009. **113**(43): p. 14480-6.

35. Arispe, N., E. Rojas, and H.B. Pollard, *Alzheimer disease amyloid beta protein forms calcium channels in bilayer membranes: blockade by tromethamine and aluminum.* Proc Natl Acad Sci U S A, 1993. **90**(2): p. 567-71.

36. Kagan, B.L., R. Azimov, and R. Azimova, *Amyloid peptide channels.* J Membr Biol, 2004. **202**(1): p. 1-10.

37. Lal, R., H. Lin, and A.P. Quist, *Amyloid beta ion channel: 3D structure and relevance to amyloid channel paradigm.* Biochim Biophys Acta, 2007. **1768**(8): p. 1966-75.

38. Cataldo, A.M., D.J. Hamilton, and R.A. Nixon, *Lysosomal abnormalities in degenerating neurons link neuronal compromise to senile plaque development in Alzheimer disease.* Brain Res, 1994. **640**(1-2): p. 68-80.

39. Kumari, S., S. Mg, and S. Mayor, *Endocytosis unplugged: multiple ways to enter the cell.* Cell Res, 2010. **20**(3): p. 256-75.

40. Yu, C., et al., *Endocytic pathways mediating oligomeric Abeta42 neurotoxicity.* Mol Neurodegener, 2010. **5**: p. 19.

41. Fuentealba, R.A., et al., *Low-density lipoprotein receptor-related protein 1 (LRP1) mediates neuronal Abeta42 uptake and lysosomal trafficking.* PLoS One, 2010. **5**(7): p. e11884.

42. Kandimalla, K.K., et al., *Mechanism of neuronal versus endothelial cell uptake of Alzheimer's disease amyloid beta protein.* PLoS One, 2009. **4**(2): p. e4627.

43. Lai, A.Y. and J. McLaurin, *Mechanisms of amyloid-Beta Peptide uptake by neurons: the role of lipid rafts and lipid raft-associated proteins.* Int J Alzheimers Dis, 2010. **2011**: p. 548380.

44. Olzscha, H., et al., *Amyloid-like aggregates sequester numerous metastable proteins with essential cellular functions.* Cell, 2008. **144**(1): p. 67-78.

45. Troy, C.M., J.E. Friedman, and W.J. Friedman, *Mechanisms of p75-mediated death of hippocampal neurons. Role of caspases.* J Biol Chem, 2002. **277**(37): p. 34295-302. .

46. Truzzi, F., et al., *p75 neurotrophin receptor mediates apoptosis in transit-amplifying cells and its overexpression restores cell death in psoriatic keratinocytes.* Cell Death Differ., 2011. **18**(6): p. 948-58.

47. Hernandez-Zimbron, L.F., et al., *Amyloid-beta peptide binds to cytochrome C oxidase subunit 1.* PLoS One, 2012. **7**(8): p. e42344.

48. Lustbader, J.W., et al., *ABAD directly links Abeta to mitochondrial toxicity in Alzheimer's disease.* Science, 2004. **304**(5669): p. 448-52.

49. Swerdlow, R.H., *Brain aging, Alzheimer's disease, and mitochondria.* Biochim Biophys Acta, 2011. **1812**(12): p. 1630-9.

50. Liu, T., et al., *Cooperative role of RanBP9 and P73 in mitochondria-mediated apoptosis.* Cell Death Dis, 2013. **4**: p. e476.

51. Hong, Y.K., et al., *Inhibition of JNK/dFOXO pathway and caspases rescues neurological impairments in Drosophila Alzheimer's disease model.* Biochem Biophys Res Commun, 2012. **419**(1): p. 49-53.

52. Sharoar, M.G., et al., *Amyloid beta binds procaspase-9 to inhibit assembly of Apaf-1 apoptosome and intrinsic apoptosis pathway.* Biochim Biophys Acta, 2014. **1843**(4): p. 685-93.

53. Formigli, L., et al., *Aponecrosis: morphological and biochemical exploration of a syncretic process of cell death sharing apoptosis and necrosis.* J Cell Physiol, 2000. **182**(1): p. 41-9.

54. Castro-Obregon, S., et al., *A ligand-receptor pair that triggers a non-apoptotic form of programmed cell death.* Cell Death Differ, 2002. **9**(8): p. 807-17.

55. Reubold, T.F. and S. Eschenburg, *A molecular view on signal transduction by the apoptosome.* Cell Signal, 2012 **24**(7): p. 1420-5. .

56. Karki, P., et al., *Intracellular K(+) inhibits apoptosis by suppressing the Apaf-1 apoptosome formation and subsequent downstream pathways but not cytochrome c release.* Cell Death Differ, 2007. **14**(12): p. 2068-75.

57. Beere, H.M., et al., *Heat-shock protein 70 inhibits apoptosis by preventing recruitment of procaspase-9 to the Apaf-1 apoptosome.* Nat Cell Biol, 2000. **2**(8): p. 469-75.

58. Zou, H., et al., *An APAF-1.cytochrome c multimeric complex is a functional apoptosome that activates procaspase-9.* J Biol Chem, 1999. **274**(17): p. 11549-56.

59. Imai, Y., et al., *The CED-4-homologous protein FLASH is involved in Fas-mediated activation of caspase-8 during apoptosis.* Nature, 1999. **398**(6730): p. 777-85.

60. Boatright, K.M. and G.S. Salvesen, *Mechanisms of caspase activation.* Curr Opin Cell Biol, 2003. **15**(6): p. 725-31.

61. Mace, P.D., S.J. Riedl, and G.S. Salvesen, *Caspase enzymology and activation mechanisms.* Methods Enzymol, 2014. **544**: p. 161-78.

62. Li, Y.P., et al., *Beta-amyloid induces apoptosis in human-derived neurotypic SH-SY5Y cells.* Brain Res, 1996. **738**(2): p. 196-204.

63. Estus, S., et al., *Aggregated amyloid-beta protein induces cortical neuronal apoptosis and concomitant "apoptotic" pattern of gene induction.* J Neurosci, 1997. **17**(20): p. 7736-45.

64. Loo, D.T., et al., *Apoptosis is induced by beta-amyloid in cultured central nervous system neurons.* Proc Natl Acad Sci U S A, 1993. **90**(17): p. 7951-5.

65. Lee do, Y., et al., *Activation of PERK signaling attenuates Abeta-mediated ER stress.* PLoS One, 2010. **5**(5): p. e10489.

66. Esler, W.P. and M.S. Wolfe, *A portrait of Alzheimer secretases--new features and familiar faces.* Science, 2001. **293**(5534): p. 1449-54.

67. Mattson, M.P., *Pathways towards and away from Alzheimer's disease.* Nature, 2004. **430**(7000): p. 631-9.

68. Neudecker, P., et al., *Structure of an intermediate state in protein folding and aggregation.* Science, 2012. **336**(6079): p. 362-6.

69. Selkoe, D.J., P. American College of, and S. American Physiological, *Alzheimer disease: mechanistic understanding predicts novel therapies.* Ann Intern Med, 2004. **140**(8): p. 627-38.

70. Duyckaerts, C., B. Delatour, and M.C. Potier, *Classification and basic pathology of Alzheimer disease.* Acta Neuropathol, 2009. **118**(1): p. 5-36.

71. Walsh, D.M., et al., *The APP family of proteins: similarities and differences.* Biochem Soc Trans, 2007. **35**(Pt 2): p. 416-20.

72. Chong, Y.H., et al., *ERK1/2 activation mediates Abeta oligomer-induced neurotoxicity via caspase-3 activation and tau cleavage in rat organotypic hippocampal slice cultures.* J Biol Chem, 2006. **281**(29): p. 20315-25.

73. Ellerby, L.M. and H.T. Orr, *Neurodegenerative disease: cut to the chase.* Nature, 2006. **442**(7103): p. 641-2.

74. Nikolaev, A., et al., *APP binds DR6 to trigger axon pruning and neuron death via distinct caspases.* Nature, 2009. **457**(7232): p. 981-9.

75. Picone, P., et al., *Abeta oligomers and fibrillar aggregates induce different apoptotic pathways in LAN5 neuroblastoma cell cultures.* Biophys J, 2009. **96**(10): p. 4200-11.

76. Fossati, S., J. Ghiso, and A. Rostagno, *TRAIL death receptors DR4 and DR5 mediate cerebral microvascular endothelial cell apoptosis induced by oligomeric Alzheimer's Abeta.* Cell Death Dis, 2012. **3**: p. e321.

77. Fossati, S., J. Ghiso, and A. Rostagno, *Insights into caspase-mediated apoptotic pathways induced by amyloid-beta in cerebral microvascular endothelial cells.* Neurodegener Dis, 2012. **10**(1-4): p. 324-8.

78. Cha, M.Y., et al., *Mitochondria-specific accumulation of amyloid beta induces mitochondrial dysfunction leading to apoptotic cell death.* PLoS One, 2012. **7**(4): p. e34929.

79. Murakami, Y., et al., *Cytoprotective role of mitochondrial amyloid beta peptide-binding alcohol dehydrogenase against a cytotoxic aldehyde.* Neurobiol Aging, 2009. **30**(2): p. 325-9.

80. Verdier, Y., M. Zarandi, and B. Penke, *Amyloid beta-peptide interactions with neuronal and glial cell plasma membrane: binding sites and implications for Alzheimer's disease.* J Pept Sci, 2004. **10**(5): p. 229-48.

81. Dahlgren, K.N., et al., *Oligomeric and fibrillar species of amyloid-beta peptides differentially affect neuronal viability.* J Biol Chem, 2002. **277**(35): p. 32046-53.

82. Resende, R., et al., *Neurotoxic effect of oligomeric and fibrillar species of amyloid-beta peptide 1-42: involvement of endoplasmic reticulum calcium release in oligomer-induced cell death.* Neuroscience, 2008. **155**(3): p. 725-37.

83. Thapa, A., et al., *Biflavonoids are superior to monoflavonoids in inhibiting amyloid-beta toxicity and fibrillogenesis via accumulation of nontoxic oligomer-like structures.* Biochemistry, 2011. **50**(13): p. 2445-55.

84. Evans, C.G., S. Wisen, and J.E. Gestwicki, *Heat shock proteins 70 and 90 inhibit early stages of amyloid beta-(1-42) aggregation in vitro.* J Biol Chem, 2006. **281**(44): p. 33182-91.

85. Sabirzhanov, B., et al., *Over-expression of HSP70 attenuates caspase-dependent and caspase-independent pathways and inhibits neuronal apoptosis.* J Neurochem, 2012. **123**(4): p. 542-54.

86. Chromy, B.A., et al., *Self-assembly of Abeta(1-42) into globular neurotoxins.* Biochemistry, 2003. **42**(44): p. 12749-60.

87. Xue, W.F., S.W. Homans, and S.E. Radford, *Systematic analysis of nucleation-dependent polymerization reveals new insights into the mechanism of amyloid*

self-assembly. Proc Natl Acad Sci U S A, 2008. **105**(26): p. 8926-31.

88. Wogulis, M., et al., *Nucleation-dependent polymerization is an essential component of amyloid-mediated neuronal cell death.* J Neurosci, 2005. **25**(5): p. 1071-80.

89. Hoffmann, J.C., et al., *A new C-terminal cleavage product of procaspase-8, p30, defines an alternative pathway of procaspase-8 activation.* Mol Cell Biol, 2009. **29**(16): p. 4431-40.

90. Cowling, V. and J. Downward, *Caspase-6 is the direct activator of caspase-8 in the cytochrome c-induced apoptosis pathway: absolute requirement for removal of caspase-6 prodomain.* Cell Death Differ, 2002. **9**(10): p. 1046-56.

91. Monnier, P.P., et al., *Involvement of caspase-6 and caspase-8 in neuronal apoptosis and the regenerative failure of injured retinal ganglion cells.* J Neurosci, 2011. **31**(29): p. 10494-505.

92. Slee, E.A., et al., *Ordering the cytochrome c-initiated caspase cascade: hierarchical activation of caspases-2, -3, -6, -7, -8, and -10 in a caspase-9-dependent manner.* J Cell Biol, 1999. **144**(2): p. 281-92.

93. Salvesen, G.S. and V.M. Dixit, *Caspase activation: the induced-proximity model.* Proc Natl Acad Sci U S A, 1999. **96**(20): p. 10964-7.

94. Morishima, Y., et al., *Beta-amyloid induces neuronal apoptosis via a mechanism that involves the c-Jun N-terminal kinase pathway and the induction of Fas ligand.* J Neurosci, 2001. **21**(19): p. 7551-60.

95. Jan, A., et al., *Abeta42 neurotoxicity is mediated by ongoing nucleated polymerization process rather than by discrete Abeta42 species.* J Biol Chem, 2011. **286**(10): p. 8585-96.

96. Majkut, J., et al., *Differential affinity of FLIP and procaspase 8 for FADD's DED binding surfaces regulates DISC assembly.* Nat Commun, 2014. **5**: p. 3350.

97. Dickens, L.S., et al., *A death effector domain chain DISC model reveals a crucial role for caspase-8 chain assembly in mediating apoptotic cell death.* Mol Cell, 2012. **47**(2): p. 291-305.

98. Hippe, D., et al., *Fas/CD95-mediated apoptosis of type II cells is blocked by Toxoplasma gondii primarily via interference with the mitochondrial amplification loop.* Infect Immun, 2008. **76**(7): p. 2905-12.

99. Kienlen-Campard, P., et al., *Intracellular amyloid-beta 1-42, but not extracellular soluble amyloid-beta peptides, induces neuronal apoptosis.* J Biol Chem, 2002. **277**(18): p. 15666-70.

100. Wirths, O., et al., *Intraneuronal Abeta accumulation precedes plaque formation in beta-amyloid precursor protein and presenilin-1 double-transgenic mice.* Neurosci Lett, 2001. **306**(1-2): p. 116-20.

101. Chui, D.H., et al., *Transgenic mice with Alzheimer presenilin 1 mutations show accelerated neurodegeneration without amyloid plaque formation.* Nat Med, 1999. **5**(5): p. 560-4.

102. Catanzariti, A.M., et al., *An efficient system for high-level expression and easy purification of authentic recombinant proteins.* Protein Sci, 2004. **13**(5): p. 1331-9.

103. De Marco, V., et al., *The solubility and stability of recombinant proteins are increased by their fusion to NusA.* Biochem Biophys Res Commun, 2004. **322**(3): p. 766-71.

104. Kapust, R.B. and D.S. Waugh, *Escherichia coli maltose-binding protein is uncommonly effective at promoting the solubility of polypeptides to which it is fused.* Protein Sci, 1999. **8**(8): p. 1668-74.

ABREVIATIONS USED

The abbreviations used are:

Aβ, amyloid β;

AD, Alzheimer's disease;

DISC, death-inducing signaling complex;

DM, prodomainless caspase-8 double mutant mimicking p30 fragment of caspase-8;

MTT, 3-(4,5-dimethylthiazol-2-yl)-2,5-diphenyl tetrazolium bromide;

p18-10, prodomainless equivalent of p41/43 fragment of caspase-8;

p30, ~30 kDa fragment of caspase-8;

p41/43, ~41/43 kDa fragment of caspase-8;

PBS, phosphate-buffered saline;

SDS-PAGE, sodium dodecylsulfate-polyacrylamide gel electrophoresis;

SEC, Size exclusion column chromatography;

STS, staurosporine;

DMEM, Dulbecco's modified Eagles medium;

DTT, Dithiothreitol;

fAβ, Fibrillar form of Aβ;

FBS, Fetal bovine serum;

ACKNOWLEDGEMENTS

Firstly, I would like to express my wholehearted gratitude to my supervisor Prof. Il-Seon Park for his continuous and judicious supervision, advice, guidance and training throughout this study. His extraordinary knowledge covering the large areas of protein biochemistry has been invaluable and a great support for my dissertation work. I would like to extend my gratitude to Prof. Song Yub Shin, Prof. Takbum Ohn and Prof. Lee Jung Hee for their valuable suggestions and support in various ways.

I reserve the deep note of appreciation to my previous supervisor Prof. Sohel Rana and my mentor in academic and personal life Prof. Gazi Mosharof Hossain for their contribution in my life. I would like to thank National Institute for International Education (NIIED) Korea, for the financial supports I got throughout my study period. I gratefully thank to my seniors Dr. Sharoar and Dr. Vijay for their training at early stage of my research and immense support during my work and to my colleague Aminul for their countless help. All the members of Molecular and cell Biology, Peptide Biochemistry, Peptide Engineering lab and Korea DNA Repair laboratory get warmest thanks for giving the chance of sharing their facilities.

Finally, I would like to thank my parents, my sisters and brothers and my wife for her inspiration, continuous supports and best care and love which made my journey a pleasant one.